Dissertation zur Erlangung des Doktorgrades

der Fakultät für Chemie und Pharmazie

der Ludwig-Maximilians-Universität München

PKC isozymes in the control of fate of prostate cancer cells

Vivian Annaluise von Burstin (geb. Därr)

aus

Houston, U.S.A.

2010

TABLE OF CONTENTS

I INTRODUCTION

I.1. Prostate Cancer

Prostate cancer is the leading cause of new cases of cancer and the second leading cause of deaths in men in the United States (Table I.1 and I.2). Among men, cancers of the prostate, lung and bronchus, and colon and rectum account for about 50% of all newly diagnosed cancers. Prostate cancer alone accounts for about 28% (217,730) of incident cases in men (Table I.1). The incidence of prostate cancer is age, race, and area dependent. Less than 1% of cases are diagnosed under the age of 40, although this may represent an underestimate as screening for disease in young men is rare. Prostate cancer is relatively uncommon in Asian populations and prevalent in Scandinavian countries, and the highest incidence (and mortality) rates known are in African Americans, being ~2-fold higher than in Caucasian Americans.

Estimated new cases of cancer in men, United States, 2010

Prostate	217,730	28%
Lung & bronchus	116,750	15%
Colon & rectum	72,090	9%
Urinary bladder	52,760	7%
Melanoma of the skin	38,870	5%
Non-Hodgkin lymphoma	35,380	4%
Kidney & renal pelvis	35,370	4%
Oral cavity & pharynx	25,420	3%
Leukemia	24,690	3%
Pancreas	21,370	3%
All sites	**789,620**	**100%**

Table I.1 Estimated new cases of cancer in men in the United States in 2010 (adapted from Jemal A, Siegel R, Xu J, Ward E. CA Cancer J Clin. 2010 Sep-Oct;60(5):277-300 [1]).

Estimated deaths of cancer in men, United States, 2010

Lung & bronchus	86,220	29%
Prostate	32,050	11%
Colon & rectum	26,580	9%
Pancreas	18,770	6%
Liver & intrahepatic bile duct	12,720	4%
Leukemia	12,660	4%
Esophagus	11,650	4%
Non-Hodgkin Lymphoma	10,710	4%
Urinary bladder	10,410	3%
Kidney & renal pelvis	8,210	3%
All sites	**299,200**	**100%**

Table I.2 Estimated deaths of cancer in men in the United States in 2010 (adapted from Jemal A, Siegel R, Xu J, Ward E. CA Cancer J Clin. 2010 Sep-Oct;60(5):277-300 [1]).

As with other common adenocarcinomas, both numerical and structural chromosomal alterations are frequent somatic changes in prostate cancer cells. Efforts have been made towards the understanding of the molecular mechanisms that initiate and lead to progression of this disease. By now, several key molecular changes were identified. Mouse models revealed the importance of the tumor suppressor *phosphate and tensin homolog 1 (PTEN)* for early tumorigenesis, as allelic deletion causes prostate intraepithelial neoplasia (PIN) and invasive cancer at later stages [2]. Loss or functional inactivation of *PTEN* results in excess input from *PI3K* and hyperactivation of the *Akt* survival pathway. Indeed, hyperactivation of Akt has been found in prostate cancer specimens, particularly in advanced stages of the disease, as well as in well-established cellular models of prostate cancer, such as LNCaP cells. Thus, loss of *PTEN* affects profoundly the regulation of the lipid based secondary messenger system. Indeed, deletion of *PTEN* obviously hits more pathways than *PI3K*, as constitutively activated Akt leads to PIN, but not invasive prostate cancer [3]. Furthermore, the occurrence of pathogenic mutations in *PTEN* in

early prostate cancer may indicate a less favorable outcome, and agents which interfere with the *PTEN* signaling pathway may provide new therapies for prostate cancer [4]. Other sites of loss/deletion in prostate cancer mainly occur in the late stages of cancer progression. Genetic inactivation of other tumor suppressor genes, such as *p53*, *RB1*, and *p16*, is seen most commonly in advanced cases of prostate cancer, although non-mutational down-regulation of these genes may frequently occur earlier.

The main focus of the research presented in this thesis is on protein kinase C (PKC), an important family of serine-threonine kinases widely implicated in cancer. Several lines of evidence suggest markedly altered mRNA and protein levels of PKC isozymes during different stages of prostate cancer progression in rodents and humans [5]. Using immunohistochemistry, Cornford et al. demonstrated elevated levels of PKCα, ε, and ζ in early stage human prostate carcinomas, whereas PKCβ levels are decreased compared to normal or benign hyperplastic prostate tissues [6]. Interestingly, the levels of PKCα mRNA and protein were decreased by 6- to 38-fold in androgen-sensitive cells when compared to androgen-insensitive cells [7], suggesting a role for PKCα in the transition from an androgen-dependent to an androgen-independent state. This is supported by the notion that treatment of male adult Wistar rats with the non-steroidal anti-androgen flutamide increased the activity of PKCα, as well as membrane translocation of PKCε, and total protein levels of PKCα, β, I, ε, and ζ compared to non-treated controls. These findings also suggest at least in part important roles for these kinases in the development of androgen-resistance, an event that results in impaired treatment options. Comparing PKC protein levels between benign prostatic hyperplasia and prostate cancer tissues from patients [8] revealed elevated levels of PKCα, β, ε, and η in prostate cancer tissues, in particular PKCε. Also, PKCε has been shown to exert oncogenic functions in

prostate and other cancer cell lines by increasing Stat3 Ser727 phosphorylation, thereby triggering Stat3-mediated transcription, and subsequently, invasion [9]. In addition, other reports indicate a role for PKCε in increased cell survival and resistance to apoptosis [10, 11]. Taken together, these studies argue for a prominent role for PKCε in the initiation and progression of prostate cancer. More recently, PKC isozymes have been implicated in certain settings to contribute to epithelial-to-mesenchymal transition (EMT) in prostate cancer cells [12]. Notably, PKCβ has been shown to phosphorylate directly histone H3 at threonine 6, which in turn prevents demethylation of methylated histone H3 lysine 4 (H3K4me) by lysine specific demethylase 1 (LSD1). In this study, PKCβ co-localized with the androgen receptor on promoters of androgen-receptor target genes, and was shown to be critical for androgen-dependent activation of transcription in prostate cancer cells [13].

The prostate cancer cell line LNCaP expresses the classical PKCα, the novel PKCδ and PKCε and the atypical PKCζ. It has been shown that androgen-dependent prostate cancer cell lines, such as LNCaP cells, undergo apoptosis upon PKC activation following treatment with the phorbol ester phorbol 12-myristate 13-acetate (PMA) in contrast to androgen-independent prostate cancer cells, such as PC3 or DU145 cells [7, 14]. Fujii et al. have also demonstrated that activation of PKCδ in LNCaP cells is responsible for the PMA-induced apoptosis in a caspase-3-independent manner [14]. Given their importance in prostate cancer biology, PKC isozymes, the mechanisms of PKC maturation and activation, and their ligands will be discussed in detail (see section I.3).

I.2 Apoptosis

I.2.1 General features of apoptosis

Apoptosis is a tightly regulated process in which a cell undergoes programmed cell death without disrupting a neighboring cell. Initially, the cell morphologically shrinks and loses its cell-cell contacts. At later stages, blebbing of the membrane occurs, and finally the cell scatters into multiple small vesicles, or apoptotic bodies. These apoptotic bodies are then subjected to phagocytosis, which allows for recycling of some of the apoptotic cell content. One of the most common features of apoptotic cells is the condensation of the nucleus, followed by its fragmentation into smaller pieces. Other organelles are subjected to fragmentation as well, *i.e.* the Golgi apparatus, the ER and the mitochondrion, which leads to the release of previously compartmentalized proteins to the cytoplasma. In case of mitochondrial lysis, one of the best studied protein in this context is cytochrome C. Cytochrome C itself triggers the assembly of the caspase-activating complex and the apoptosome, which ultimately leads to caspase activation [15].

I.2.2 Caspases

The name caspase is derived from 'cys-dependent asp-specific protease'. Caspases are the main players in executing the apoptotic program. They harbor a conserved cysteine side chain and specifically cleave target proteins after an aspartate (Asp) residue. Given the specificity of the caspase recognition motif, the family of caspases does not merely chop up proteins and foster their degradation, but modify proteins at specific residues, which may lead to altered conformation and function of these targets. This holds also true for the mode of activation of caspases themselves.

The apoptotic process involves two different kinds of caspases, the initiator and the effector caspases. Caspases-8, -9 and -10 are initiator caspases upstream in the caspase signaling cascade. Whereas caspase-8 and -10 are involved in the activation of the extrinsic pathway and can be found in the death-ligand induced signaling complex (DISC), caspase-9 is the initiator caspase of the intrinsic pathway (see below). Initiator caspases are comprised out of a large and a small subunit connected via a linker region that has an unusual length within the catalytic domain. Initiator caspases are activated upon dimerization, and, in contrast to effector caspases, not through cleavage (Fig. I.1A). The main function of initiator caspases is the activation of effector caspases by cleavage. Examples for effector capases are caspases-3 and -7. They are composed out of a large and a small subunit and exist in constitutive dimers, both in the inactive and in the active state (Fig. I.1B). Cleavage of the latent form results in the rearrangement within the protein, thereby unblocking the catalytic residues and leading to the proper alignment of the substrate binding site (Fig. I.1C) [16].

A

B

C
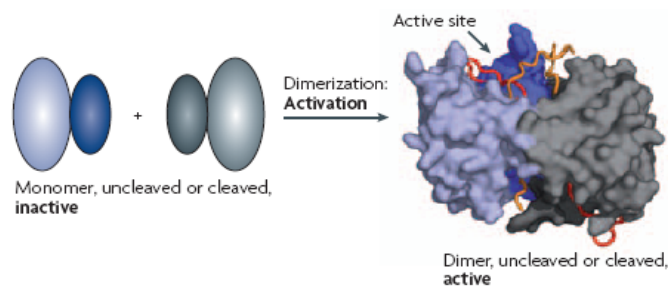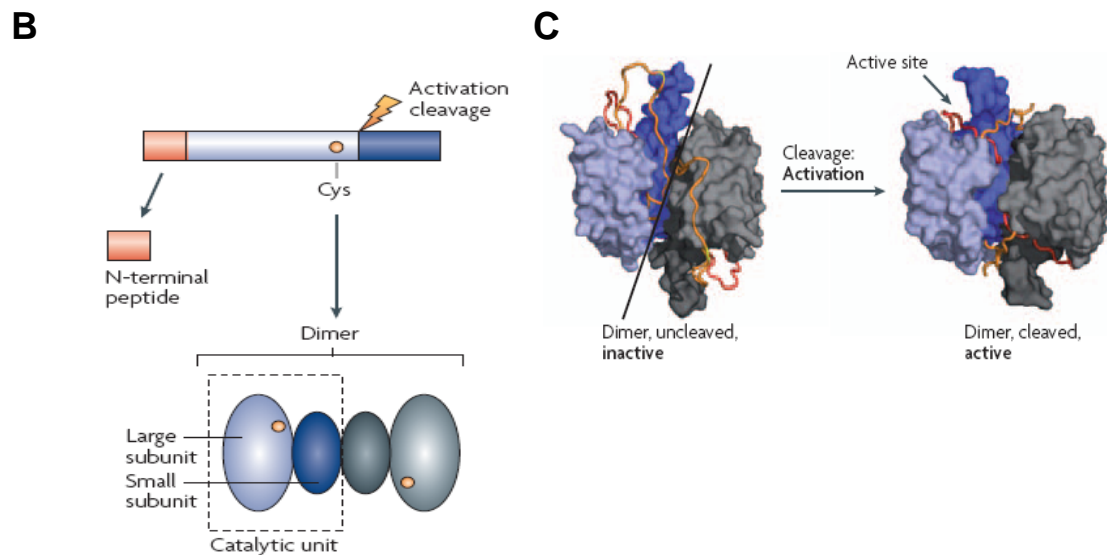
Figure I.1 **Structure and activation of initiator and effector caspases.** *Panel A.* Activation of initiator caspases through dimerization. *Panel B.* Schematic overview of the cleavage induced activation of effector caspases. *Panel C.* An activating cleavage of effector caspases leads to conformational changes and exposure of the enzymes's active site.

I.2.3 Pathways of caspase activation

In mammalian cells there are three well known pathways that lead to the activation of caspases and subsequent apoptotic cell death: The *extrinsic pathway,* the *intrinsic pathway* and the *granzyme b pathway*. The *extrinsic pathway* is induced by extracellular ligands that bind to specific cell surface receptors. Typical ligands are FasL, tumor necrosis factor-α (TNFα) and TNF-related apoptosis-inducing ligand (TRAIL). Binding of the ligand provokes the recruitment of adaptor proteins, such as the Fas-associated death domain protein (FADD) which in turn activates caspase-8 and caspase-10. This complex assembly is also termed Death Inducing Signaling Complex (DISC). Caspase-8 and -10 then proteolytically process and activate caspase-3 and -7 leading to further caspase activation, and finally apoptotic cell death.

The *intrinsic pathway* is characterized by various death signals that ultimately lead to the release of cytochrome C from the mitochondrial membrane. Typically, this is achieved by activation of one or more members of the BH3-only family through cell stress or damage. BH3-only proteins act as pathway-specific sensors for a variety of stimuli. Importantly, their activation overcomes the inhibitory effect of the anti-apoptotic B-cell-lymphoma-2 (BCL-2) family members and promotes the assembly of BAK-BAX oligomers within mitochondrial outer membranes. These oligomers in turn allow the release of cytochrome C from the mitochondrial intermembrane space, which then triggers the formation of the apoptosome and subsequent activation of caspases. The extrinsic and the intrinsic pathways are interconnected through the caspase-8-mediated activation of the BH3-only protein BID (BH3-interacting domain death agonist) which can promote mitochondrial cytochrome C release followed by assembly of the apoptosome (see section I.2.6) (Fig. I.2).

The *granzyme b (GrB)-mediated pathway* involves the delivery of this protease into the target cell through specialized granules that are released from cytotoxic T lymphocytes (CTL) or natural killer (NK) cells. CTL and NK granules contain numerous granzymes, as well as the pore-forming protein perforin. Perforin oligomerizes in the membrane of target cells, thereby permitting the granzymes to enter the target cell. [17-19]. Although several different granzymes have been described to induce cell death in a perforin-dependent manner [17], the most potent and best characterized is GrB. GrB is, like all other known granzymes, a pro-apoptotic serine protease with the ability, like caspases, to cleave proteins after specific Asp residues. These properties enable GrB to directly activate BID and caspases-3 and -7 (Fig. I.2) [15]. Although caspase activation is an important function of GrB, it has been shown that GrB-mediated apoptosis can occur in the absence of active caspases [20, 21]. GrB can directly cleave some nuclear proteins such as nuclear matrix antigen and poly(ADP-ribose) polymerase [22], and these properties may account for its caspase-independent action. Recently, another

caspase-independent pathway has been described, the granzyme A (GrA) pathway. Like GrB, GrA enters the target cell through perforin-mediated pores. It has been demonstrated that GrA activation results in DNA fragmentation in a caspase-independent manner in cell extracts. The GrA apoptotic pathway is characterized by the formation of single-stranded DNA nicks and the appearance of apoptotic morphology [23-26]. The pathways leading to caspase activation are summarized in Figure I.2.
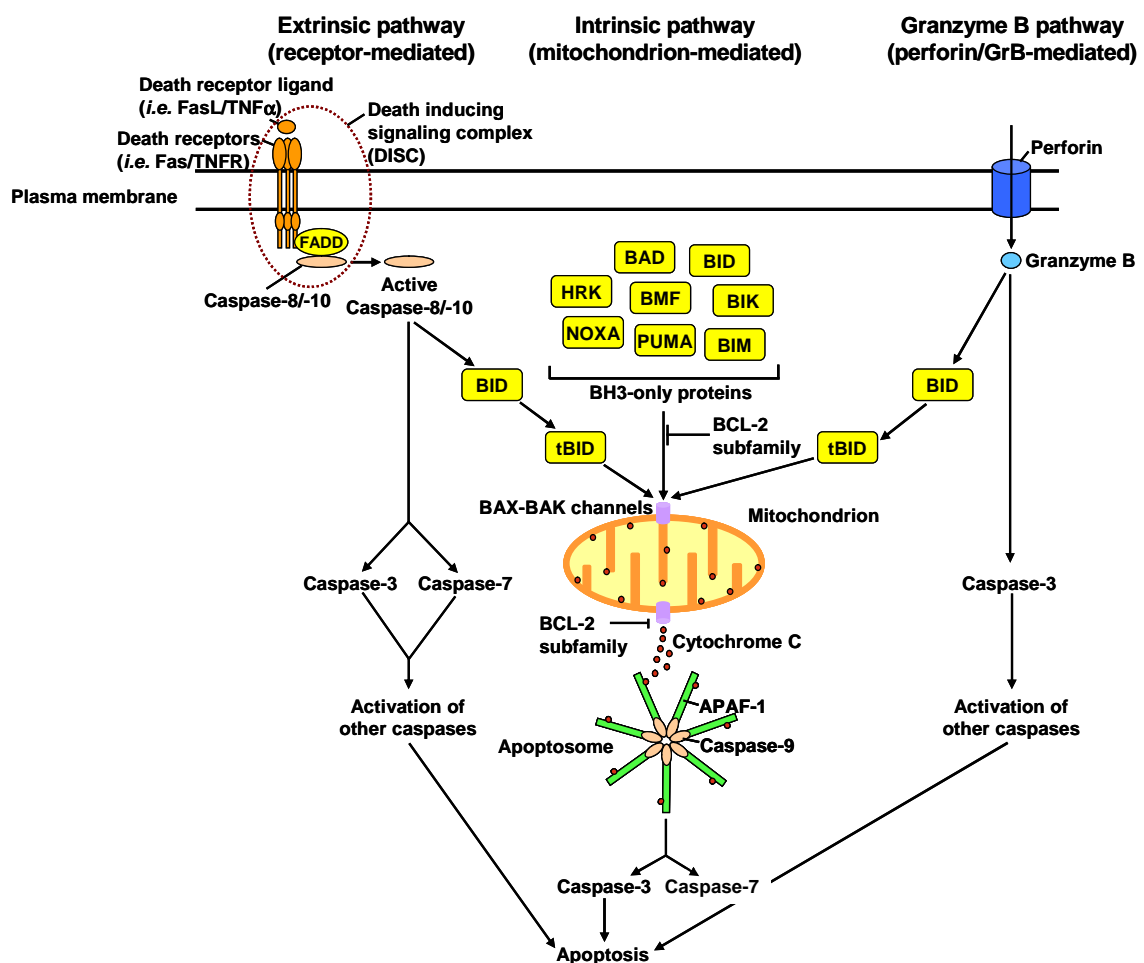
Adapted from Taylor, R.C. et al., Nat Rev Mol Cell Biol. 2008 Mar;9(3):231-41 [15].

Figure I.2 Three well-known pathways of caspase activation and initiation of apoptosis. The extrinsic and intrinsic pathways are caspase-dependent, whereas the granzyme B activated pathway can be caspase-dependent or -independent.

I.2.4 Apoptosis versus necrosis

As opposed to apoptosis, cells can also undergo necrosis which is the uncontrolled form of cell death. Necrosis is characterized by rapid loss of membrane integrity and subsequent swelling and membrane rupture. This in turn results in the release of cellular contents into the extracellular space. This release damages neighboring cells and in addition it initiates an immune response. Necrotic cells trigger inflammation by attracting neutrophils, macrophages and other cells of the innate immune system. The molecules causing the attraction of immune cells are called danger-associated molecular patterns (DAMPs) or alarmins. They include the high mobility group protein B1 (HMGB1), uric acid, certain heat shock proteins, single-stranded RNA and genomic DNA. In contrast, apoptotic bodies retain those alarmins and additionally facilitate the fast removal of apoptotic cells from the tissue. Therefore, apoptotic cell death does not initiate an immune response [15].

I.2.5 B-cell lymphoma-2 (BCL-2) family

Proteins of the BCL-2 family are critical regulators of apoptosis and can be classified into three subfamilies: *the anti-apoptotic BCL-2 family*, the *pro-apoptotic BCL-2 family,* and the *BH3-only family*. All of them contain one to four BCL-2 homology (BH) domains, and most of them also contain transmembrane domains (TM). The anti-apoptotic BCL-2 proteins possess four BH domains and all family members inhibit apoptosis by differential binding to BH3-only proteins. This in turn prevents BH3-only protein-induced oligomerization of the pro-apoptotic BCL-2 family members BAX and/or BAK in mitochondrial outer membranes, which is a required event for the induction of the intrinsic apoptotic pathway. The pro-apoptotic BAX-like family is characterized by the absence of a BH4 domain. Proteins of this family are required for the pore formation in the outer mitochondrial membrane, where they act

in form of hetero-oligomers, and are responsible for the subsequent release of cytochrome C. The BH3-only protein subfamily currently contains eight family members and is a structurally diverse group where the proteins only display homology within the BH3 motif. The BH3-only members serve as upstream sentinels that respond to specific, proximal death, and survival signals [27]. Some BH3-only proteins, such as BID and BIM, interact with all anti-apoptotic BCL-2 protein members, whereas others, such as NOXA, interact only with certain family members [15]. The regulation of BH3-only proteins is very distinct. For instance, NOXA, PUMA and BID are target genes of p53 and are transcriptionally up-regulated by p53. Therefore, levels of these proteins are found at increased levels in DNA-damage induced apoptosis. BID can be activated by caspase-8 mediated cleavage, resulting in tBID mediated BAX/BAK oligomerization. Whereas BAD is regulated by phosphorylation, BIM and BMF are freed from their intracellular binding partner dynein upon disruption of the cytoskeleton. In addition to that, BIM can be regulated by phosphorylation through ERK, resulting in proteasome-mediated degradation of BIM [15, 27]. An overview of the BCL-2 family members and their structure is given in Fig. I.3.
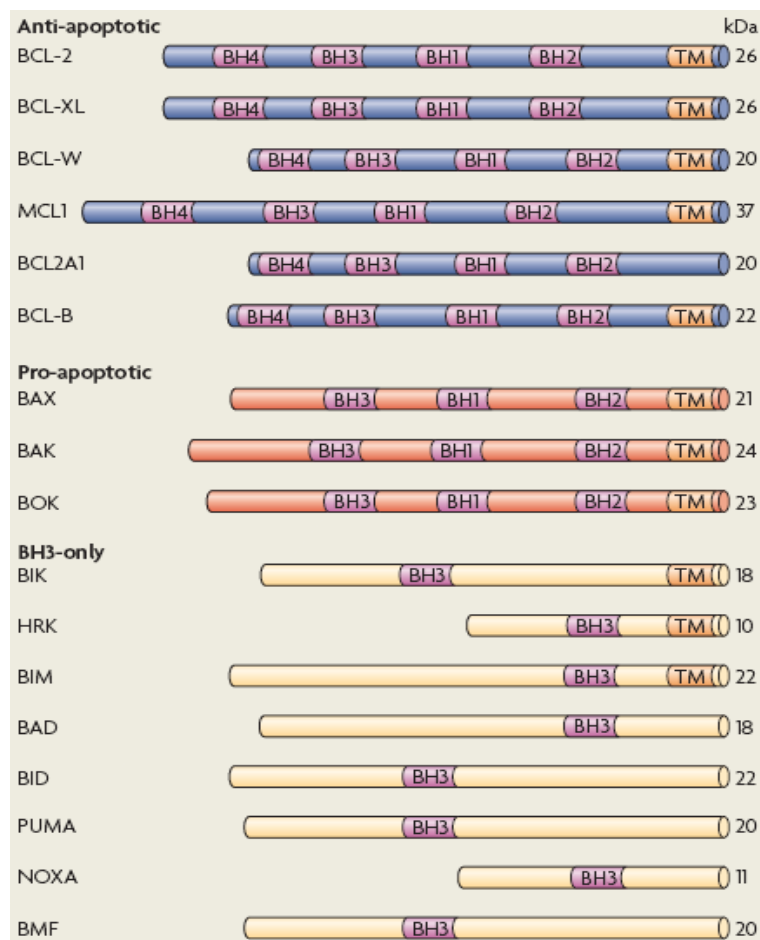
Figure I.3 Overview of the BCL-2 family members and their structures. There are three BCL-2 subfamilies, the anti-apoptotic subfamily, the pro-apoptotic subfamily, and the BH3-only subfamily.

BCL-2, B-cell lymphoma-2; BCL-XL, BCL2-like 1; BCL-W, BCL2-like 2; MCL1, myeloid cell leukemia sequence 1; BCL2A1, BCL2-related protein A1; BCL-B, BCL2-like 10; BAX, BCL-2-associated X protein; BAK, BCL-2 antagonist/killer-1; BOK, BCL-2-related ovarian killer; BIK, BCL-2-interacting killer; HRK, harakiri (also known as death protein -5); BIM, BCL-2-like-11; BAD, BCL-2 antagonist of cell death; BID, BH3-interacting domain death agonist; PUMA, BCL-2 binding component-3; BMF, BCL-2 modifying factor.

I.2.6 The apoptosome

The formation of the apoptosome is an essential step in the promotion of the apoptotic cascade as it leads to the activation of caspase-9. The activation process

requires caspase-9 to interact with the cofactor apoptotic protease activating factor-1 (Apaf-1). In the absence of an apoptotic signal Apaf-1 exists in a monomeric form. Upon binding to cytochrome C, Apaf-1 recruits caspase-9 in the presence of ATP or 2'-deoxy ATP (dATP). Apaf-1 consists of three functional regions, an N-terminal caspase-recruitment domain (*CARD*) which binds caspase-9, a nucleotide-binding and oligomerization domain (*NOD* or *NB-ARC*) which consists of three domains, and the C-terminal *WD40 repeats* (Fig. I.4A) [16, 27]. The *WD40 repeats* consist of two domains and are responsible for the binding of cytochrome C after its release from mitochondria. The *NB-ARC* region is the center for oligomerization and the formation of the apoptosome. There is evidence that it also contains an ATPase domain [28]. As long as Apaf-1 is in its monomeric form *WD40 repeat* domains are bound and keep it in a locked form. Most likely ATP/dATP is bound to the ATPase domain during the locked state of Apaf-1 [29, 30]. Upon an apoptotic signal cytochrome C is released from mitochondria and binds to the *WD40 repeat* region of Apaf-1. dATP is hydrolyzed by Apaf-1 which creates a dADP bound conformation of the Apaf-1 monomer. Now, the lock of the Apaf-1 is released and in a semi-open, but still autoinhibited form. In this autoinhibited form the *CARD* closely interacts with the ATPase domain and the winged-helix domain of the *NB-ARC* region. Therefore, the CARD is not accessible and cannot recruit caspase-9, and the blockage of the ATPase domain impairs the ability of Apaf-1 to form oligomers. Only a nucleotide exchange (dATP for dADP) and interactions with other Apaf-1 monomers or with caspase-9 monomers lead to an extended conformation that assembles heptamers into the wheel shaped apoptosome (Fig. I.4B). The reason for the ability to form oligomers (hexa- or heptamers) is the ATPase domain of Apaf-1. It contains domains which are found in a large family of ATPases, the AAA+ family, and without a nucleotide exchange Apaf-1 forms the inactive aggregate [16, 29, 30]. Once the oligomer is formed, it brings monomers of caspase-9 in close proximity of each other and facilitates the formation of caspase-9 dimers, which is the active form of

caspase-9 (see I.2.2), thereby triggering the intrinsic apoptotic cascade. The importance of Apaf-1 has been demonstrated in Apaf-1 knockout mice, which exhibit craniofacial and profound neuronal defects, leading to intrauterine or perinatal death of Apaf1$^{-/-}$ mice. This study also demonstrated the strict involvement of Apaf-1 in the intrinsic but not extrinsic apoptotic pathway, as FasL-induced apoptosis was largely unaffected [31].

A
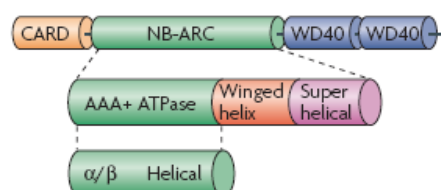
B
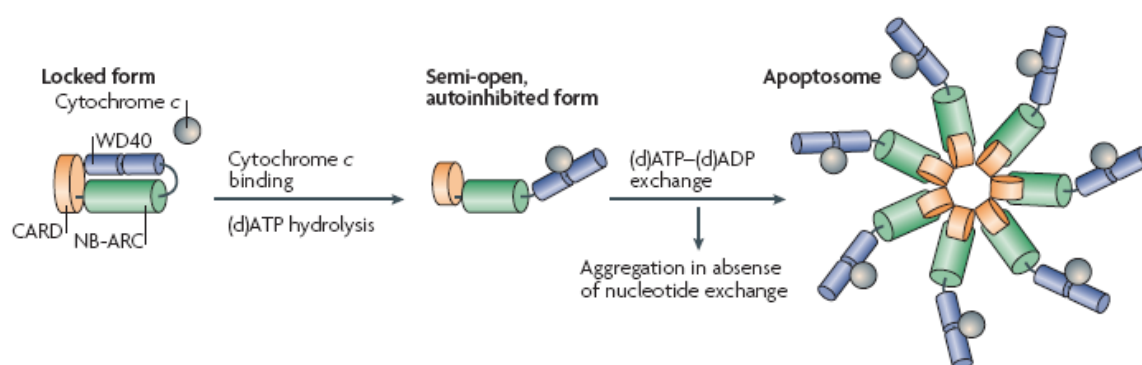
Taylor, R.C. et al., Nat Rev Mol Cell Biol. 2008 Mar;9(3):231-41 [15].

Figure I.4 Structure of Apaf-1 and apoptosome formation. *Panel A.* The structure of the apoptotic protease activating factor-1 (Apaf-1) contains three functional units: the N-terminal caspase-recruitment domain (*CARD*) which is responsible for recruiting caspase-9; a nucleotide-binding and oligomerization domain (*NOD* or *NB-ARC*) which is responsible for (d)ATP (ATP or 2′-deoxy ATP)-dependent oligomerization, and the *WD40* region which is responsible for binding of cytochrome C. The *NB-ARC* harbors an ATPase region. It belongs to the superfamily of AAA+ ATPases which are generally organized into an α/β- and a helical domain [32]. In the case of Apaf-1, this region is followed by a winged-helix and a superhelical domain. *Panel B.* In the absence of a signal Apaf-1 exists in a locked autoinhibited form. Upon binding of cytochrome C to the WD40 domain and (d)ATP hydrolysis the lock is released which leads to a semi-open but still autoinhibited form of Apaf-1. A nucleotide exchange is necessary to allow the release of the autoinhibition and the formation of an oligomerized, active state.

I.2.7 Induction of apoptosis by DNA double strand breaks

DNA double strand breaks (DSBs) may occur in a low frequency within a cell and can be repaired. If DSBs occur at a higher frequency or cannot be repaired, the cell in which this happens normally becomes apoptotic. However, DSBs may lead to genomic rearrangements and to silencing of tumor suppressor genes and/or amplification of oncogenes, eventually leading to malignant transformation. Indeed, inactivation or loss of DNA repair genes, such as *BRCA1*, can be found in multiple types of cancer. DSBs can be provoked through intrinsic and extrinsic stimuli. Common intrinsic stimuli include endogenously generated ROS and mechanical stress on the chromosomes, whereas ionizing radiation and chemicals represent typical extrinsic stimuli. In the event of a DSB, multiple factors are recruited to the site of damage. One key regulating factor upstream of the repair cascade is the kinase ATM. This kinase has multiple downstream targets, including BRCA1 and p53 [33, 34]. Phosphorylation of p53 through ATM leads to its stabilization [35] and activation [36]. p53 itself is now able to trigger a pro-apoptotic cascade by up-regulating several BH3-only protein upstream of BAX/BAK formation, including PUMA, NOXA and BID [37]. Activation of these BH3-only proteins merges then in the formation of BAX/BAK complexes and the induction of apoptosis. In addition, BAX itself is downstream target of p53.

The fact that DSB induces apoptosis can be used for cancer treatment. One classical chemotherapeutic agent that is widely used to generate DSBs is etoposide. Etoposide is a semisynthetic derivate of the naturally occurring mandrake root podophyllotoxin. It binds to topoisomerase II, a critical enzyme for DNA unwinding, cleavage and ligation. Binding of etoposide particularly inhibits the religation of cleaved DNA, thereby increasing the number of DSBs [38]. These DSBs can overwhelm the cell and lead to the triggering of death pathways. Interestingly, PKCδ has been shown to induce the expression of topoisomerase IIα which is also a PKCδ binding partner, in response to genotoxic stress [39], and aberrant activation of

topoisomerase IIα can trigger the intrinsic apoptotic pathway. The structure of etoposide is included in Figure I.5.

Other DSB-inducing agents are listed in Table I.3. Of note, the pro-apoptotic effect of DSB-inducing agents appears to be reduced in cells lacking functional p53 [40].
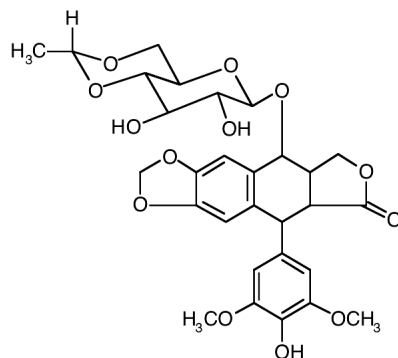
Figure I.5 Structure of etoposide. Etoposide binds to topoisomerase II. In this manner it inhibits religation of cleaved DNA, and thus leading to DNA damage.

DNA double-strand breaking agents	Mechanism of DNA double-strand break
Cyclophosphamide Melphalan Busulfan Chlorambucil Mitomycin	Alkylating agents; form interstrand and/or intrastrand crosslinks
Cisplatin	Forms crosslinks
Bleomycin	Cuts DNA strands between GT or GC
Etoposide Irinotecan Mitoxantrone	Inhibit the proper functioning of enzymes (**topoisomerases**) needed to unwind DNA for replication and transcription
Dactinomycin	Inserts into the double helix preventing its unwinding

Table I.3 DNA double-strand breaking agents and their mechanisms of action.

I.3 PKC isozymes

I.3.1 Structure of PKC isozymes

The PKC isozymes belong to the family of lipid-regulated serine-threonine kinases. The PKC family includes at least 10 isozymes which are classified into three groups by their structural and biochemical properties: "classical" calcium-sensitive cPKCs α, βI, βII and γ, "novel" nPKCs δ, ε, η and θ which are calcium-independent and "atypical" aPKCs ζ and ι/λ [41, 42]. aPKCs do not respond to diacylglycerol (DAG) or phorbol esters as opposed to cPKCs and nPKCs. The PKC structure consists of four well defined conserved domains (C1-C4) located in two regions, the N-terminal (or regulatory) and the C-terminal (or catalytical) domain. The N-terminal region possesses the motifs involved in the binding of the phospholipid cofactors, DAG/phorbol esters and calcium (Ca^{2+}), and it also participates in the associations with interacting proteins that control localization. The C1 domain contains a cysteine-rich motif and serves as the binding site for DAG/phorbol ester. Furthermore, the regulatory domain possesses an autoinhibitory pseudosubstrate sequence (PS) upstream of the cysteine-rich motif. The PS keeps the protein in its inactive state by binding to the catalytic domain of the kinase. The C2 domain contains the recognition site for acidic lipids and, in the classical PKC isozymes, the calcium binding site. The C3 and C4 domains are located in the C-terminus and form the ATP and substrate binding lobes of the kinase, respectively. Upon binding of a C1-ligand, *i.e.* DAG or PMA, to the C1 domains an allosteric conformational change relieves the autoinhibition and activates the enzyme. The regulatory and the catalytic domain are connected through a highly flexible hinge region which harbors sites for protease cleavage. The four conserved (C1-C4) and the five variable (V1-V5) domains of PKC isozymes are shown in Table I.3 and Fig. I.6.

4 conserved domains (C1-C4)

C1 in cPKCs and nPKCs	Binding of phorbol esters and DAG
C2	Lipid binding
C3	ATP binding site
C4	Substrate-binding site

Table I.4 PKC isozymes contain four conserved (C1-C4) domains.
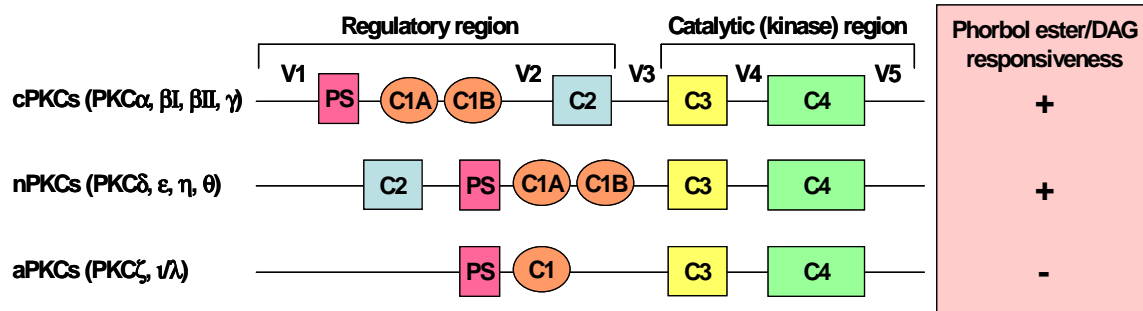
Adapted from Kazanietz, M.G., Biochim Biophys Acta. 2005 Dec 30;1754(1-2):296-304 [42] and Griner, E.M. et al., Nat Rev Cancer. 2007 Apr;7(4):281-94 [41].

Figure I.6 Structure of PKC isozymes. Only cPKCs and nPKCs respond to phorbol esters or DAG.

I.3.2 Mechanisms of PKC activation and inactivation

I.3.2.1 PKC maturation

PKC isozymes undergo a process of maturation through a series of phosphorylation steps before they become activated. In their C-terminal domain PKC isozymes contain an 'activation-loop site', a 'turn motif', and a 'hydrophobic motif'. For the priming phosphorylation step the enzyme needs to be in an 'open' conformation. This is the naturally occurring conformation of newly synthesized PKC isozymes in which the autoinhibitory PS sequence does not bind to the substrate-binding cavity. The priming phosphorylation step is initialized by 3-phosphoinositide-dependent protein kinase-1 (PDK1) which phosphorylates newly synthesized PKCs

at the activation-loop site. Once the phosphorylated C-terminus of PKC is released from PDK1, the 'turn' and the 'hydrophobic motif' are autophosphorylated, and conformational changes then free the catalytic domain to bind the autoinhibitory PS domain. The mature PKC, now primed for activation by DAG, is released into the cytosol and kept in an inactive conformation by intramolecular interactions between the N-terminal PS region and the kinase domain (Fig. I.7) [41, 43].

I.3.2.2 PKC activation

Stimulation of G-Protein-Coupled Receptors (GPCR) or Tyrosine-Kinase Receptors leads to the activation of different isoforms of phospholipase C (PLC) which cleave phosphoinositol-4,5-bisphosphate (PIP2) into DAG and inositol-1,4,5-trisphosphate (IP3). IP3 is released to the cytosol and interacts with a Ca^{2+} channel in the endoplasmatic reticulum (ER), releasing Ca^{2+} into the cytoplasm. Ca^{2+} binds to the C2 domain of PKCs and translocates it to the plasma membrane. The binding to Ca^{2+} is a low-affinity binding and is not sufficient to activate PKCs. nPKCs are not pre-targeted to membranes by Ca^{2+}. As a consequence, they translocate slower to membranes than cPKCs. Once the PKC has reached the plasma membrane, it diffuses in the plane of the membrane to bind to its membrane embedded ligand DAG (Fig. I.7). Binding of DAG to the C1 domain results in a high-affinity interaction of PKC with the membrane. The energy of this interaction leads to a conformational change which releases the PS domain from the substrate-binding site. In this activated open conformation, mature PKC binds substrates and effects downstream signaling [41, 43].

I.3.2.3 PKC inactivation

Biochemical studies revealed that membrane bound, activated PKC is highly sensitive to dephosphorylation [44]. Furthermore, it is known that prolonged activation, *i.e.* by treatment of cells with phorbol esters, results in increased dephosphorylation and turn-over of PKC [45]. Thus, dephosphorylation is a frequently occurring event and often involves the protein phosphatase 2A (PP2A) [46, 47], among others [48]. The dephosphorylated isozyme localizes to the detergent-insoluble fraction of cells, where it is eventually proteolyzed. Studies suggest that PKCα is degraded by the involvement of caveolin-dependent targeting to endosomes [49]. Additionally, limited evidence suggests that proteolysis of PKCs may occur through an ubiquitin-mediated pathway (Fig.I.7) [50, 51]. However, one efficient way by which the cell prevents degradation of dephosphorylated PKC is through its association with the heat shock protein HSP70. Association with HSP70 leads to stabilization of dephosphorylated PKC and allows for re-phosphorylation, thus recycling 'used' PKC [52].
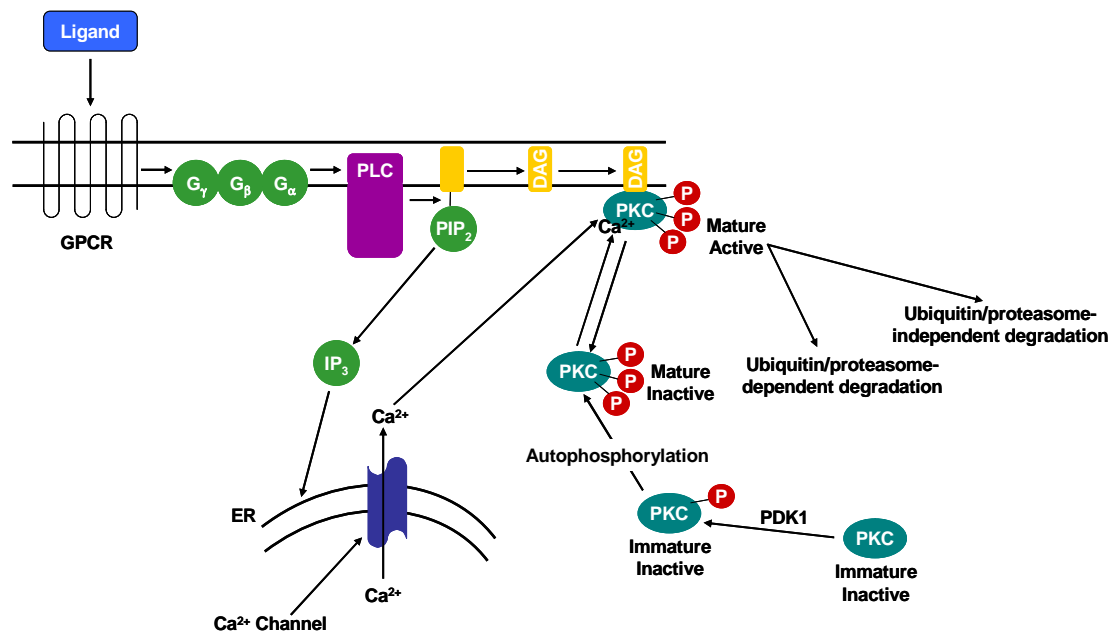
Figure I.7 Mechanisms of PKC maturation activation and inactivation. This model reflects the mechanisms for cPKCs. nPKCs are calcium-insensitive and therefore translocate slower to the plasma membrane. aPKCs do not respond to phorbol ester or DAG and are calcium-insensitive.

I.4 Regulation of apoptotic pathways by PKC isozymes

Although PKC isozymes share a high degree of homology, the cellular roles of PKC isozymes are very distinct. Upon binding of a C1 ligand, activation of a specific PKC may lead to apoptosis, *i.e.* as described for the activation of PKCδ in LNCaP cells. In contrast, PKCε leads to pro-survival signaling in various cell types. It has been shown that PKCε protects cells from apoptosis through activation of the anti-apoptotic BCL-2, and conversely, silencing of PKCε induces apoptosis in LNCaP cells (Fig. III.9). Over-expression of PKCε in lung cancer cells induces mitogen-activated protein kinase kinase (MAPKK or MEK) - ERK activation and has been shown to up-regulate the pro-survival factors BCL-X$_L$ and X-linked inhibitor of apoptosis (XIAP). In breast cancer cells PKCε is involved in Akt activation and hence pro-survival signaling. Moreover, PKCε fails to protect Akt-depleted cells from apoptosis, suggesting that Akt is the major pro-survival pathway activated by PKCε. In addition, increased expression of PKCε has been linked to resistance to chemotherapeutic agents as shown in non-small-cell lung carcinoma cells [41].

PKCδ on the other hand can trigger pro-apoptotic signaling. Because PKCδ is highly susceptible to caspase-3 cleavage at the hinge region, its proteolytic activation is a common event during apoptosis. Cleavage in the hinge region results in a physical separation of the regulatory domain and catalytic domains. The catalytic fragment, which has a molecular weight of 40 kDa, is constitutively active. Some chemotherapeutic agents, such as etoposide or cisplatin, or UV radiation are capable to induce the generation of the catalytic fragment, and their apoptotic efficacy is impaired when PKCδ function or expression is inhibited. Interestingly, PKCδ is involved upstream and downstream of caspase-3, as PKCδ cleavage serves as a positive feedback signal by relocation of the catalytic fragment to mitochondria and increasing cytochrome C release (Fig. I.8).

A

UV or other DNA-damaging agents

B

Phorbol ester/DAG

TNFα and TRAIL
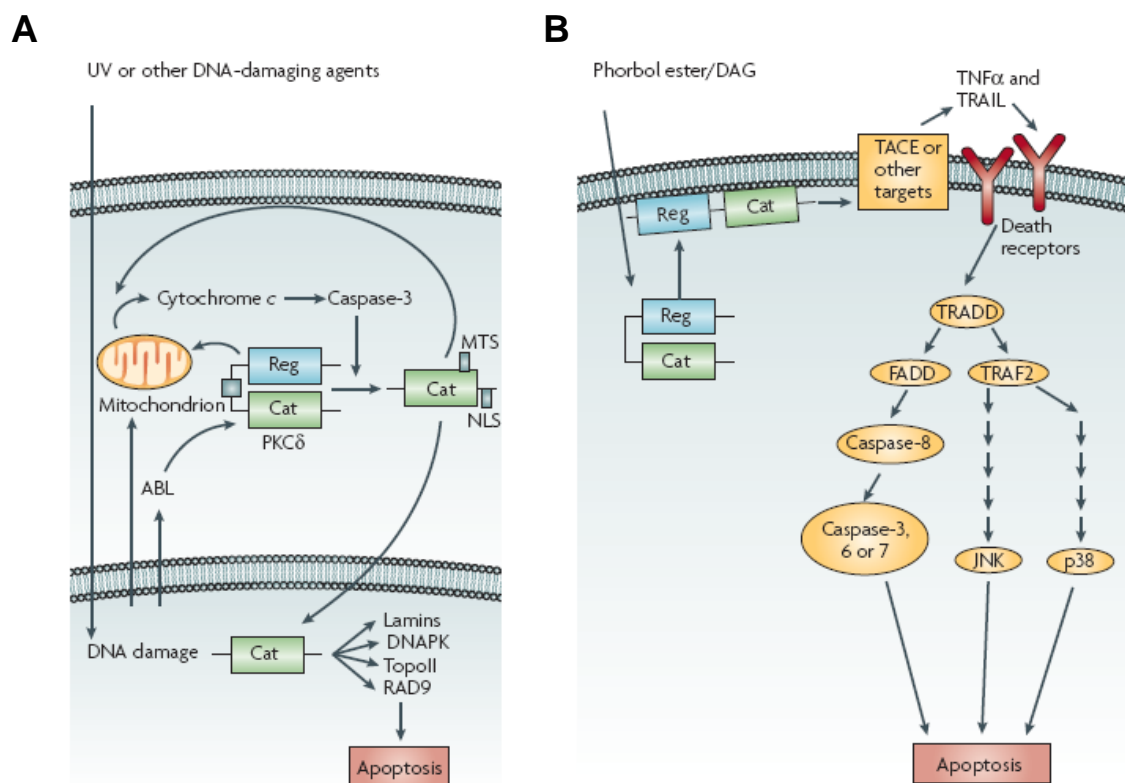
Figure I.8 Pathways of PKCδ-mediated apoptosis. *Panel A.* PKCδ is subject to caspase-3-mediated cleavage, *i.e.* as a consequence of DNA damage, which results in the release of the catalytic domain. This in turn facilitates mitochondrial translocation and also exposes a cryptic nuclear localization sequence (NLS). Once the catalytic domain of PKCδ translocates into these compartments, it may lead to increased release of cytochrome C and phosphorylation of nuclear targets, respectively. The latter may be important for the regulation of the cell cycle and other nuclear events that occur during apoptosis. *Panel B.* PKCδ is also capable of triggering the extrinsic cascade by modulating the release of death factors, such as TNFα, which then leads to the assembly of the DISC and subsequently the induction of apoptosis.

Cleaved PKCδ can also translocate to the nucleus in response to chemotherapeutic agents, which is due to the exposure of a cryptic nuclear localization signal (NLS) located at the C-terminus of PKCδ. Impairing the nuclear translocation of PKCδ was found to inhibit the apoptotic effect of etoposide. In addition, many other apoptotic stimuli can redistribute full length PKCδ to mitochondria, promoting cytochrome C release, caspase-3 activation, and initiation of the intrinsic apoptotic cycle [53-55].

Oxidative and genotoxic stress can also lead to phosphorylation of full length PKCδ at a C-terminal tyrosine residue. Importantly, PKCδ-mediated apoptosis could be regulated by tyrosine-phosphorylation. This event is likely to be mediated through the c-Abl protein tyrosine kinase and promotes nuclear translocation of PKCδ through the induction of conformational changes, thereby exposing the otherwise cryptic NLS [56]. Previous work from our laboratory demonstrated that activation of PKCδ triggers an autocrine apoptotic loop through the secretion of TNFα and TRAIL [57] in LNCaP cells. The integrity of this autocrine loop appears to be critical for the induction of apoptosis by phorbol esters [58].

The third DAG/PMA-responsive PKC isoform expressed in LNCaP cells is the classical PKCα. In LNCaP cells this PKC isoform facilitates apoptosis through activation of PP2A, a phosphatase that dephosphorylates and inactivates Akt. Expression of a constitutive active form of Akt (Myr-Akt) prevents PMA-induced apoptosis in LNCaP cells. PMA fails to reduce phospho-Akt levels in the presence of the PP2A inhibitor okadaic acid. It was also shown that induction of apoptosis by PMA could be attenuated by specific blockade of PKCα [58]. In addition, activation of PKCs by PMA leads to increased levels of phosphorylated p38, and functional inhibition of p38 with SB 203580 reduced PMA-induced apoptosis. Interestingly, this effect could be ascribed to both PKCα and δ [58]. In summary, the above mentioned findings demonstrate once more that the effect of PKC activators on apoptosis is both cell type and PKC-isozyme dependent. A summary of the pro-apoptotic functions of PKCα and PKCδ in LNCaP cells is shown in Fig. I.9, and the effects of PMA in LNCaP cells is summarized in Fig. I.10.
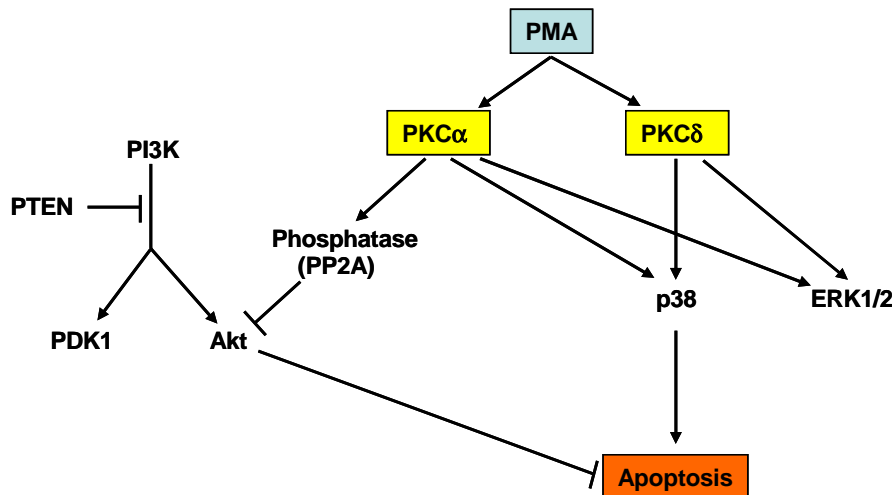
Adapted from Gonzalez-Guerrico, A.M., et al., J Biochem Mol Biol. 2005
Nov 30;38(6):639-45 [138].

Figure I.9 Signaling pathways of the PKC isoforms involved in apoptosis in LNCaP cells. Pro-apoptotic PKCs activate the p38 cascade in LNCaP prostate cancer cells and lead to the inactivation of the survival kinase Akt. Whereas both PKCα and PKCδ promote phosphorylation of p38, it is thought that only PKCα triggers the dephosphorylation of Akt by activating a phosphatase (PP2A).
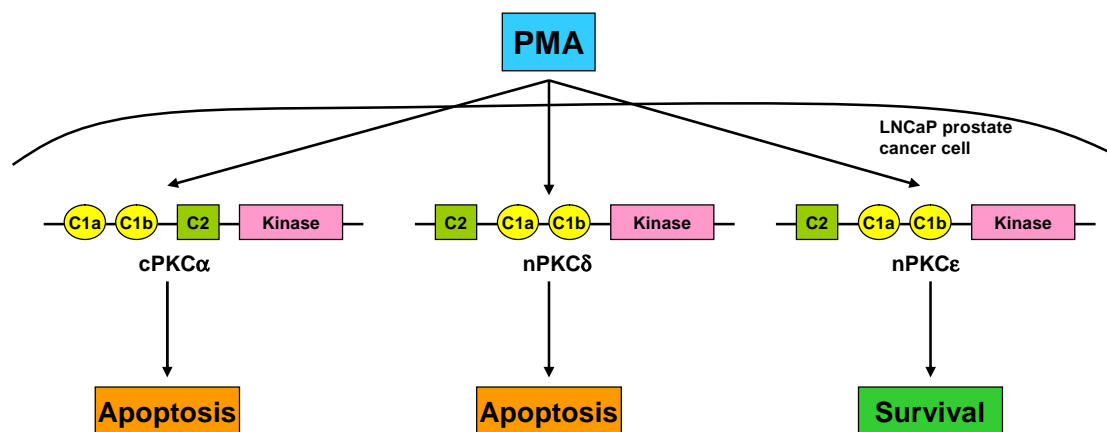
Adapted from Gonzalez-Guerrico, A.M., et al., J Biochem Mol Biol. 2005
Nov 30;38(6):639-45 [138].

Figure I.10 Overview of PKC functions. In LNCaP cells PKCα, δ and ε respond to phorbol esters after its binding to the C1 domain of the PKCs. Each PKC isozyme has distinct roles in cellular processes, such as proliferation, differentiation, apoptosis and survival. PKCα and PKCδ are pro-apoptotic kinases, whereas PKCε is a pro-survival kinase.

I.5 Naturally occurring DAG analogs: Phorbol esters and Bryostatins

Phorbol esters are generally known for their tumor promoting activity, and naturally occur in *Thymelaeaceae* and *Euphorbiaceae*, here especially in *Jatropha curcas* (Fig. I.11). This shrub is widely distributed in many Latin American, Asian and African countries. The seed kernels contain up to 60% oil with a fatty acid composition similar to that of common eatable oils. However, the seeds and seed oil are toxic to humans and animals [59], and the toxicity of the seeds of *J. curcas* has been ascribed mainly to the presence of phorbol esters [60, 61].

A
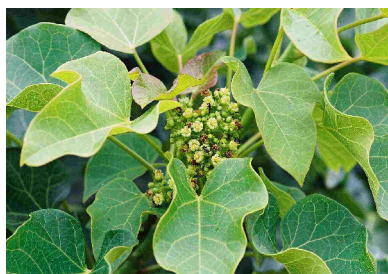
B
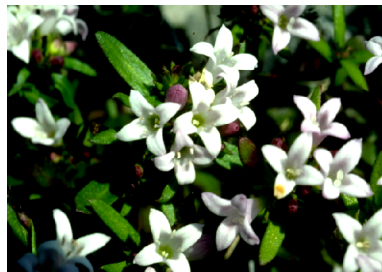
Figure I.11 **Phorbol ester naturally occur in *Euphorbiaceae* and *Tyhmelaeaceae*.** *Panel A.* The plant *Jatropha curcas* L. (*Euphorbiaceae*) *(left panel)* bears oil containing seed kernels with phorbol ester (*right panel*). *Panel B. Gnidia capitata* L.f. (*left panel*) and *Daphne alpine* (right panel) belong to the phorbol ester bearing *Thymelaeaceae*.

Although a few phorbol ester derivatives are known for their antitumor activities [62], phorbol esters have been widely used in cancer research because of

their high potency as tumor promoters in the mouse skin [63]. It has been in the early 1980s that PKC isozymes have been identified as the target of the phorbol esters. One of the best studied phorbol ester in this regard is phorbol 12-myristate 13-acetate (PMA), also known as tetradecanoyl phorbol acetate (TPA) which has been used for decades as a PKC activator. It mimics the action of DAG and binds to the C1 domain of PKCs with high affinity. Of note, PMA has higher potency and stability than DAG itself which makes it one of the most valuable pharmacological tools to study multistage carcinogenesis *in vivo*. In addition to its tumor promoting activity, PMA leads to numerous cellular responses, including mitogenesis, cell growth arrest, survival, apoptosis, differentiation, and transformation, depending on the cell type. Other natural products mimicking DAG activity are the daphnane derivatives, mezerein and thymeleatoxin, ingenol esters, aplysiatoxins, teleocidines such as indolactam V (ILV), and bryostatins [64, 65].

Bryostatin 1 is of particular interest, since it has been described to have effects on PKCs that only partially recapitulate the effects provoked by PMA. Bryostatins are macrocyclic lactones which were first isolated in the late 1960s by George Pettit and co-workers from extracts of a species of the bryozoan *Bugula neritina*. Currently, there are 20 known natural bryostatins differing mainly in the nature of the substituents at positions C7 and C20 [66]. Importantly, the bryostatins have been shown to competitively inhibit the binding of phorbol esters and endogenous diacylglycerol to PKCs at low nanomolar to picomolar concentrations and to stimulate comparable kinase activity *in vitro* by binding to the C1 domains of cPKCs and nPKCs [66, 67]. However, while bryostatins mimic several phorbol ester responses, they display unusual pharmacological properties as they fail to induce phorbol ester-like responses in many cellular models. More interestingly, bryostatins functionally antagonize phorbol ester responses that they themselves are unable to elicit, including tumor promotion [68, 69].
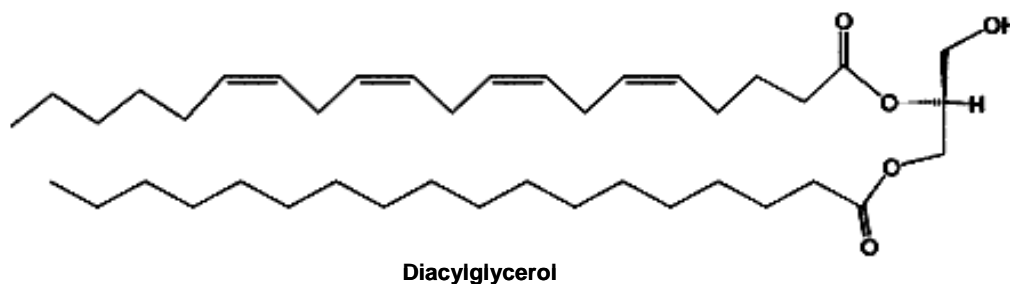
Diacylglycerol
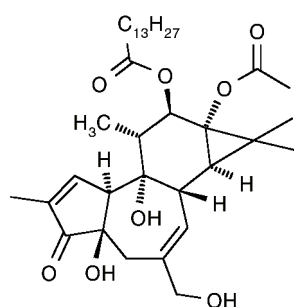
Phorbol 12-myristate 13-acetate
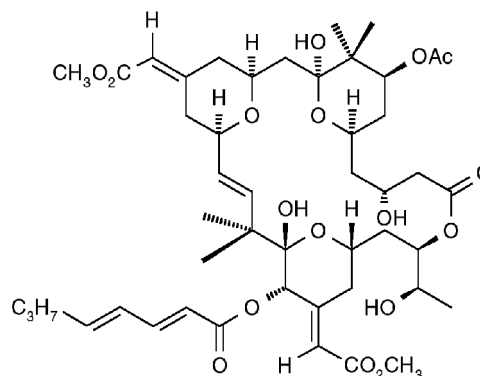
Bryostatin 1

Figure I.12 Structures of PKC activators. Diacylglycerol (DAG), phorbol 12 myristate 13-acetate (PMA), and bryostatin 1 activate PKC isozymes by binding to their C1 domain.

Preliminary biological screening had revealed bryostatins to be powerful antitumor agents *in vitro*, and efforts were made to identify the structure of bryostatin 1, which was achieved in 1982, also by George Pettit and co-workers (Fig I.12) [70]. The *in vitro* antitumoral effects of bryostatin 1 were later confirmed *in vivo* in a number of established murine tumor models [71, 72]. In addition, it was found that the bryostatins exhibit potent anti-tumor activity against a broad range of human cancer cell lines and provide significant *in vivo* life extensions in murine xenograft tumor models [66]. Currently, bryostatin 1 is evaluated alone and in combination with other chemotherapeutic agents in over 25 phase I and II human clinical trials for melanoma, myeloma, chronic lymphocytic leukemia (CLL), AIDS- related lymphoma, non-Hodgkin's lymphoma, colorectal, renal, prostate, head and neck, cervix, ovarian,

breast, peritoneal, stomach, esophagus, anus, prostate, and non-small cell lung cancer [73-77]. Results of several clinical trials have indicated that bryostatin 1 is well tolerated with no acute toxicities. The dose-limiting toxicity in all cases has been myalgia (muscle pain) which is relieved upon cessation of treatment. Efficacy has been observed in these clinical studies including several partial and complete responses for advanced, refractory forms of cancer [66].

I.6 Aims of the study

As outlined above, PKC isozymes play a fundamental role in the induction of apoptosis in LNCaP cells. In particular, PKCδ has been suggested to be of major importance for the induction of apoptosis in this cell line. PKCs can be influenced by multiple stimuli, both endogenous (DAG) and exogenous (PMA and bryostatin 1). However, PMA and bryostatin 1 only partially provoke identical responses upon binding to the C1 domain of PKCs, and have opposing effects with regard to the responses they do not share. Because bryostatin 1 is in clinical trials for various cancers, but not prostate cancer, the following question should be investigated in this study:

Specific Aim 1: To assess the effect of bryostatin 1 on LNCaP prostate cancer cells and whether it affects PMA-induced apoptosis in this cell line.

In addition, different C1 domain containing PKC isozymes have different targets, which is reflected in isoform-specific responses of a cell to PMA. Phosphorylation of target proteins may ultimately lead to changes in gene expression, *i.e.* through stabilization/destabilization or subcellular translocation of a phosphorylated signaling molecule or transcription factor. However, it has not been

systematically addressed so far whether and to which extend PKC activation by PMA and subsequent apoptosis in LNCaP cells involves transcriptional regulation in an isoform-dependent manner. To address these issues, the specific aim 2 is as follows:

Specific Aim 2: To elucidate the impact of PKC isozyme activation on transcriptional regulation in LNCaP cells in the context of PMA-induced apoptosis.

II MATERIALS AND METHODS

II.1 Compounds for cell culture treatment

Bryostatin 1 was purchased from EMD (Gibbstown, NJ, USA). A stock of 100 µM was prepared in DMSO and stored at -20°C. Phorbol 12-myristate 13-acetate (PMA) was obtained from LC Laboratories (Woburn, MA, USA). A 1 mM stock prepared in 100 % ethanol was stored at -80°C. Etoposide was purchased from EMD (San Diego, CA, USA) and dissolved in DMSO at a concentration of 100 µM. Cycloheximide was purchased from Sigma (St. Louis, MO, USA) and dissolved in 100% ethanol to concentration of 50 mM. TNFα was purchased from Peprotech (Rocky Hill, NJ, USA).

II.2 Cell Culture

II.2.1 Cultivation of cells

The prostate cancer cell line LNCaP, clone FGC (CRL-1740), was cultured in RPMI 1640 medium supplemented with inactivated 10% FBS, penicillin (100 units/ml) and streptomycin (100 µg/ml) (complete RPMI 1640) at 37°C in a humidified 5% CO_2 atmosphere. Cells were grown in an adherent monolayer in tissue culture dishes on an area of 60 cm^2 and were passaged twice a week. Cells were washed with pre-warmed (37°C) RPMI 1640 medium to avoid detachement of the cells. One ml of 0.05% Trypsin/EDTA was added to a p100 plate and incubated for 3 to 5 min at 37°C in a humidified 5% CO_2 atmosphere. After cell detachment, 11 ml of complete RPMI 1640 medium were added to inactivate the Trypsin/EDTA solution. Cells were thoroughly resuspended and either passaged in a ratio of 1:3 or 1:4 into 3 or 4 p100 plates, respectively. To avoid loss of androgen-dependency the cell density never exceeded 70-80%, and cells were only used from passage 2 to 8 for all experiments.

II.2.2 Materials

Product	Company
LNCaP clone FGC (CRL-1740) Prostate Carcinoma; human	American Type Culture Collection, Manassas, VA, USA
RPMI 1640 medium	American Type Culture Collection
Fetal bovine serum (FBS)	Hyclone, Logan, UT, USA
Penicillin/Streptomycin solution	Invitrogen, Carlsbad, CA, USA
0.05% Trypsin-EDTA	Invitrogen
Dimethylsulfoxide (DMSO)	Thermo Fisher Scientific, Rochester, NY, USA
Tissue culture dishes (22.1 cm^2, 60.1 cm^2)	TPP, Trasadingen, Switzerland
BD Falcon™ 6- and 12-well Multiwell Plates	BD Biosciences, San Jose, CA, USA
BD Falcon™ Serological pipets	BD Biosciences
15 and 50 ml conical tubes	GeneMate/ISC BioExpress, Kaysville, UT, USA
Corning® 2ml External Threaded Polypropylene Cryogenic Vial	Corning Incorporated Life Sciences, Lowell, MA, USA
13 mm syringe filter (0.45 μm pore size)	Thermo Fisher Scientific
5100 Cryo 1°C Freezing Container, "Mr. Frosty"	Nalgene Labware, Thermo Fisher Scientific
Jouan CR 312 centrifuge	Jouan, now Thermo Fisher Scientific
US AutoFlow NU-4750 incubator	Nuaire, Plymouth, MN, USA

Table II.1 Materials used for cell culture.

II.2.3 Freezing and thawing of LNCaP cells

Freezing medium with 5% of DMSO	
DMSO	2.5 ml
Complete RPMI 1640	47.5 ml

Table II.2 Composition of freezing medium

The purchased LNCaP cells were warmed up at 37°C by holding the cryovial into a pre-warmed water bath (37°C) until they started thawing (30-60 sec). Cells were completely defrosted by gently dissolving in 30 ml pre-warmed medium. Subsequently, cells were centrifuged (1,000 rpm, 5 min) to remove DMSO and cell debris. After resuspending the cell pellet in 10 ml fresh medium, cells were plated and left to grow (considered as passage 1) in a 100 mm dish. After reaching a confluency of 70-80% cells were passaged in a 1:3 ratio (passage 2). Cells were again 70-80% confluent before freezing or using them for experiments (passage 3).

To freeze cells a special freezing medium was prepared (Table II.2: Freezing medium for LNCaP cells) containing DMSO to avoid cell rupture. Complete RPMI 1640 medium was removed from the cells. Cells were washed once with 7 ml of complete RPMI 1640, and 1 ml of 0.05 % Trypsin/EDTA was added to the cells and incubated for 3 to 5 min at 37°C in a humidified 5% CO_2 atmosphere. After detachment, cells were resuspended thoroughly in 11 ml of complete RPMI 1640, transferred into a 15 ml conical tube and centrifuged (1000 rpm, 5 min, 4°C). The supernatant was removed and the cell pellet was resuspended in 2 ml (1:2) of ice-cold freezing medium for LNCaP cells. One ml of the cell suspension was transferred into each cryovial and transferred into a pre-cooled (4°C) freezing container. This special freezing container provides a cooling rate of -1°C/minute. The freezing container was then transferred into the -80°C freezer. Two days later the cryovials were transferred into liquid nitrogen for long-term storage.

II.2.4 Inactivation of fetal bovine serum (FBS)

Frozen fetal bovine serum was thawed overnight at 4°C. Thawed serum was left at room temperature for 2 h. Afterwards, the bottle of serum was heated at 56°C for 30 min in a water bath containing enough water to immerse the bottle to just above the level of the serum. The bottle with serum was swirled every 5 to 10 min to assure equal temperature throughout the entire bottle. After 30 min, serum was cooled down on ice immediately, aliquoted in 50 ml aliquots, and stored at -20°C.

II.3 Apoptosis assay

II.3.1 Materials

Product	Company
4´,6-Diamidine-2´-phenylindole dihydrochloride (DAPI)	Roche Applied Science, Indianapolis, IN, USA
Phosphate Buffered Saline (PBS) 7.4 (1X)	Invitrogen
Dimethylsulfoxide (DMSO)	Thermo Fisher Scientific
0.05% Trypsin/EDTA	Invitrogen
15 ml conical tube	GeneMate/ISC BioExpress
Fluoromount-G™	SouthernBiotech, Birmingham, AL, USA
Corning® 75 x 25mm Microscope Slides, Frosted OneSide, One End	Corning Incorporated Life Sciences,
Corning® 22 x 50mm Rectangular #1 Cover Glass	Corning Incorporated Life Sciences
Nikon Eclipse Microscope TE 2000-U	Nikon Instrument Inc., Melville, NY, USA
Microscope Camera: Dual-View Optical Insights OJ-05-EM	Nikon Instruments Inc.
Dual-View wavelength splitter with an OI-05-Ex excitation filter (436 ± 20 nm) and OI-05-Em emission filter (480 ± 30 nm)	Optical Insights, Tucson, AZ, USA
Microscope Software: Northern Eclipse	Empix Imaging Inc., Cheektowaga, NY, USA

Table II.3 **Materials for apoptosis assay.**

II.3.2 DAPI staining

DAPI was reconstituted in distilled H_2O to obtain a stock solution at a concentration of 1 mg/ml, aliquoted and stored in the dark at -20°C. A working solution of 1 μg/ml DAPI in PBS was prepared prior to use.

2×10^5 cells were seeded into a 6-well plate and cultured for 2 days. Cells were then treated with either vehicle (ethanol and/or DMSO), PMA 100 nM and/or bryostatin at various concentrations (1, 10 or 100 nM). Forty-eight h after treatment the medium containing detached apoptotic cells was transferred into a 15 ml conical tube. To wash the remaining attached cells 2 ml of PBS/well were added, removed and transferred to the same tube as the detached cells. The attached cells were trypsinized with 0.5 ml of 0.05% Trypsin-EDTA/well at 37°C in a humidified 5% CO_2 atmosphere. Two ml of PBS were added to the trypsinized cells and combined with the already collected cells of one sample in the 15 ml conical tube. The tube was then centrifuged for 5 min at 1,000 rpm at 4°C. The supernatant was removed and the cell pellet carefully resuspended in 200 μl of PBS. One hundred μl of the cell suspension were mounted on glass slides and fixed in 70% pre-cooled (-20°C) ethanol for 20 min at -20°C. Morphological changes in chromatin structure were assessed after staining with DAPI/PBS solution for 20 min in the dark at 4°C [11, 58]. Apoptosis was characterized by chromatin condensation and fragmentation when examined by fluorescence microscopy (Fig. II.1). The percentage of apoptosis was determined by counting a total of 300 cells per preparation. In previous studies our laboratory found that the results with this method match those obtained by flow cytometry and correlate with DNA laddering analysis [14, 57].
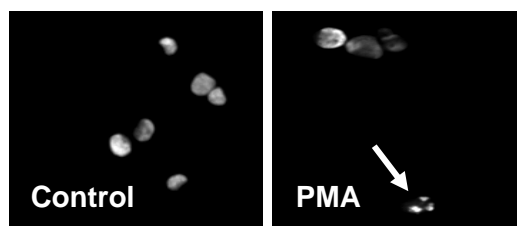
Figure II.1 Micrographs of LNCaP cells stained with DAPI. LNCaP cells treated with 100 nM PMA for 1 h undergo apoptosis as indicated with an arrow (*right panel*).

II.3.3 Generation of Conditioned medium (CM)

1.5×10^6 LNCaP cells were seeded in a tissue culture dish (100 mm) (secretor cells) and 2×10^5 cells in a 6-well plate (receptor cells). Two days later secretor cells were washed and medium prepared with agent, *i.e.* PMA or bryostatin 1 was added to the cells for 60 min. Then, cells were washed twice with RPMI 1640 medium to remove residual compounds and 7 ml of medium were added to the cells. Receptor cells were washed with RPMI-1640 and 2 ml of fresh medium were added. After 24 h, the conditioned medium generated by the secretor cells was collected in 15 ml conical tubes or in 1.5 ml eppendorf tubes and centrifuged at 1,000 rpm for 5 min at 4°C or 4,000 rpm for 5 min at 4°C, respectively. The supernatant was filtered through a 13-mm syringe filter (0.45 μm pore size) and the medium of the receptor cells was replaced with 1 ml CM. LNCaP cells were ~70% confluent at the time they were treated with CM. Receptor cells were collected 24 h later for evaluation of apoptosis as described in section 3.2. For experiments using a TNFα rescue approach, TNFα was added to CM to achieve final concentrations of 0.1, 1.0 and 10 ng/ml.

II.3.4 Treatment of LNCaP cells with etoposide

LNCaP cells were serum starved (RPMI 1640 without FBS) and 48 h later treated with 400 µM etoposide. Cells were harvested (see section 8.1) and RNA was isolated 5 h after treatment with the RNeasy Mini Kit (Qiagen Inc., Valencia, CA, USA) as described in section II.10.1 To assess the percentage of apoptosis cells were collected and stained with DAPI 48 h after treatment with etoposide.

II.3.5 Treatment of LNCaP cells with cycloheximide

Cycloheximide, an antibiotic produced by *Streptomyces griseus*, inhibits translation in eukaryotes by interfering with the binding and transfer of tRNA to and from the ribosome during protein synthesis [78]. 2×10^5 LNCaP cells were seeded in 6-well plates. Two days later cells were treated with 50 µM cycloheximide for 40 min, and then 100 nM PMA was added for 1 h. After extensive washing with medium, 50 µM cycloheximide were added again. After 24 h, cells were stained with DAPI and the percentage of apoptosis was assessed as described in section II.3.2.

II.4 Transfection

Transfection is the process of introducing nucleic acids into eukaryotic cells by nonviral methods. The negatively charged phosphate backbones of DNA or RNA are coated by chemicals like calcium phosphate, DEAE-dextran, or cationic lipid-based reagents. This leads to neutralization or a positive charge of the nucleic acids which makes it easier for the DNA/RNA-transfection-reagent-complex to cross the membrane. Especially lipids will fuse more easily with the lipid bilayer. By contrast, physical transfection methods like microinjection or electroporation create little pores in the plasma membrane and the DNA is introduced directly into the cell [79].

II.4.1 Transfection by electroporation

Product	Company
Amaxa® Nucleofector® Device	Lonza, Walkersville, MD, USA
Nucleofector® Kit R	Lonza

Table II.4 Transfection devices.

Plasmid DNA or siRNA were introduced into LNCaP cells by electroporation using the Amaxa Nucleofector®. Here, an electrical pulse perturbs the cell membrane and forms transient pores that allow the passage of nucleic acids into the cell [80].

LNCaP cells were cultured 2-3 days before the nucleofection and cultured as described above until they reached a confluency of 70-80%. The Nucleofector® solution R was prepared as described in Table II.5. One to five µg of DNA were mixed with 100 µl of Nucleofector® solution R. Cells were trypsinized and counted. For each transfection 2×10^6 cells were transferred into a 15 ml conical tube and centrifuged (1,000 rpm, 4°C, 5 min). The supernatant was discarded and the cell pellet resuspended in 100 µl of DNA containing Nucleofector® solution R (room temperature). One nucleofection® sample contained:

2×10^6 cells

1-5 µg plasmid DNA

100 µl Nucleofector® solution R

The nucleofection sample was transferred into an Amaxa certified cuvette. For LNCaP cells the Nucleofector® program T-009 was used. To avoid damage of the cells the sample was removed from the cuvette immediately after the program had finished. Five hundred µl of pre-warmed complete RPMI 1640 medium were

added to the cuvette. The sample was transferred to a 15 ml conical tube containing pre-warmed complete RPMI 1640 medium using the plastic pipette provided in the Nucleofector® Kit R. The appropriate volume to obtain a cell number of 3×10^5/ 6-well was transferred into a 6-well plate.

The transfected cells were incubated at 37°C in a humidified 5% CO_2 atmosphere for 24 to 48 h depending on the plasmid and experiment.

Nucleofector® solution R (4°C)	
Nucleofector® solution	2.25 ml
Supplement I	0.5 ml

Table II.5 Composition of Nucleofector® solution R.

II.5 Immunofluorescence and confocal microscopy

Product	Company
Fisherbrand Microscope Cover Glass	Thermo Fisher Scientific
Anti-Myc Tag (rabbit polyclonal IgG)	Upstate (Millipore), Billerica, MA, USA
Alexa-Fluor 488 goat anti-rabbit IgG	Invitrogen

Table II.6 Additional materials for immunofluorescence and confocal microscopy.

For localization studies of GFP-fused PKCs, 2×10^6 LNCaP cells were transfected with 2 μg of pEGFP-N1-PKCα, pEGFP-N1-PKCδ or pEGFP-N1-PKCε [81, 82] as described in section II.4.1. 10^5 cells were plated on sterile round cover-slides in 12-well plates. After 48 h cells were stimulated for 20 min with 100 nM PMA, 100 nM bryostatin 1, or 100 nM PMA/100 nM bryostatin 1. Cells were then washed with

PBS and fixed with pre-cooled methanol (-20 $^{\circ}$C) for 10 min at -20°C. Samples were stained with DAPI (1 µg/ml) for 10 min at 4°C, mounted on a glass slide, and visualized with a Zeiss LSM510 META NLO laser scanning confocal microscope.

In a different set of experiments, cells were transfected with plasmids encoding myc-tagged PKCs generated (see section II.8 for details). Twenty-four h post-transfection, cells of one 12-well were fixed in 1 ml of pre-cooled methanol (-20 $^{\circ}$C) for 10 min at -20°C. After blocking with 500 µl of 5% BSA/PBS for 1 h at room temperature cells were incubated with a rabbit polyclonal anti-myc antibody (Millipore) for 1 h at room temperature in 5% BSA/PBS (1:500). Following wash steps (3 x 5 min PBS on an orbital shaker), samples were probed with a secondary Alexa Fluor 488 coupled anti-rabbit antibody (Invitrogen) for 1 h at room temperature (1:2000). Finally, slides were washed, counterstained with DAPI (1 µg/ml) for 10 min at 4°C, and visualized by confocal microscopy.

II.6 Measurement of cytokines in the CM

Enzyme-linked Immunosorbent Assay (ELISA) is a highly sensitive technique for detecting and measuring antigens in a solution. The solution is run over a surface to which immobilized antibodies (capture antibodies) specific to the antigen have been attached. If the antigen is present it will bind to the immobilized antibody layer. Next, the enzyme linked antibodies (detection antibodies) are added and will bind specifically to a different epitope of the same antigen. The enzyme converts a chemical into a color, fluorescent, or electrochemical signal to detect the presence of the antigen. The absorbance, fluorescence, or electrochemical signal is proportional to the concentration of the antigen.

II.6.1 ELISA for humhan TNFα (Sandwich ELISA)

Product	Company
Human TNFα-ELISA Development Kit	Peprotech, Rocky Hill, NJ, USA
ELISA microplates	Nunc MaxiSorb, Rochester, NY, USA
Tween-20	Sigma, St.Louis, MO, USA
BSA	Sigma
ABTS Liquid Substrate Solution	Sigma
Phosphate Buffered Saline (PBS) pH 7.4	Invitrogen

Table II.7 Materials for ELISA.

ELISA components

Capture antibody	Antigen-affinity purified rabbit anti-hTNFα
Detection antibody	Biotinylated antigen-affinity purified rabbit anti-hTNFα
Human TNFα standard	Recombinant hTNFα
Avidin-HRP conjugate	

Table II.8 Components of ELISA. The components were reconstituted as instructed by the manufacturer, aliquoted, and stored at -20°C.

To determine TNFα levels in CM, 2×10^5 cells were plated in a 6-well plate and treated 48 h later cells with bryostatin 1 +/- PMA for 60 min. After 60 min cells were washed and 1 ml of fresh RPMI 1640 medium was added for 24 h. The CM was collected in microcentrifuge tubes and centrifuged at 4,000 rpm (4°C, 5 min) and either used immediately for ELISA or stored at -80°C.

The 96-well ELISA plate was prepared by adding 100 μl of capture antibody (1 μg/ml in PBS) to each well. The plate was sealed with parafilm and incubated on

an orbital shaker overnight at 4°C. The following day the plate was washed 4 times with 300 µl of wash buffer (0.05% Tween-20/PBS). After the last wash the plate was inverted to remove residual buffer and blotted on a paper towel. To minimize any non-specific binding sites, plates were incubated for 1 h at room temperature with 300 µl of blocking buffer.

Different dilutions of the recombinant hTNFα standard were added immediately to each well in triplicate and incubated on an orbital shaker at room temperature for 2 h to allow for binding of TNFα to the capture antibody. Afterwards, the plate was washed as described above, 100 µl of the biotinylated detection antibody (0.5 µg/ml) were added, and incubated at room temperature for 2 h. Once more the ELISA plate was washed and incubated with 100 µl of avidin-HRP conjugate (1:2000 in diluent) for 30 min at room temperature. The plate was washed again. One hundred µl of a room temperature aliquot of ABTS liquid substrate solution was added to each well. After 20 min the color development was measured with the Emax precision microplate reader at 405 nm. The data analysis was conducted with the software SoftMax® Pro (both Molecular Devices, Sunnyvale, CA, USA).

Solutions for ELISA	
PBS	
Wash buffer	0.05% Tween-20 in PBS
Block buffer	1% BSA in PBS
Diluent	0.05% Tween-20, 0.1% BSA in PBS

Table II.9 Solutions for ELISA experiment.

II.6.2 RayBio® Human Cytokine Antibody Array

To detect different cytokines simultaneously in CM the RayBio® Human Cytokine Array 5 (4) was used (RayBiotech, Inc., Norcross, GA, USA).

Membranes were blocked for 30 min with blocking buffer provided by the manufacturer. Afterwards, membranes were washed with provided wash buffers and subsequently incubated with 1 ml of CM generated from cells treated with either 10 nM bryostatin 1 or 100 nM PMA, alone or in combination or vehicle for 2 h. The membranes were washed again and each membrane was incubated with 1 ml of a solution with diluted biotin-conjugated antibodies for 90 min. After subsequent washing, the membranes were incubated for 2 h at room temperature with 2 ml of HRP-conjugated streptavidin. Finally, membranes were incubated for 2 min with the provided detection buffers (Fig. II.2). The signal was detected by enhanced chemiluminescence using the LAS-3000 imaging system and Multi Gauge software (both Fujifilm, Edison, NJ, USA). Exposure time was 40 sec. Every step of the protocol was performed at room temperature.
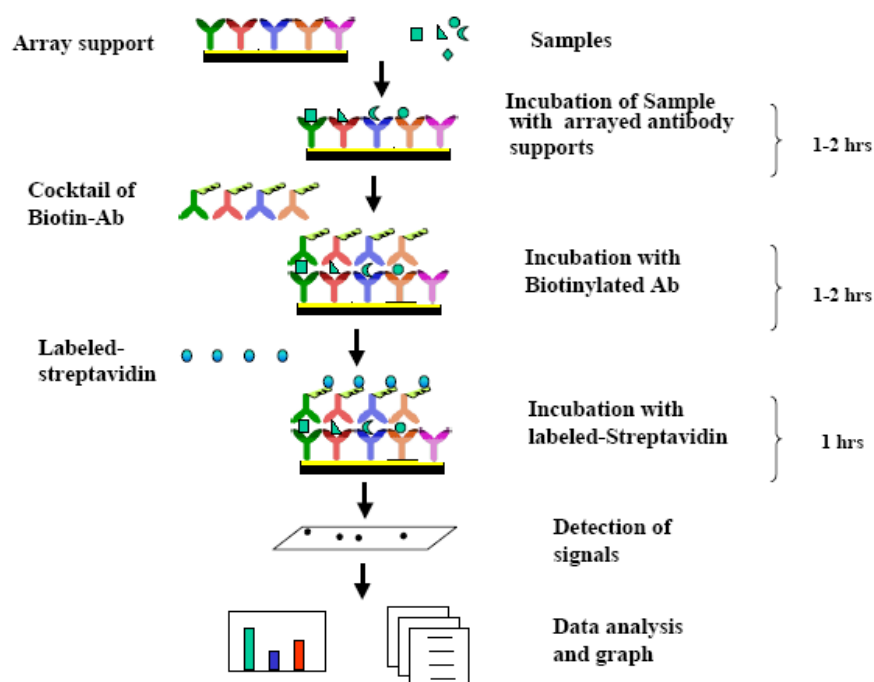
Figure II.2 RayBio® Human Cytokine Antibody Array Protocol (Ray Biotech, Inc.).

II.7 Western Blot Analysis

II.7.1 Isolation of proteins

Lysis buffer (4°C)

	Final concentration	Volume
HEPES 1 M	25 mM	2.5 ml
NaCl 5 M	150 mM	3.0 ml
NP40 10%	1%	10.0 ml
Sodium deoxycholate 10%	0.25%	2.5 ml
Glycerol	10%	10 ml
MgCl$_2$ 1 M	10 mM	1 ml
EDTA 0.5 M	1 mM	0.2 ml
dH$_2$O		to 100 ml

Table II.10 Composition of protein lysis buffer. Protease inhibitor (PI) (Sigma, St. Louis, MO) was added to the lysis buffer 1:500 right before use.

4x Sample buffer

	Final concentration	Volume
Tris HCl 0.5M, pH 6.8	250mM	5.0 ml
Glycerol	30%	3.0 ml
SDS	8%	0.8 g
-> 60°C to dissolve SDS		
Bromophenol blue 0.1%	0.001%	100 µl
dH$_2$O		to 10.0 ml

Table II.11 Composition of 4x Sample buffer. 2% β-mercaptoethanol were added before use.

2 x 10^5 LNCaP cells were seeded in 6-well plates. After treatment cells were carefully washed with 1 ml of PBS. PBS was at room temperature to avoid detachement of the cells. The plates were then transferred on ice and 100 µl of complete lysis buffer were added to each well. Cells were scraped off the well with a cell scraper and transferred to a 1.5 ml microcentrifuge tube, placed on ice and

incubated for 20 min. Subsequently, cells were centrifuged at 13,000 rpm (4°C for 10 min). The supernatant was transferred to new tubes and the protein concentration was determined by the Bradford method as described in section 7.2. Lysates were stored at -80°C or prepared for Western Blot as follows. Proteins were kept on ice, and 20 μg of protein were pipeted into a new tube. All samples were adjusted with protein lysis buffer containing protease inhibitor (PI) (Sigma) to the same volume. Subsequently, the appropriate volume of 4X sample buffer was added to achieve a final concentration of 1X sample buffer. The samples were then incubated in a 95°C water bath, and 20 μg of protein were subjected to SDS-PAGE.

II.7.2 Protein Quantification

The protein concentration was measured by the Bradford method [83]. To obtain a standard curve, Bovine Serum Albumin Standard (BSA, Pierce Biotechnology, Inc., Rockford, IL, USA) was used from 0 to 8 μg/ml. For protein quantification the Bio-Rad Protein Assay (Bio-Rad Laboratories, Hercules, CA, USA) solution was diluted 1:5 in dH$_2$O. Protein concentrations were assessed in standard disposable polystyrene cuvettes and measured in a SmartSpec Plus Spectrophotometer (Bio-Rad Laboratories) at 595 nm.

II.7.3 SDS-PAGE

Protein samples are separated by discontinuous denaturizing SDS-PAGE according to Laemmli [84]. The discontinuous electrophoresis system used here consists of two layers: the stacking gel, where the proteins are concentrated and the separating gel, where the proteins are separated according to the molecular size.

The compositions of the gels and buffers used for SDS-PAGE are shown in Tables II.12, II.13, II.14, II.15, and II.16.

Separating gel (10%)	
dH$_2$O	4 ml
1.5 M Tris HCl, pH 8.8	2.5 ml
10% SDS	100 µl
30% Acrylamide/Bis Solution	3.3 ml
APS 10%	100 µl
TEMED	4 µl

Table II.12 Working solution for separating gel 10%.

Stacking gel	
dH$_2$O	6 ml
0.5 M Tris HCl, pH 8.8	2.5 ml
10% SDS	100 µl
30% Acrylamide/Bis Solution	1.3 ml
APS 10%	50 µl
TEMED	4 µl

Table II.13 Working solution for stacking gel 3.9%.

Electrophoresis buffer (1X)	
Tris-Glycine (10X)	100 ml
SDS 10%	10 ml
dH$_2$O	to 1 l

Table II.14 Working solution for electrophoresis

Tris-Glycine (10X)	
Tris Base	30 g
Glycine	144 g
dH$_2$O	to 1 l

Table II.15 Tris-glycine stock solution (10X).

Proteins	Acrylamide concentration
PKCα	7.5 or 10%
PKCδ	7.5 or 10%
PKCϵ	7.5 or 10%
Akt	10%
phospho-Akt (Ser473)	10%
P44/42 MAP Kinase	10%
phospho-p44/42 MAP Kinase (Thr202/Tyr204)	10%
SAPK/JNK	10%
phospho-SAPK/JNK (Thr183/Tyr185)	10%
P38 MAP Kinase	10%
phospho-p38 MAP Kinase (Thr180/Tyr182)	10%
p21[Cip1]	12%

Table II.16 Acrylamide concentrations in the separating gel. The concentration varies according to the analyzed protein

To determine the molecular weight of the proteins, samples were compared to a prestained low range molecular weight marker (SDS-PAGE Standard, Bio-Rad Laboratories, Hercules, CA, USA). Electrophoresis was performed using a vertical Mini-PROTEAN Tetra Cell (Bio-Rad Laboratories, Hercules, CA, USA) connected to a power supply (Bio-Rad Laboratories, Hercules, CA, USA).

Electrophoresis was run at 60 V until the proteins started separating in the separation gel. When the marker dye had entered the separation gel the current was set at 110 V until completion of the electrophoretic separation.

II.7.4 Western Blotting and detection

After the electrophoresis, proteins were transferred from the gel onto a polyvinylidenflouride (PVDF) blotting membrane. The membrane was activated by soaking in methanol for 30 sec. Subsequently, the activated membrane was soaked

in 1X transfer buffer together with the blotting pads, Whatman paper, and the gel. These transfer supplies were assembled in transfer sandwiches in the order described below (Table II.17 and II.18).

Sandwich holder anode side
wetted pad
Whatman paper
Membrane
Gel
Whatman paper
wetted pad
Sandwich holder cathode side

Table II.17 Setup of transfer sandwich.

Transfer buffer 1x (4°C)	
Tris-Glycine (10x)	100 ml
Methanol	200 ml
dH$_2$O	to 1 l

Table II.18 Components of transfer buffer (1X).

Transfer sandwíches were transferred into the Western blot tank (Bio-Rad Laboratories) containing Transfer buffer 1X. The transfer was conducted at 100 V for 1 h at 4°C or at 30 V overnight at 4°C.

Afterwards, PVDF membranes were stained with Ponceau S (Sigma) for 5 sec to verify the efficieny of the transfer and equal loading, washed with dH$_2$O and blocked with 5% skim milk/TBS-T 0.1% for 1 h at room temperature. Membranes were shortly washed 3 times for 5 min with TBS-T 0.1% and incubated with primary antibody at 4°C over night (see Table II.20 for primary antibodies and dilutions). All primary antibodies were diluted in 5% BSA/TBS-T 0.1%.

The following day, membranes were washed 3 times for 5 min with 5% TBS-T 0.1% and incubated for 1 h with either anti-mouse or anti-rabbit secondary antibodies

conjugated to horseradish peroxidase (1:5000 in 5% skim milk/TBS-T 0.1%, Bio-Rad) (see Table II.21 for secondary antibodies and dilutions). Subsequently, the membrane was washed 3 times for 10 min with TBS-T 0.1%. Bands were visualized by enhanced chemiluminescence using the LAS-3000 imaging system and Multi Gauge software (both Fujifilm, Edison, NJ).

Ponceau S solution		
Ponceau S	0.2%	0.2 g
glacial acetic acid	3%	3 g
dH$_2$0		to 100 ml

Table II.19 Composition of Ponceau S solution.

primary antibody	isotype	dilution	Company
PKCα, clone M4	mouse IgG$_1$	1:1000	Upstate (Millipore),
PKCδ	rabbit IgG	1:1000	Cell Signaling Technology; Danvers, MA, USA
PKCϵ	rabbit IgG	1:500	Santa Cruz Biotechnology, Santa Cruz, CA, USA
Akt	rabbit IgG	1:1000	Cell Signaling Technology
phospho-Akt (Ser473)	rabbit IgG	1:1000	Cell Signaling Technology
p44/42 MAP Kinase	rabbit IgG	1:1000	Cell Signaling Technology
phospho-p44/42 MAP Kinase (Thr202/Tyr204)	rabbit IgG	1:1000	Cell Signaling Technology
SAPK/JNK	rabbit IgG	1:1000	Cell Signaling Technology
phospho-SAPK/JNK (Thr183/Tyr185)	rabbit IgG	1:1000	Cell Signaling Technology
p38 MAP Kinase	rabbit IgG	1:1000	Cell Signaling Technology
phospho-p38 MAP Kinase (Thr180/Tyr182)	rabbit IgG	1:1000	Cell Signaling Technology
p21^{Cip1}	mouse IgG$_{2a}$	1:1000	Cell Signaling Technology
β-actin, clone AC-15	mouse IgG$_1$	1:40000	Sigma, St. Louis, MO, USA
vinculin, clone hVIN-1	mouse IgG$_1$	1:5000	Sigma, St. Louis, MO, USA

Table II.20 Primary antibodies for Western Blot.

secondary antibody	dilution	Company
goat anti-mouse IgG (H+L)-HRP conjugate	1:5000	Bio-Rad Laboratories
goat anti-rabbit IgG (H+L)-HRP conjugate	1:5000	Bio-Rad Laboratories

Table II.21 **Secondary antibodies for Western Blot.**

II.8. Generation of myristoylated PKCδ constructs

II.8.1 Cloning of myristoylated PKCδ constructs

To investigate the effects of targeting PKCδ to the plasma membrane, an NH2-terminal in-frame insertion of a myristoylation signal sequence was added as it has been described for PKCα [85]. Myristate, a 14-carbon saturated fatty acid, is covalently attached to the N-terminal glycine by the enzyme N-myristoyltransferase, usually during translation. To discriminate between endogenously and exogenously expressed PKCδ and to determine transfection efficiencies and also successful membrane localization of MyrPKCδ by immunofluorescence, a sequence coding for the myc tag was added. To obtain the desired insert, PKCδ was amplified from pShooter PKCδ (a generous gift from Dr. Chaya Brodie, Henry Ford Hospital) and flanked with 5'-*XbaI* and 3'-*EcoRI* restriction sites. Primers used for amplification were as follows (*restriction sites*):

Forward primer (FW): 5'- CCAAG*TCTAGA*GCACCCTTCCTTCGCATCTCCTT -3'

Reverse primer (RV): 5'- TCCAA*GAATTC*CTATGCGGCCCCATTCAGATCC -3'

Since the resulting product will be used for cloning and subsequent protein expression from the resulting plasmid, it is desirable to minimize errors during replication. This can be achieved by using a proofreading enzyme, the *Pfx* Platinum Taq polymerase (Invitrogen, Carlsbad, CA). The PCR reaction was set up as follows:

PCR reaction mix	
10x PCR buffer	5 µl
dNTP (2.5 mM each)	4 µl
MgSO$_4$ (50 mM)	1 µl
FW primer (10 mM)	2.5 µl
RV primer (10 mM)	2.5 µl
H$_2$O	33 µl
Template	1 µl
Platinum® *Pfx* polymerase	1 µl

Table II.22 Components for PCR reaction buffer.

The reaction tube was then briefly mixed by gently tapping, spun down, and placed into a thermocycler. The following conditions were used for amplification:

PCR reaction		
96°C	5 min	
96°C	45 s	
61°C	1 min	25 cycles
68°C	3 min	
68°C	10 min	

Table II.23 Conditions for PCR reaction.

One fifth of the reaction was run on a 1% agarose gel in Tris-Acetate-EDTA (TAE) buffer and DNA was stained with ethidium bromide and visualized with a BioRad Gel Doc system to verify the expected insert size of 2.1 kb (Figure II.3).
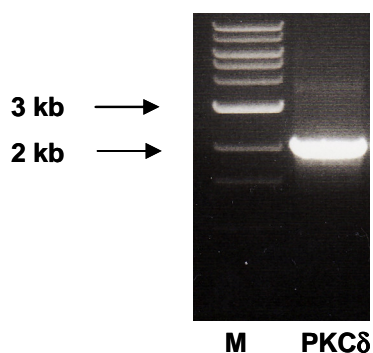
Figure II.3 PCR amplification of PKCδ. The coding sequence of PKCδ was amplified from the plasmid template and restriction sites were attached. Successful amplification is demonstrated by DNA agarose gel, and DNA was visualized with ethidium bromide. M = marker

In the next step, both PCR product and target vector were prepared. To this end, pCMV6-MyrPKCα (generous gift from Dr. Alex Toker, Harvard Medical School), was obtained (Figure II.4).
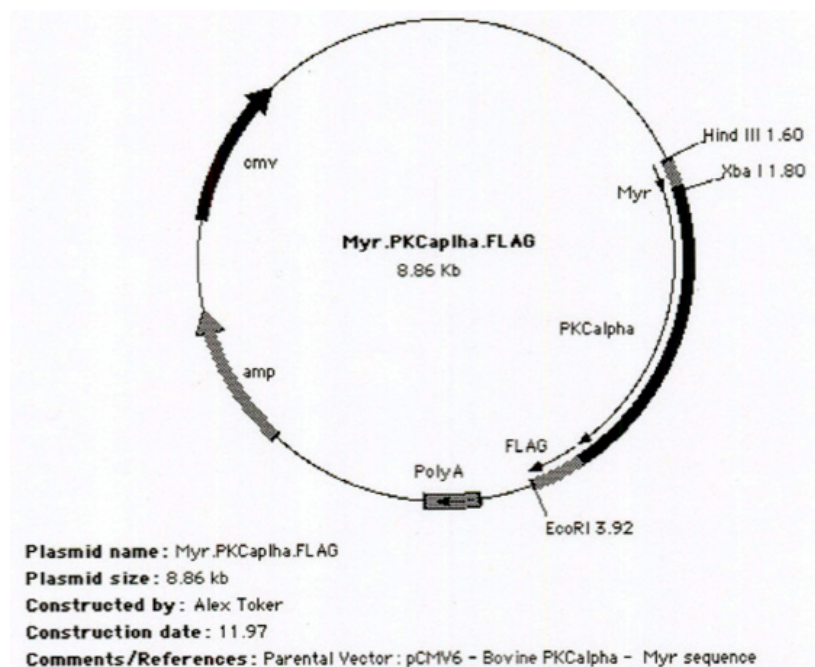

Plasmid name: Myr.PKCaplha.FLAG
Plasmid size: 8.86 kb
Constructed by: Alex Toker
Construction date: 11.97
Comments/References: Parental Vector: pCMV6 – Bovine PKCalpha – Myr sequence

Figure II.4 Vector Map of MyrPKCα.

The PCR product was purified using the QiaQuick PCR Purification Kit (Qiagen, Valencia, CA), and both the purified PCR product and pCMV6-MyrPKCα were digested with *EcoRI* and *XbaI* (New England Biolabs, Ipswich, MA) for 2 h at 37°C. The restriction digestion had the following effects: First, PKCα was removed from the pCMV6 plasmid while the myr sequence was retained. Second, digestion of the PKCδ PCR product and the vector created compatible ends that facilitate directional insertion of PKCδ. Following digestion, PCR fragment and vector were first visualized on a 1% agarose gel in TAE buffer (Figure II.5) and then gel-purified prior to ligation using the QiaQuick Gel purification Kit (Qiagen).
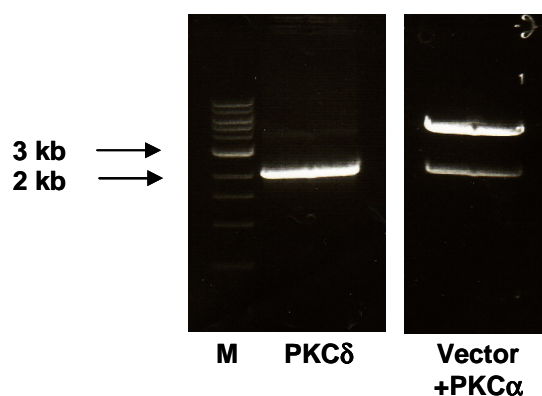
Figure II.5 Gel purification of digested DNA. DNA was loaded on an ethidium bromide containing 1% agarose gel and run at 110 V for 60 min. *Left panel.* PKCδ PCR. *Right panel.* Successful removal of PKCα coding sequence from MyrPKCα. M = marker

Ligation was carried out in a 5:1 ratio of PCR-product:vector, using 50 ng of vector DNA and 78 ng of the PCR product. The formula used to calculate the required amount of PCR product when using 50 ng of vector DNA is

X ng PCR-DNA = 50 ng vector DNA * n(bp PCR-DNA)/n(bp vector DNA)

For ligation of the PCR product and vector, the T4 ligase (New England Biolabs) was used in the presence of an ATP containing buffer in a total reaction volume of 20 µl at 16°C for 4 h and additional 30 min at room temperature. As a control for digestion efficiency, an additional tube was set up under identical conditions except that the PCR-product had been replaced with sterile water.

From the experimental agar plate containing putative Myr PKCδ positive clones, eight colonies were picked and cultured for mini preparations (see section II.8.2). Between 2 and 4 µg plasmid were used for restriction analysis using *XbaI* and *EcoRI* as described above and analyzed on a 1% agarose gel (Figure II.6).
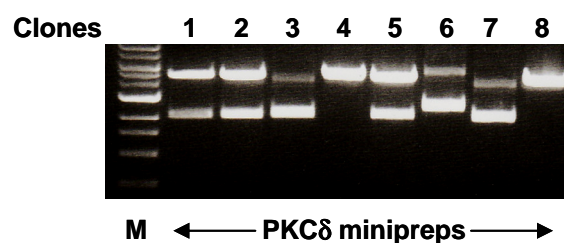
Figure II.6 Digestion of PKCδ minipreps. After digestion with *XbaI* and *EcoRI*, only a subset of preparations show the correct pattern (clones 1, 2, and 5). DNA was run on a 1% agarose gel for 45 min at 110 V and stained with ethidium bromide. M = marker

From these, clones number 1, 2 and 5 were sequenced at the DNA sequencing facility of the Department of Genetics of the University of Pennsylvania (http://www.med.upenn.edu/dnaseq/). The primer used for sequencing anneals within the CMV promoter and has the sequence 5´-CGCAAATGGGCGGTAGGCGTG-3´. All three clones were identified to harbor the desired insert in the correct orientation. Clone #1 was then grown in a 250 ml LB/ampicillin culture and DNA was isolated using the EndoFree Plasmid Maxi Kit (see section II.8.2).

II.8.2 Transformation

The following reagents were used:

Product	Company
LB Broth, Lennox, powder	Thermo Fisher Scientific Inc.
One Shot® TOP10F´ Chemically Competent *E. coli*	Invitrogen
S.O.C. medium	Invitrogen
Agar plates Ampicillin (50 μg/ml)	Cell Center Service Facility of the University of Pennsylvania
14 ml round bottom tubes	BD Biosciences
EndoFree Plasmid Maxi Kit	Qiagen Inc., Valencia, CA, USA
QIAprep Spin Miniprep Kit	Qiagen Inc.

Table II.24 Materials for plasmid transformation.

Day 1: One Shot® TOP10F´ Chemically Competent *E. coli* were thawed on ice. For each transformation 25 μl of competent bacteria were used. 10 ng of plasmid (~ 2 μl) were added to the bacteria and incubated for 30 min on ice. Tubes containing competent bacteria and plasmid were placed in a 42°C waterbath for 30 sec (heat shock). Bacteria were placed back immediately on ice for 5 min and incubated in 1 ml of S.O.C. medium for 1 h. After the incubation, 100 μl of the bacteria suspension were evenly spread out on the agar plate with ampicillin and incubated at 37°C overnight.

Day 2: LB medium containing 50 μg/ml of antibiotic was prepared.

a) Two colonies (clones) per transformation were picked and transferred into separate tubes containing 3 ml of LB/antibiotic, followed by incubation for

6-7 h (250 rpm, 37°C) (pre-culture). Then, 400 µl of the pre-culture were incubated over night in 200 ml LB/antibiotic (250 rpm, 37°C). In parallel, a bacteria glycerol stock of each colony was prepared. Therefore, the pre-culture was mixed with autoclaved glycerol/LB 50% in a ratio 1:1 and stored at -80°C.

b) Two or more colonies per transformation were picked and transferred into separate tubes containing 4 ml of LB/antibiotic and grown by shaking overnight (250 rpm, 37°C).

Day 3: a) Bacteria were centrifuged at 4,000 rpm for 1 h at 4°C. The bacteria pellet was either stored at -20°C or directly subjected to purification with the EndoFree Plasmid Maxi Kit to obtain endotoxin-free plasmid DNA or *b)* bacteria were centrifuged at 4,000 rpm for 15 min at 4°C and purified with the QIAprep Spin Miniprep Kit.

The EndoFree Plasmid Maxi Kit and QIAprep Spin Miniprep Kit (both Qiagen) were used according to the manual provided by the manufacturer.

LB medium	
LB Broth, Lennox, powder	20 g
dH$_2$O	to 1000 ml

Table II.25 Components for LB medium.

II.9 RNA interference (RNAi)

Double-stranded RNA (dsRNA) is an important regulator of gene expression in many eukaryotes. It triggers different types of gene silencing that are collectively referred to as RNA silencing or RNA interference (RNAi). RNAi is widely used as an experimental approach to silence the expression of proteins in cells. This method utilizes short dsRNAs, which guide sequence-specific degradation of complementary

or near-complementary target mRNAs by specific and distinct mechanisms [86]. Here, RNAi was used to deplete individual PKC isozymes from prostate cancer cells.

II.9.1 siRNAs for experimental gene silencing

The Silencer Negative Control siRNA#1 (AM4615) and Negative Control siRNA#2 (AM4644) were obtained from Applied Biosystems/Ambion Inc. (Austin, TX, USA). One hundred μl of 50 μM siRNA were diluted with 150 μl of storage buffer 1X to obtain a concentration of 20 μM.

The siRNAs listed in Table II.26 and II.27 were purchased from Dharmacon Inc., now Thermo Fisher Scientific Inc.. The vial containing the siRNA as a powder was shortly centrifuged, reconstituted in storage buffer 1x to obtain a concentration of 20 μM, mixed on an orbital shaker for 20 min at room temperature, and again shortly centrifuged. All siRNAs were aliquoted and stored at -20°C.

Product	Target sequences of siRNA	Used concentration
PKCα #1	CCAUCCGCUCCACACUAAA	120 pmol
PKCα #2	GAACAACAAGGAAUGACUU	120 pmol
PKCδ #1	CCAUGAGUUUAUCGCCACC	120 pmol
PKCδ #2	CAGCACAGAGCGUGGGAAA	120 pmol
PKCϵ #1 (ON-TARGETplus)	GUGGAGACCUCAUGUUUCA	120 pmol
PKCϵ #2 (ON-TARGETplus)	GACGUGGACUGCACAAUGA	120 pmol
BCL2A1 #1	GCAGUGCGUCCUACAGAUA	240 pmol
BCL2A1 #2	UAUCUCUCCUGAAGCAAUA	240 pmol
FOSL1 #1	GCUCAUCGCAAGAGUAGCA	240 pmol
FOSL1 #2	GAGCUGCAGUGGAUGGUAC	240 pmol

Table II.26 dsRNAi target sequences.

For the following genes an ON-TARGETplus SMARTpool was used:

Gene	Catalog number
Human FOSL1	L-004341-00
Human BCL2A1	L-003306-00
Human SERPINB2	L-010859-00
Human TRAF1	L-017438-00

Table II.27 ON-TARGETplus SMARTpool siRNAs for four selected genes.

dsRNAs were transfected into LNCaP cells using the Amaxa$^{®}$ Nucleofector$^{®}$ as described in section II.4.1. Briefly, 2×10^6 cells were nucleofected with 120 or 240 pmol of siRNA in 100 µl Nucleofector$^{®}$ solution R using the program T-009. Experiments were carried out 12 or 48 h post-transfection.

II.10 RNA isolation

II.10.1 RNA isolation with the Qiagen RNeasy Mini Kit

For RNA isolation 2×10^5 cells/6-well were plated or cells were transfected with siRNA as described in II.9.1. Experiments were carried out 12 or 48 h later and RNA was isolated by means of the Qiagen RNeasy Mini Kit (Qiagen) according to the manufacturer's instructions.

II.10.2 RNA isolation for microarray

For microarray applications TRIzol® Reagent (Invitrogen) and the Qiagen RNeasy Mini Kit were combined. This method adds the tissue disruption and extraction power of TRIzol® to the purification and yield of RNeasy columns, while avoiding RNA precipitation.

Homogenization and phase separation were conducted as described in the instructions for the use of TRIzol® (Invitrogen). Cells in 6-well plates were homogenized using 1 ml of TRIzol®. To separate the phases 200 µl of chloroform were added to each sample, incubated for 1 min at room temperature and vigorously shaken for 15 sec. Another incubation step of 2-3 min followed. Samples were centrifuged (12,000 x g, 4°C, 15 min). Subsequently, 250 µl of the colorless upper aqueous phase containing the RNA were transferred into a new tube and an equal volume of 70% ethanol was added. All following purification steps were performed as described in the Qiagen RNeasy instructions, including DNase digestion. RNA was eluted in 50 µl of RNase-free water. One µl of Superase-In (Applied Biosystems/Ambion) per 50 µl RNA elution was added and briefly mixed. RNA samples were stored at -80°C.

II.11 cDNA synthesis

In vitro complementary DNA or copy DNA (cDNA) is synthesized from RNA molecules in a reaction called reverse transcription (RT) using the enzyme reverse transcriptase. As there is no amplification involved, the number of cDNA molecules corresponds to the mRNA expression level for any given gene in a particular cell type or setting, *i.e.* treatment *vs.* control (see section II.13).

The Reverse Transcription Reagent Master Mix (Applied Biosystems, Branchburg, NJ, USA) was prepared as shown in Table II.28. One µg of RNA and 30.75 µl of the prepared Master Mix per sample were used. To adjust the volume to 50 µl nuclease-free H_2O (Genemate ISC Bioexpress) was used.

compound	final concentration	μl per reactions 10 reactions	add
10 x TaqMan® RT Buffer	1X	50	first
MgCl$_2$ (25 mM)	5.5 mM	110	
dNTP-Mix	500 μM each	100	
Random hexamers	2.5 μM	25	
RNase Inhibitor	0.4 U/μl	10	then
Multiscribe RT (50 U/μl)	1.25 U/μl	12.59	

Table II.28 Composition of the Reverse Transcription Master Mix.

In the following order compounds were pipetted:

Nuclease-free H$_2$O	To 50 μl
Master Mix	30.75 μg
RNA	1 μg

Once the samples have been mixed and briefly centrifuged, the RNA was transcribed into cDNA using the following conditions in a MJ Research PTC-100 Peltier Thermal Cycler (GMI Inc., Ramsey, MN, USA):

25°C	10 min
48°C	60 min
95°C	5 min

II.12 Reverse transcriptase real-time PCR

II.12.1 Experimental conditions

Real-time PCR or quantitative PCR (qPCR) is a variation of the standard PCR used to quantify DNA in a sample. Additionally, the relative expression of a particular mRNA sequence can be determined. This technique compares the expression between different genes or one particular gene expressed under different conditions

(*i.e.* treatment *vs.* control) relative to a specific housekeeping gene which in this study was 18S rRNAs (ribosomal RNAs).

The amount of amplified product is measured at each cycle of the PCR, and PCR products from genes with higher expressions appear after fewer PCR cycles. To quantify the amplified product fluorescent probes are necessary. The used TaqMan® Gene Expression Assays (Applied Biosystem) are probes which all have a FAM™ reporter dye at the 5' end of the TaqMan® MGB probe and a non-fluorescent quencher at the 3' end of the probe. These probes hybridize to an internal region of a PCR product. In the unhybridized state, the proximity of the fluor and the quench molecules prevents the detection of fluorescent signal from the probe. During PCR, when the polymerase replicates a template on which a TaqMan® probe is bound, the 5'-nuclease activity of the polymerase cleaves the probe. This decouples the fluorescent and quenching dyes. Thus, fluorescence increases in each cycle, proportional to the amount of probe cleavage.

In order to measure fluorescence while the temperature changes due to the PCR conditions (see Table II.29) we used the 7300 Real-Time PCR System (Applied Biosystems). The data were analyzed using the 7300 System Software (Applied Biosystems).

Stage 1	50°C, 2 min	Repetitions: 1
Stage 2	95°C, 10 min	Repetitions: 1
Stage 3	95°C, 15 sec	Repetitions: 40
	60°C, 1 min	

The sample volume was 20 μl.

Data were collected at stage 3, step 2 (60°C,1 min).

II.12.2 Quantification with the 2$^{-\Delta\Delta Ct}$ method (comparative C$_t$ method)

To quantify the results obtained by RT-PCR a comparative C$_t$ threshold method was used. Here, the C$_t$ values of the samples of interest and the control sample were normalized to the housekeeping gene 18S rRNAs and compared to each other. This 2$^{-\Delta\Delta Ct}$ method or comparative C$_t$ method is defined as follows:

$$2^{-\Delta\Delta Ct} = 2^{(\Delta Ct\ sample\ -\ \Delta Ct\ reference)}$$

$\Delta C_{t\ sample}$:   C$_t$ value for any sample normalized to 18S rRNAs

$\Delta C_{t\ reference}$:   C$_t$ value for the control normalized to 18S rRNAs

II.12.3 Materials and primers for RT-PCR using TaqMan®

Materials and TaqMan® Gene Expression Assays were obtained from Applied Biosystem, Foster City, CA, USA.

RT-PCR
7300 Real-Time PCR System
Software: 7300 System Software
MicroAmp® Optical Adhesive Film
MicroAmp® Optical 96-Well Reaction Plate with Barcode

Table II.29 Materials and equipment for RT-PCR.

probe	reporter dye at the 5' end
Eukaryotic 18S rRNA Endogenous Control	VIC™ dye - MGB
BCL2A1 (Hs00187845_m1)	FAM™ dye-MGB
FOSL1 (Hs00759776_s1)	FAM™ dye-MGB
TRAF1 (Hs00194639_m1)	FAM™ dye-MGB
SERPINB2 (Hs00234032_m1)	FAM™ dye-MGB
PPP1R15A (Hs00169585_m1)	FAM™ dye-MGB

Table II.30 TaqMan® Gene Expression Assays.

II.13 DNA Microarray and Analysis of Array Data

Two experiments were performed, using the Affymetrix GeneChip® Human Genome U133A 2.0 Array (Affymetrix Inc., Santa Clara CA, USA), which represents the expression level of 18,400 transcripts and variants, including 14,500 well-characterized human genes. Microarray services were provided by the Penn Microarray Facility, including quality control tests of the total RNA samples by Agilent Bioanalyzer and Nanodrop spectrophotometry. All protocols were conducted as described in the NuGEN Ovation manual and the Affymetrix GeneChip Expression Analysis Technical Manual. Briefly, 100 ng of total RNA was converted to first-strand cDNA using reverse transcriptase primed by a poly(T) oligomer that incorporated a synthetic RNA sequence. Second-strand cDNA synthesis was followed by ribo-SPIA (Single Primer Isothermal Amplification, NuGEN Technologies Inc., San Carlo, CA, USA) for linear amplification of each transcript. The resulting cDNA was transcribed into cRNA, which was also labeled with biotin during this process. Biotinylated cRNA was subsequently fragmented and assessed by Bioanalyzer. Then, 3.75 µg of the fragmented and labeled cRNA were added to Affymetrix hybridization cocktails, heated at 99ºC for 2 min and hybridized for 16 h at 45ºC to GeneChip® Human Genome U133A 2.0 Array. The microarrays were then washed at low (6X SSPE) and high (100 mM MES, 0.1 M NaCl) stringency and stained with streptavidin-phycoerythrin. Fluorescence was amplified by adding biotinylated anti-streptavidin and an additional aliquot of streptavidin-phycoerythrin stain. A confocal scanner was used to collect the fluorescence signal after excitation at 570 nm.

The first experiment that was carried out addressed the expression of genes at different time points after treatment with the phorbol ester PMA (100 nM). Cells were treated in triplicates with either vehicle or PMA (1 h, 100 nM) and total RNA was isolated at different times post-treatment (0, 4, 8, 12 and 24 h). Vehicle (ethanol)-treated samples were collected at 24 h post-treatment. All samples (18 samples in total) were used for the experiment and hybridized to the array. CEL-files which

include the probe level data from the array were extracted from DTT-files. For background correction, normalization, and probe summarization the GCRMA algorithm (GeneChip Robust Multiarray Averaging) was applied to all 18 CEL-files. For this purpose, the program ArrayAssist Lite version 3.4 (Stratagene, LaJolla, CA) was used. In addition to the GCRMA signal we calculated Affymetrix absent (A), present (P) or marginal (M) MAS5 flags. Data were transferred to Spotfire (TIBCO, Palo Alto, CA) in order to filter and to visualize the data. Data were filtered retaining only those probe sets that were flagged as present in at least two of the 18 samples. For statistical analysis the flag-filtered data were evaluated using Partek Genomics Suite (Partek Inc., St Louis, MO). Log_2 ratios for each probe set in each condition were calculated versus ethanol (vehicle). A one-way ANOVA was used across the 6 conditions. Additionally, we calculated the five pairwise contrasts between each PMA-treated condition and the ethanol control. This yielded a p value for the Anova and a p value and log_2 ratio for each of the pairwise comparisons for all of the filtered probe sets. For these six p values the false discovery rate (FDR)-corrected p value was calculated according to the method of Benjamini and Hochberg [87, 88]. Additionally, the maximum of the absolute value of each of the log_2 ratios was calculated. Genes were considered for further evaluation if their FDR-corrected p values for the ANOVA were ≤ 0.001 and the maximum absolute value was at least 1 (± 2 fold in at least one of the five pairwise comparisons). These criteria yielded 4949 probe sets. The procedure is summarized in Fig. II.7.
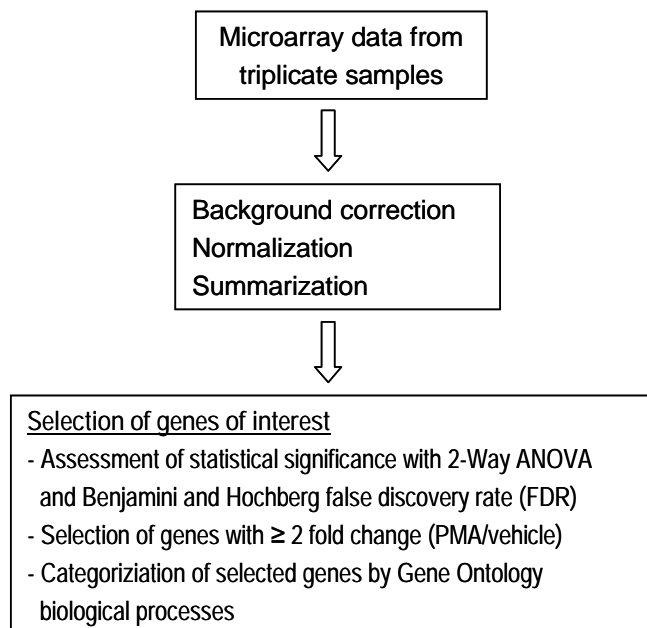
Fig. II.7 Gene expression analysis at a glance. Flow chart of data evaluation and selection criteria.

The second experiment that I carried out addresses PKC isoform-specific regulation of expression. Cells transfected separately with two different RNAi duplexes for either control or each of the PKC isoforms (PKCα, δ, ϵ) were treated with vehicle (1h, ethanol) or PMA (1 h, 100 nM), and total RNA was isolated 4 h post-treatment. Experiments were conducted in triplicates, resulting in a total of 48 samples. RNA from all 48 samples was prepared and subjected to microarray analysis. CEL files were background corrected, normalized, summarized and transformed as described above. A two-way ANOVA (treatment, RNAi) was calculated. Triplicate samples were averaged and a p value and a $\log_2$ ratio was calculated for each PKC RNAi relative to control RNAi, both for vehicle and PMA conditions. Only genes with a minimum induction by PMA of two fold were filtered ($\log_2$ ratio PMA vs. vehicle $\geq$ 1), yielding 2670 probe sets.

II.14 Validation of data by quantitative RT-PCR

Fold changes were referred to samples transfected with control siRNA and treated with vehicle. GCRMA values were normalized to GAPDH. In order to analyze PKCδ-specific genes two different RNAis for PKCδ (siRNA sequences see Table II.26 in II.9.1) were used. For control and the PKCα and PKCε isoforms one specific siRNA (siRNA #1 of each PKC; siRNA sequences see Table II.26 in section II.9.1) was used.

II.15. Statistical analysis

All experiments were performed three times. For statistical analysis, two tailed *Student's t-test* for equal sample variance was used. A p value <0.05 was considered as significant. The results are represented as the mean value ± S.E.M..

III RESULTS

III.1 Phorbol ester and bryostatin have opposing effects in LNCaP cells

III.1.1 PMA induces apoptosis in the prostate cancer cell line LNCaP

Most PKC agonists, including phorbol esters, DAGs, and ingenol-3-angelate (PEP005), bind to the C1 domains in cPKCs and nPKCs leading to kinase activation *in vitro*. In androgen-dependent prostate cancer cells, these PKC activators induce a strong apoptotic response [57, 81, 89, 90].

To first confirm previous findings, the apoptotic effect of PMA on LNCaP cells was assessed. To that end cells were treated with vehicle or different concentrations of PMA and the percentage of apoptotic cells determined. Apoptosis in response to PMA increased in a dose-dependent manner (Fig. III.1). In all future experiments the PMA concentration was kept constant at 100 nM as the maximal apoptotic response had been achieved at this concentration in previous work [81].
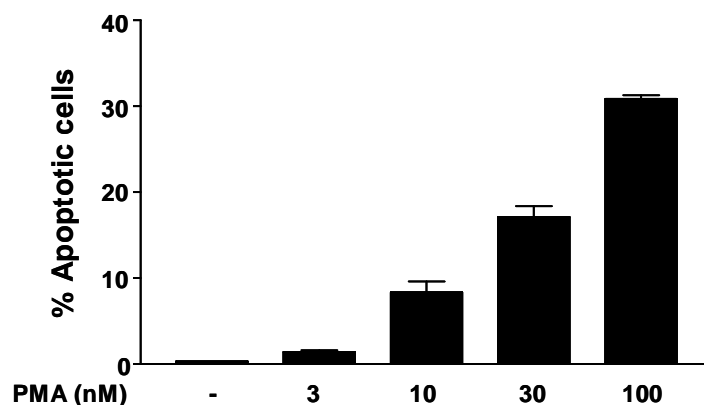

Figure III.1 PMA induces apoptosis in LNCaP cells in a dose-dependent manner. LNCaP cells were treated with vehicle or various concentrations of PMA as indicated for 1 h and then washed extensively with medium. Apoptosis was assessed 24 h later by DAPI staining. Data represent the mean ± S.E.M. of three independent experiments.

III.1.2 The C1 domain ligand bryostatin 1 fails to induce cell death and inhibits PMA-induced apoptosis in LNCaP cells

Previous studies showed that long-term treatment (24-72 h) of LNCaP prostate cancer cells with 10 nM bryostatin 1, another C1 domain ligand for PKCs, does not affect LNCaP cell viability. Such long-term treatment causes a marked down-regulation of PKC isozymes, primarily PKCα [91]. The main interest of this study was focused on the effects of short-term treatment with bryostatin 1 on LNCaP cells, an effect that should be independent of PKC down-regulation. Indeed, short treatment (1 h) of LNCaP cells with bryostatin 1 (0.1-100 nM) did not appreciably change the expression of PKCα, PKCδ, or PKCε, which are the C1 domain containing PKC isoforms expressed in these cells (Fig. III.2A).

As previously reported [58], a 1 h treatment with PMA caused a marked apoptotic response in LNCaP cells. On the other hand, bryostatin 1 failed to cause apoptosis at all concentrations tested (0.1-100 nM) under similar experimental conditions. Moreover, co-incubation of bryostatin 1 with PMA inhibited the apoptotic effect of the phorbol ester in a dose-dependent manner (Fig. III.2B and III.2C). In agreement with a previous study [91], a 24 h treatment with bryostatin 1 also failed to promote LNCaP apoptotic cell death. Representative micrographs of LNCaP cultures and nuclear DAPI stainings in response to the different treatments are shown in Fig. III.2C. These results suggest that bryostatin 1 acts as a functional antagonist of PMA-induced apoptosis in LNCaP prostate cancer cells.
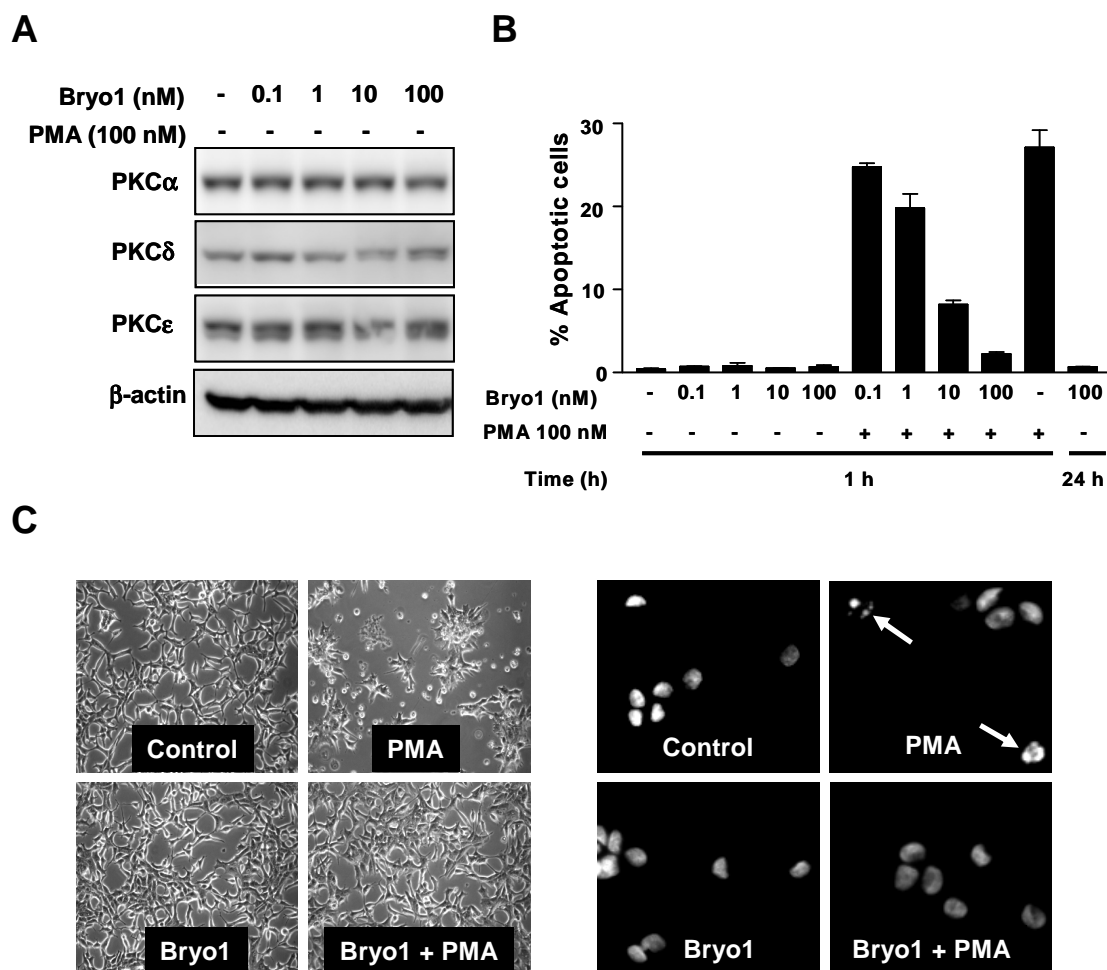
A

B

C

Figure III.2 **Short-term bryostatin 1 treatment prevents PMA-induced apoptosis in LNCaP cells.** *Panel A.* LNCaP cells were treated with different concentrations of bryostatin 1 (0.1-100 nM, 1 h) and subjected to Western blot analysis using specific antibodies for PKC isozymes. *Panel B.* LNCaP cells were treated for 1 h with PMA or bryostatin 1 alone or in combination at the concentrations indicated in the figure, and the percentage of apoptotic cells determined 24 h later. The effect of 24 h of bryostatin 1 treatment is also shown. Data represent the mean ± S.E.M. of three independent experiments. *Panel C.* Representative micrographs of LNCaP cell cultures (*left panel*) and DAPI stainings (*right panel*), after treatment with PMA and/or bryostatin 1 (100 nM). Apoptotic cells are indicated with arrows.

III.1.3 Bryostatin 1 does not affect the expression of survival factors or the phosphorylation status of Akt or p38

Apoptosis is a well orchestrated process and is controlled by multiple pathways, both pro- and anti-apoptotic. These pathways need to be perfectly

balanced, and imbalances can result in premature cell death of an otherwise intact cell or to apoptotic resistance in a cell that normally needs to be eliminated from the organism, *i.e.* cancer cells. Well studied factors that contribute to the apoptotic resistance are MCL1, BCL-XL and BCL-2 [92, 93]. Therefore, LNCaP cells were treated with PMA alone or in combination with bryostatin 1 as described above and cells lysed at different times, and subjected to Western blot analysis using antibodies against the aforementioned factors. The results shown in Figure III.3 demonstrate that expression of MCL1, BCL-XL, and BCL-2 was not increased and therefore are not likely to contribute to the anti-apoptotic effect of bryostatin 1.
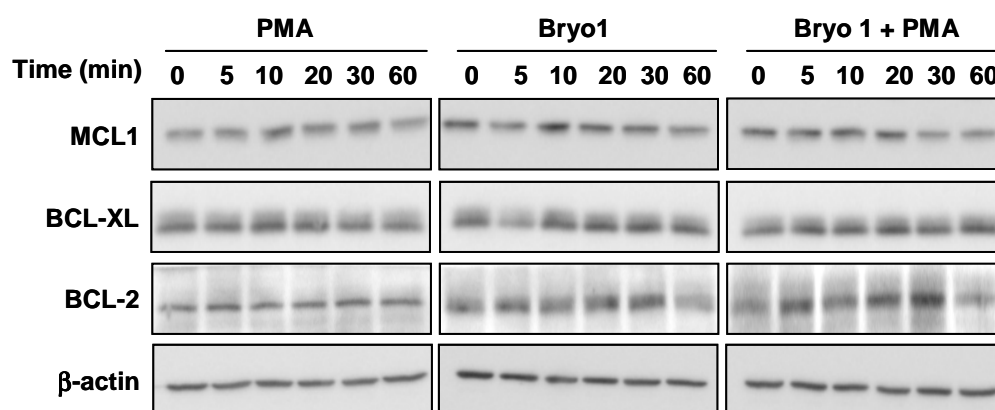
Figure III.3 PMA-induced expression of MCL1, BCL-XL, and BCL-2 does not change after treatment with bryostatin 1. LNCaP cells were treated at the indicated time points with 100 nM PMA alone or in combination with 10 nM bryostatin 1 and subjected to Western blot analysis.

In addition to these factors, an interesting question was whether changes in the phosphorylation status of Akt and p38 occur. It has been described previously that phosphorylation of these factors is altered in LNCaP cells upon treatment with PMA [58]. Western blot analysis shows clearly that Akt was rapidly dephosphorylated after treatment with PMA, and phospho-p38 levels increased over time, while total levels of these proteins remained unchanged. When cells were treated with

bryostatin 1 either alone or in combination with PMA, the kinetics of phospho-Akt

dephosphorylation and the phosphorylation of p38 were not affected (Fig. III.4A and
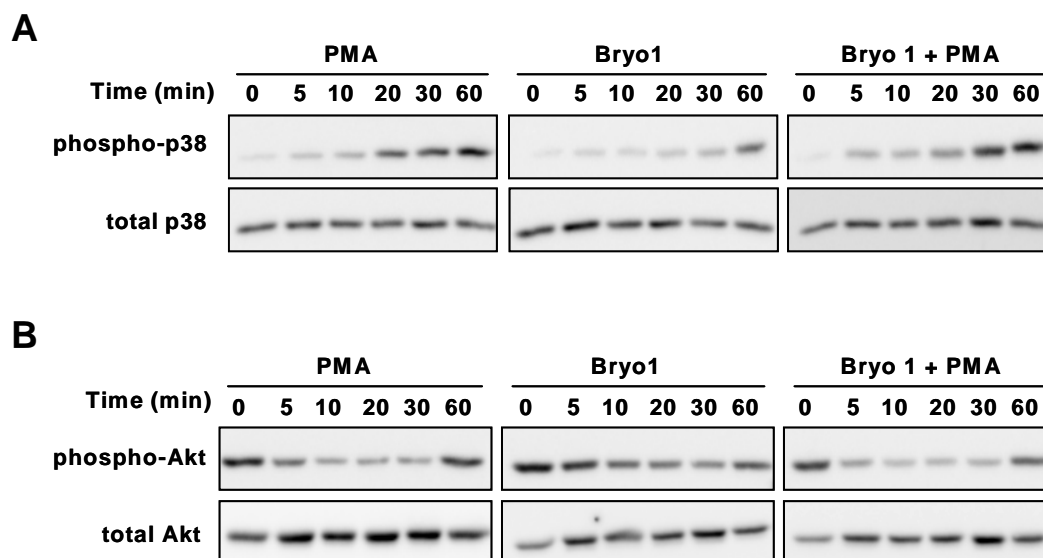
III.4B).

A

B

Figure III.4 The PMA-induced phosphorylation status of p38 and Akt is not affected upon treatment with bryostatin 1. LNCaP cells were treated with 100 nM PMA, 10 nM bryostatin 1, alone or in combination at the indicated time points. Proteins were subjected to Western Blot analysis. *Panel A.* Western Blot analysis for p38. *Panel B.* Western Blot analysis for Akt.

III.1.4 Conditioned medium (CM) from bryostatin 1-treated LNCaP cells inhibits PMA-induced apoptosis in naïve LNCaP cells

As shown in Figure III.3 and III.4A and 4B neither MCL-1, BCL-XL or BCL-2

nor changes in the phosphorylation status of Akt or p38 are implicated in the anti-

apoptotic effect of bryostatin 1. Therefore, a more broad-based approach was

chosen to clarify the anti-apoptotic effect of bryostatin 1 and the role of factors

secreted by LNCaP cells upon treatment with PMA. Previous studies from our

laboratory have shown that PMA-induced apoptosis in LNCaP cells is mediated by

the autocrine release of death factors primarily TNFα. Therefore, the failure of

bryostatin 1 to promote LNCaP cell apoptosis might relate to its inability to induce the

secretion of death factors. Also it could be possible that bryostatin 1 alters the pattern of secreted factors, thereby inhibiting PMA-induced apoptosis. To this end, CM was prepared as described in the Materials and Methods section II.3.3. As shown in Figure III.5, treatment with CM collected from cells treated with PMA (CM-PMA) resulted in increased apoptosis of recipient LNCaP cells. In contrast, CM collected from cells treated with bryostatin 1 + PMA (CM-Bryo1+PMA) did not yield an apoptotic response when added to naïve LNCaP cells.
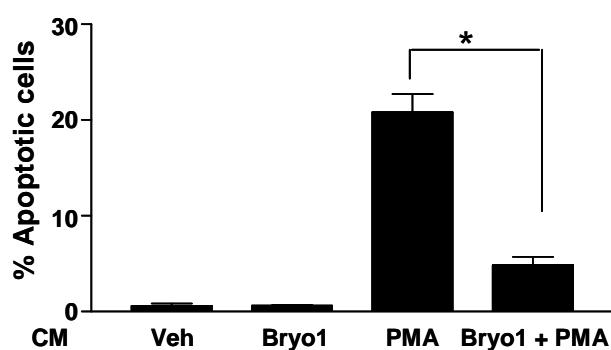
Figure III.5 CM from bryostatin 1-treated cells inhibits apoptosis in LNCaP receptor cells. LNCaP cells were treated with bryostatin 1 (10 nM) and/or PMA (100 nM), or vehicle. CM was collected 24 h later and added to a naïve culture of LNCaP cells. The percentage of apoptotic cells was determined 24 h later. Data represent the mean ± S.E.M. of three independent experiments, *$p < 0.05$.

Again, the common and well studied signaling cascades of the p38/MAPK, Akt and, in addition, the JNK pathways were investigated. To exclude that bryostatin 1 influences these pathways through an altered composition of the CM, time-course experiments with CM were performed. Time-courses were chosen to be longer than in previous experiment to include late events. No changes in the phosphorylation status of p38, JNK or Akt were observed. (Fig. III.6A). Therefore, it appears that these signaling pathways are regulated by PMA independently of bryostatin 1-induced changes of the CM.

We also tested if the time-course of p38 phosphorylation was shortened upon treatment with PMA and bryostatin 1 as compared to treatment with PMA alone. However, no differences in the phosphorylation of p38 were observed over 8 hours (Fig. III.6B).
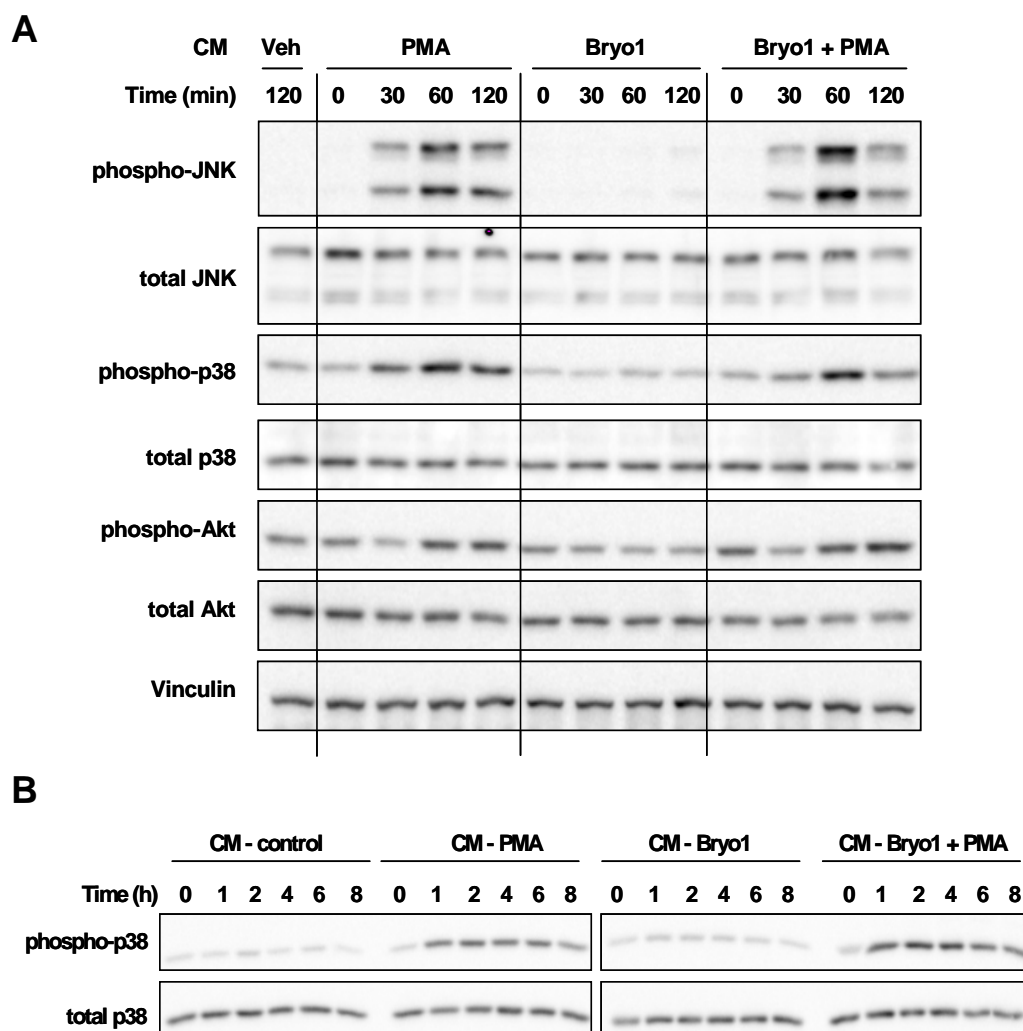
A

B

Figure III.6 CM-Bryo1+PMA does not alter the phosphorylation status of p38/MAPK, JNK, and Akt. *Panel A.* LNCaP cells were treated with 10 nM bryostatin 1 ± 100 nM PMA for 1 h and CM was collected 24 h later. Fresh LNCaP cells were then treated with CM and harvested at indicated time points. Protein lysates were subjected to Western Blot analysis. The phosphorylation status of both JNK and p38 as well as of Akt was not altered when cells were treated with CM from LNCaP cells treated with PMA alone or in combination with bryostatin 1. *Panel B.* LNCaP cells were treated with 10 nM bryostatin 1 ± 100 nM PMA for 1 h and CM was collected 24 h later. Fresh LNCaP cells were then treated with CM and harvested at indicated time points. p38 remains phosphorylated even after 8 h of treatment. No differences were observed between cells receiving CM from PMA or bryostatin 1 + PMA.

III.1.5 Analysis of the secreted factors to the CM using a cytokine array does not reveal significant changes upon treatment with bryostatin 1

In order to identify changes in the release of cytokines, chemokines and growth factors into the medium after treatment with bryostatin 1 (10 nM) and/or PMA (100 nM), a commercial cytokine array (Ray Biotech, No. 5) was used. Membranes were incubated with CM from LNCaP cells subjected to the different treatments or vehicle and the relative changes in cytokine expression was determined. Using the Map of RayBio Human Cytokine Antibody Array 5 the cytokines of the array could be identified (Table. III.1). No major changes upon treatment with bryostatin 1 were found (Fig. III.7A). The densitometric evaluation of several cytokines is shown in Fig. III.7B. All samples on one membrane were normalized to the intensity of the internal control. In a second step, the relative intensities were normalized to the samples treated with CM-Vehicle, and the corresponding samples were then displayed as fold-changes compared to vehicle-treated cells. As shown in Fig. III.7B, there was a marked increase in the release of a broad range of secreted cytokines to CM in response to PMA. However, there were no relevant differences in these cytokines from CM-Bryo1+PMA, making these factors unlikely to be candidates for the inhibitory effect of Bryo1 on PMA-induced apoptosis in LNCaP cells.

	A	B	C	D	E	F	G	H	I	J	K
1	Pos	Pos	Pos	Pos	Neg	Neg	ENA-78	GCSF	GM-CSF	GRO	GRO-α
2	I-309	IL-1α	IL-1β	IL-2	IL-3	IL-4	IL-5	IL-6	IL-7	IL-8	IL-10
3	IL-12 p40p70	IL-13	IL-15	IFN-γ	MCP-1	MCP-2	MCP-3	MCSF	MDC	MIG	MIP-1β
4	MIP-1β	RANTES	SCF	SDF-1	TARC	TGF-β1	TNF-α	TNF-β	EGF	IGF-I	Angio-genin
5	Onco-statin M	Thrombo-poietin	VEGF	PDGF-BB	Leptin	BDNF	BLC	Ck β 8-1	Eotaxin	Eotaxin-2	Eotaxin-3
6	FGF-4	FGF-6	FGF-7	FGF-9	Flt-3 Ligand	Fract-alkine	GCP-2	GDNF	HGF	IGFBP-1	IGFBP-2
7	IGFBP-3	IGFBP-4	IL-16	IP-10	LIF	LIGHT	MCP-4	MIF	MIP-3 α	NAP-2	NT-3
8	NT-4	Osteo-protegerin	PARC	PIGF	TGF-β 2	TGF-β 3	TIMP-1	TIMP-2	Neg	Pos	Pos

Table III.1 Map for RayBio® Human Cytokine Antibody Array 5 (adapted from www.raybiotech.com).

A

CM-Vehicle   CM-PMA

CM-Bryo1   CM-Bryo1+PMA
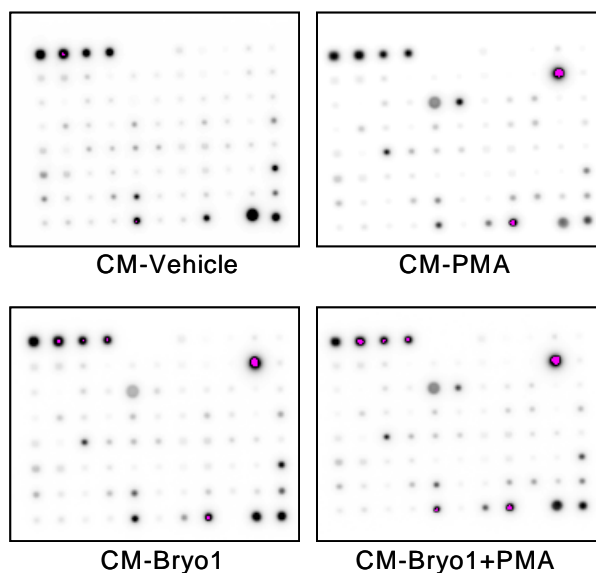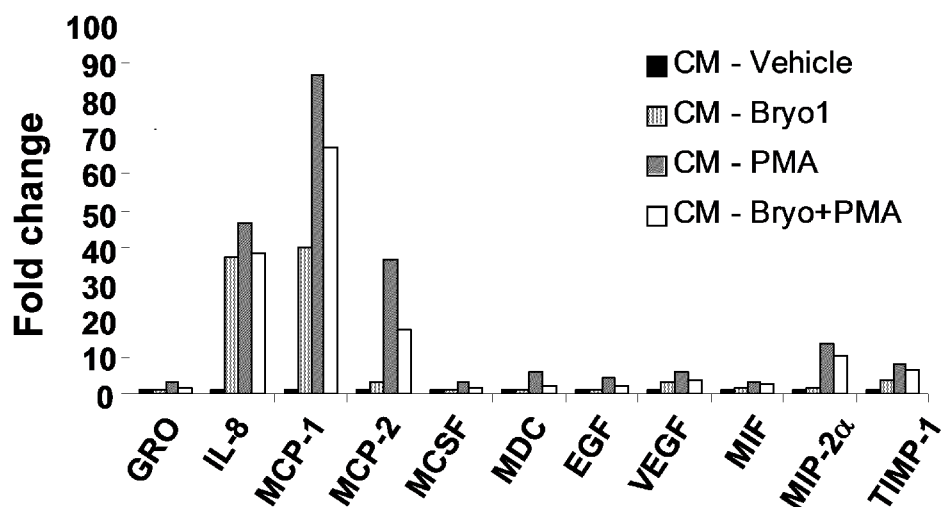
B

<u>**Figure III.7**</u> **The cytokine array does not reveal any major changes in the secretion of cytokines upon treatment with bryostatin 1.** *Panel A.* LNCaP cells were treated with 10 nM bryostatin 1 and/or 100 nM PMA or vehicle. CM was collected 24 h later and expression of cytokines determined with a cytokine array. Array Membranes were incubated for 2 h with 1 ml of CM from cells treated with PMA or bryostatin 1 alone or in combination, and detection was achieved by enhanced chemiluminescence. *Panel B.* Changes in the concentrations of selected cytokines in the cytokine array, as determined by densitometry, did not show relevant differences in cytokine concentrations in the medium of cells treated with Bryo1 + PMA compared to cells treated with PMA alone.

One caveat of this approach might be the limited dynamic range of the HRP-based detection system as compared to fluorescent detection systems [94]. In other words, a change in protein concentration on the lower detection limit might not be detected because proteins present at high levels (such as IL-8) are at detection ranges in which saturation already occurs. Therefore, we decided to focus on TNFα as an interesting candidate cytokine using ELISA technology. As indicated before, TNFα is an important factor released by LNCaP cells when treated with PMA [57]. Moreover, it was shown to be involved in triggering the pro-apoptotic signaling cascade in this cell system [57].

III.1.6 Bryostatin 1 prevents PMA-stimulated release of TNFα from LNCaP cells

Previous studies have established that PMA promotes the release of death factors from LNCaP cells, primarily TNFα. RNAi depletion or inhibition of TACE (the enzyme responsible for TNFα shedding [95]), neutralization of TNFα in the CM, or blockade/depletion of TNFα receptors, markedly reduces PMA-induced apoptosis in LNCaP cells, arguing for a critical involvement of this autocrine loop in the death effect of the phorbol ester [57]. To determine if autocrine mechanisms are involved in the inhibition of PMA-induced apoptosis by bryostatin 1, the effect of bryostatin 1 on TNFα release from LNCaP cells was examined. As shown in Fig. III.8A, TNFα specific ELISA clearly demonstrates that unlike PMA, bryostatin 1 treatment failed to induce any measurable release of TNFα from LNCaP cells, and more importantly, it essentially blunted TNFα release by PMA.

In order to determine whether reduced secretion of TNFα is a critical determinant for the impaired apoptotic response of PMA in the presence of bryostatin 1, a rescue approach by adding exogenous TNFα to the CM was pursued. The assumption for this experiment was that by supplementing this cytokine to CM-Bryo1/PMA to levels similar as those normally observed in CM-PMA, it should be possible to restore the apoptotic response. A caveat in this experiment, is that, as shown in Fig. III.8C, the recovery of TNFα was less than 20% of the amount added. Possible reasons for this reduced recovery may be decreased stability and/or misfolding of the synthetic TNFα. Importantly, addition of exogenous TNFα was able to rescue the pro-apoptotic effect of CM-Bryo1/PMA in a concentration-dependent manner (Fig. III.8B). Based on the linear correlation established between the added and measured TNFα concentrations in the medium we were able to estimate the actual TNFα concentrations in CM-Bryo1/PMA. Data clearly show that complete rescue could be achieved at concentrations of TNFα similar to those present in CM (compare with Fig. III.8A).
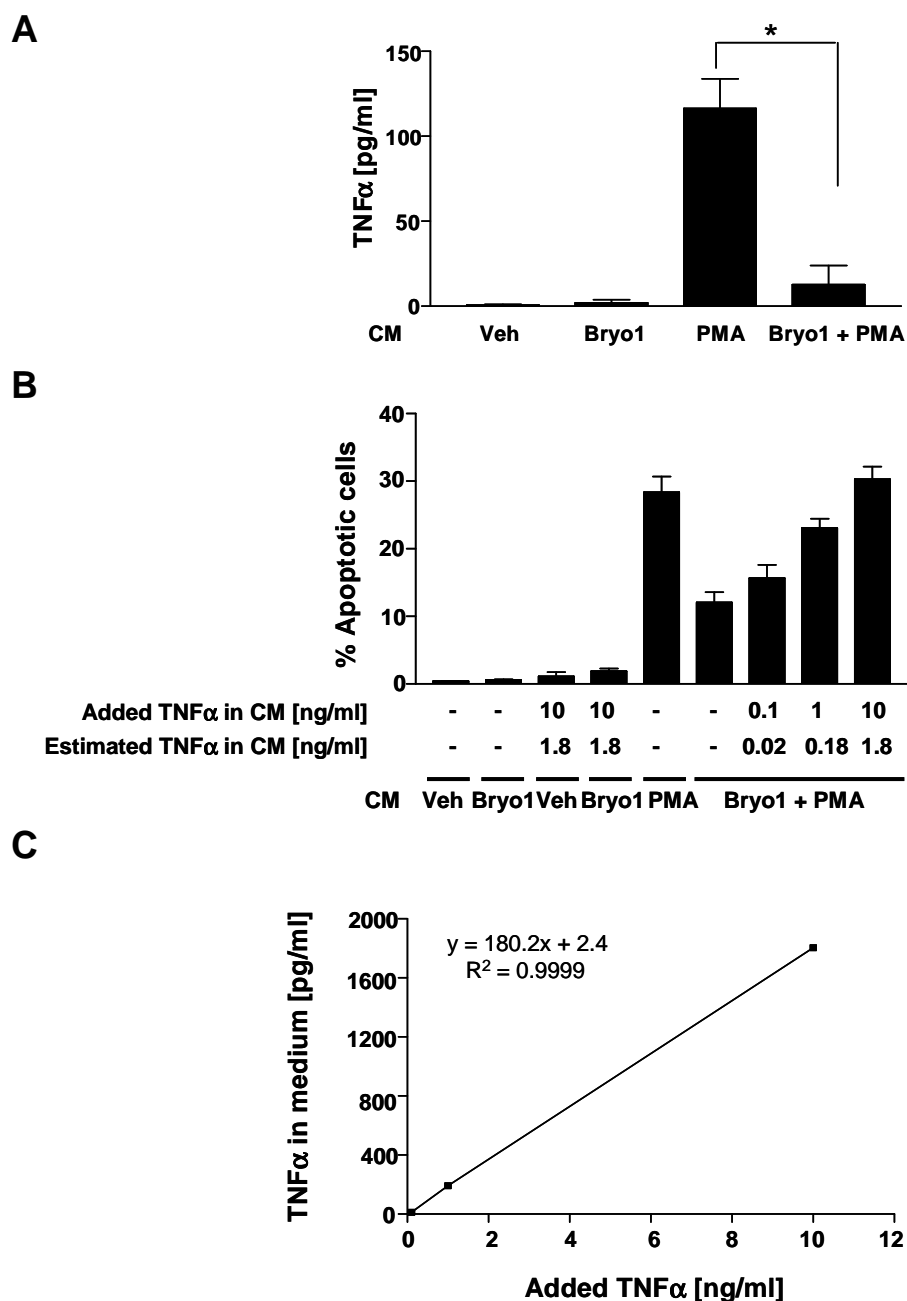
A

B

C

Figure III.8 Bryostatin 1 prevents the release of TNFα from LNCaP cells. *Panel A.* TNFα levels were measured by ELISA in CM collected 24 h after the different treatments. Data represent the mean ± S.E.M. of three independent experiments. *Panel B.* LNCaP cells were treated with vehicle, bryostatin 1, PMA, or bryostatin 1 in combination with PMA at the concentrations indicated in the figure. CM was collected 24 h later, supplemented with TNFα at the indicated concentrations, and added to naïve LNCaP cells. After 24 h the percentage of apoptotic cells was determined. The concentrations of TNFα in CM calculated according to the relation given in *Panel C* is also shown. Data represent the results of three independent experiments (mean ± S.E.M.). *Panel C.* Determination of TNFα concentrations by ELISA in medium after supplementation with exogenous TNFα.

III.1.7 PKCδ is a key regulator of PMA-induced TNFα release from LNCaP cells

A previous report has shown that the ability of bryostatin 1 to impair PMA-induced apoptosis is related to its ability to down-regulate PKCα from LNCaP cells, although unlike the studies presented here this occurred upon long-term (24-72 h) treatment [91]. Also, a key role has been assigned to PKCδ in PMA-induced apoptosis [58]. Therefore, in the present studies this issue was explored in more detail by means of a RNAi approach. The three PMA-responsive PKCs expressed in LNCaP cells were silenced using two different siRNA duplexes for each PKC isoform, which minimized the possibility of "off-target" effects of RNAi. Isozyme-specific depletion for each PKC was successfully achieved with either duplex relative to cells transfected with control siRNA (Fig. III.9A). These experiments revealed that the apoptotic effect of PMA was substantially reduced in PKCδ-knockdown LNCaP cells, but not in cells in which either PKCα or PKCε were depleted (Fig. III.9B). A greater apoptotic effect of PMA was observed in PKCε-depleted LNCaP cells, consistent with its pro-survival effect in this model [96]. Most importantly, only PKCδ depletion could significantly impair TNFα release by the phorbol ester, while depletion of either PKCα or PKCε failed to block secretion of the death factor (Fig. III.9C). These data not only suggest that PKCδ is crucial for PMA-induced TNFα release in LNCaP cells, but it also argues in favor of PKCδ as the main PKC implicated in the protection of PMA-induced apoptosis by bryostatin 1.
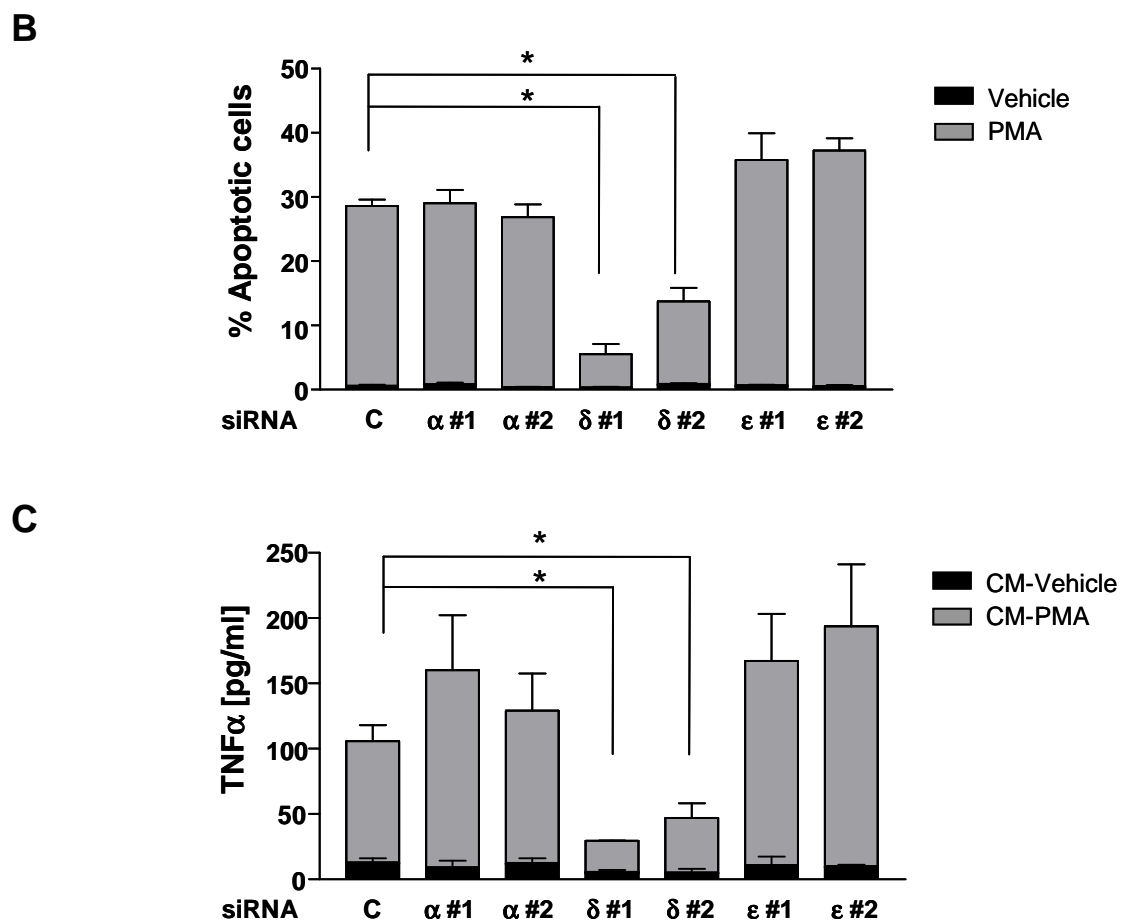
A

B

C
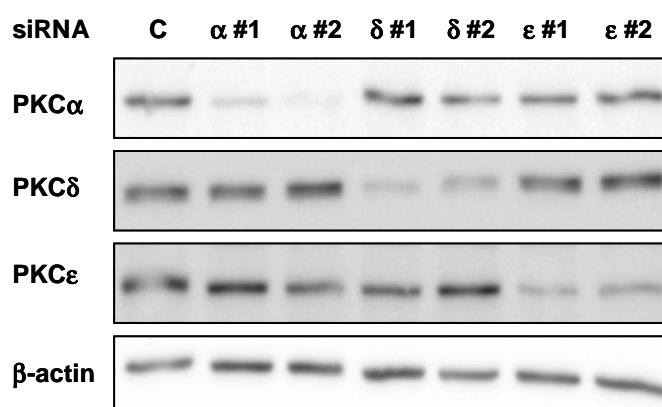
Figure III.9 PKCδ is essential for TNFα release induced by PMA. LNCaP cells were transfected with two different siRNA duplexes (#1 or #2) for each PKC isoform or a control siRNA (240 pmol). After 48 h, cells were treated with PMA (100 nM, 1 h). *Panel A.* Western Blot for PKCα, PKCδ, and PKCε 48 h after transfection. *Panel B.* Effect of individual PKC isozyme depletion on PMA-induced apoptosis, as determined 24 h after treatment. Data represent the mean ± S.E.M. of three independent experiments, *p<0.05 vs. control siRNA. *Panel C.* TNFα levels in CM from vehicle- or PMA-treated LNCaP cells subject to PKC isozyme RNAi depletion. Data represent the mean ± S.E.M. of three independent experiments, *p<0.05 vs. control siRNA.

III.1.8 Bryostatin 1 selectively inhibits the translocation of PKCδ to the plasma membrane in LNCaP cells

At this point, the data obtained so far called for the question whether bryostatin 1 could induce changes in the subcellular localization of PKCδ. It is well established that translocation of PKC isozymes is a hallmark of enzyme activation [97]. It is tempting to speculate that the failure of bryostatin 1 to induce apoptosis in LNCaP cells may relate to its failure to translocate PKCδ to the plasma membrane, which may ultimately lead to the inability to release TNFα. To this end, translocation of PKCs was assessed using GFP-fused PKCs. LNCaP cells were transfected with pEGFP-N1-PKCα, pEGFP-N1-PKCδ, or pEGFP N1-PKCε and 48 h after transfection, cells were treated with PMA or bryostatin 1, alone or in combination. Localization of the GFP-fused PKCs was determined by confocal microscopy. PMA redistributed PKCα and PKCε to the plasma membrane, while PKCδ was dually translocated to the plasma and nuclear membranes (Figs. III.10C, 10G, and 10K). Similar patterns of translocation for these PKCs have been reported in various cell types [81, 82, 98]. Like PMA, treatment with bryostatin 1 caused significant translocation of PKCα and PKCε to the cell periphery, although the effect was less pronounced for PKCα (Fig. III.10B and J). In contrast, bryostatin 1 caused a pronounced translocation of PKCδ to the nuclear membrane, but remarkably, translocation to the plasma membrane could not be readily detected (Fig. III.10F). Co-treatment of LNCaP cell with PMA and bryostatin 1did not affect the translocation of PKCα and PKCε to the cell periphery (Fig. III.D and L). In contrast, under these conditions peripheral translocation of PKCδ by PMA was significantly reduced in cells treated with bryostatin 1, whereas accumulation of PKCδ at the nuclear membrane remained essentially unaffected (Fig. III.10H). These findings demonstrate a different subcellular relocalization of PKCδ depending on the ligand used for treating LNCaP cells. Most importantly, they reveal that bryostatin 1 has the ability to prevent the translocation of PKCδ to the plasma

membrane without significantly altering the distribution of other PKCs. It is therefore conceivable that translocation of PKCδ to the plasma membrane is a pre-requisite for the induction of apoptosis in LNCaP cells by PKC activators.
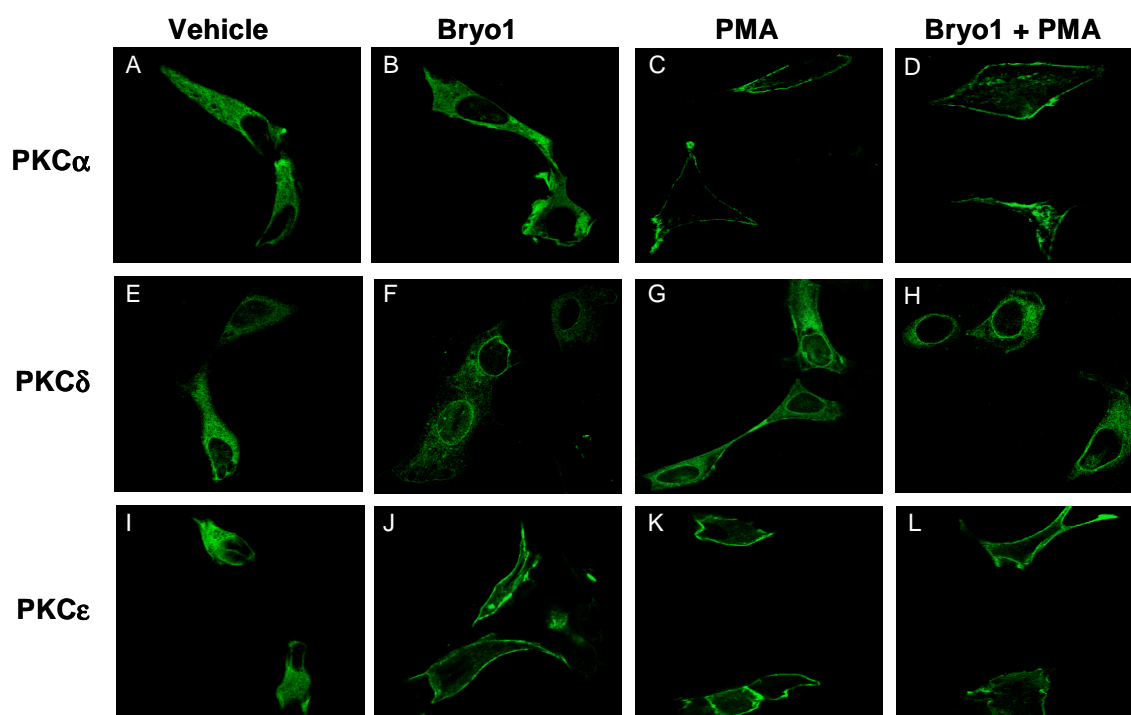

Figure III.10 Bryostatin 1 impairs PMA-induced peripheral translocation of PKCδ in LNCaP cells. LNCaP cells expressing GFP-PKCα, GFP-PKCδ, or GFP-PKCε were stimulated for 20 min with vehicle, 100 nM PMA or bryostatin 1, alone or in combination. Localization was determined by confocal microscopy. Representative micrographs are shown. Similar results were observed in multiple cells in at least three individual experiments.

III.1.9 Translocation of PKCδ to the plasma membrane is essential for the induction of apoptosis in LNCaP cells

Localization of PKC isozymes is key for determining the nature of the cellular response to PKC activators. PKCs can differentially translocate to multiple compartments in a cell type-specific manner, leading ultimately to a differential access to substrates or accessory interacting proteins [99, 100]. The data of the

present studies point to plasma membrane redistribution of PKCδ as an essential step for PMA-induced apoptosis in LNCaP cells. To test this hypothesis, a construct in which PKCδ was fused at the N-terminus to a myristoylatation signal sequence (myr) and at the C-terminus to a myc-tag was generated. PKCδ expressed from this construct will be targeted to the plasma membrane through its myristoylated N-terminus, while detection could be achieved through staining or immunoblotting against the C-terminal myc tag. LNCaP cells were transfected with plasmids encoding either wild-type PKCδ, which localizes essentially in the cytoplasm (PKCδ*cyto*), or the membrane-targeted PKCδ (PKCδ*myr*), and apoptosis assessed 24 h later. Transfection efficiencies were ~15% as determined by the fraction of myc-tag positive cells. Expression by Western blot is shown in Fig. III.11A. Upon ectopic expression of PKCδ*cyto* in LNCaP cells no measurable apoptotic response could be detected. In contrast, ectopic expression of PKCδ*myr* resulted in significant cell death (Fig. III.11B). To confirm the localization of PKCδ*myr* at the plasma membrane, confocal microscopy was performed. As shown in Fig. III.11C, this modified form of the kinase localized exclusively in the cell periphery, while PKCδ*cyto* was found essentially in the cytoplasm of LNCaP cells. Thus, targeting PKCδ to the plasma membrane is sufficient to promote apoptosis in LNCaP cells. Taken together, the data presented here strongly argue that the lack of apoptosis in response to bryostatin 1 and the abrogation of PMA-induced apoptosis by bryostatin 1 are due to the inability of PKCδ to translocate to the plasma membrane.
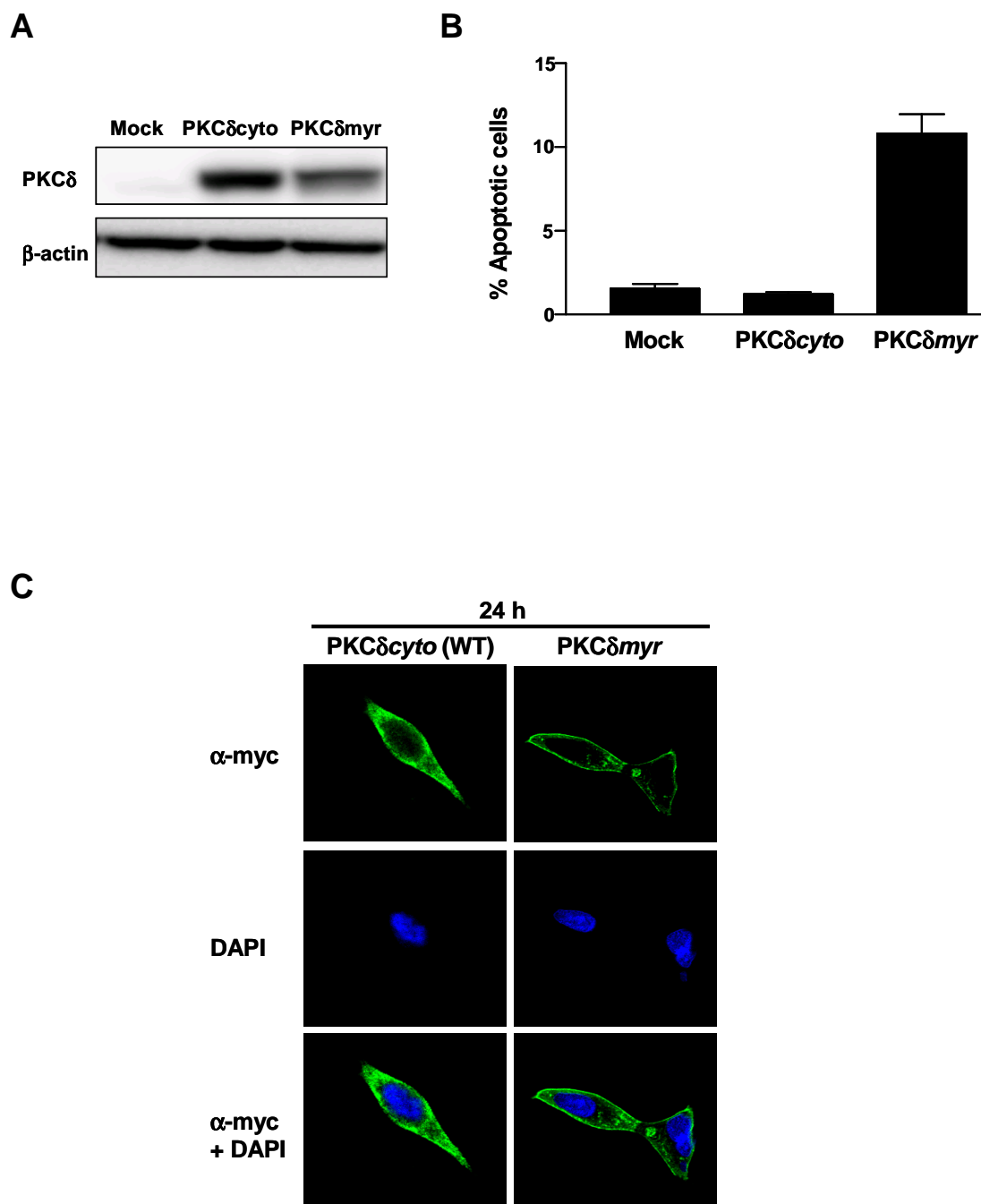
A

B

C

Figure III.11 Targeted localization of PKCδ to the plasma membrane induces apoptosis in LNCaP cells. LNCaP cells were transfected with myc-tagged vectors encoding PKCδ*cyto*, PKCδ*myr*, or empty vector as a control. *Panel A.* Expression was determined by Western blot using an anti-myc-tag antibody. *Panel B.* Percentage of apoptotic cells 24 h after transfection. Data represent the mean ± S.E.M. of three independent experiments. *Panel C.* Localization of PKCδ*cyto* and PKCδ*myr* in LNCaP cells 24 h after transfection. Transfection efficiency was ~15%.

III.2. Genome-wide expression analysis reveals PKCδ as master regulator of transcription in LNCaP cells

III.2.1 Inhibition of protein synthesis by cycloheximide significantly decreases PMA-induced apoptosis

Although PKCs are known to play an important role in the regulation of gene expression through TPA/PMA-responsive elements in gene promoters, our understanding of how individual PKC isozymes control gene expression is poor. The well-established differential effects of PKC isozymes in survival and apoptosis in prostate cancer cells prompted us to investigate whether transcriptional regulation might be involved in phorbol ester induced apoptosis in prostate cancer cells. To address this question, LNCaP cells were treated with the inhibitor of protein synthesis cycloheximide (50 μM) prior and during the exposure to PMA (100 nM, 1 h). The efficiency of cycloheximide was confirmed by its ability to inhibit the induction of the cell cycle regulator p21 (Fig. III.12A). Notably, the apoptotic effect of PMA was significantly reduced from $27.9 \pm 3.1\%$ in vehicle-treated cells to $15.6 \pm 0.7\%$ in cycloheximide-treated cells (Fig. III.12B). Thus, the inhibition of *de novo* protein synthesis significantly decreased the apoptotic response by 44%. These results argue for a potential involvement of transcriptional mechanisms in the induction of apoptosis by PMA. Therefore, global gene expression analyses were carried out to address the following two questions: First, what is the overall change in gene expression upon treatment with PMA and when do these changes occur; and second, what is the relative contribution of PKC isozymes to the control of gene expression?
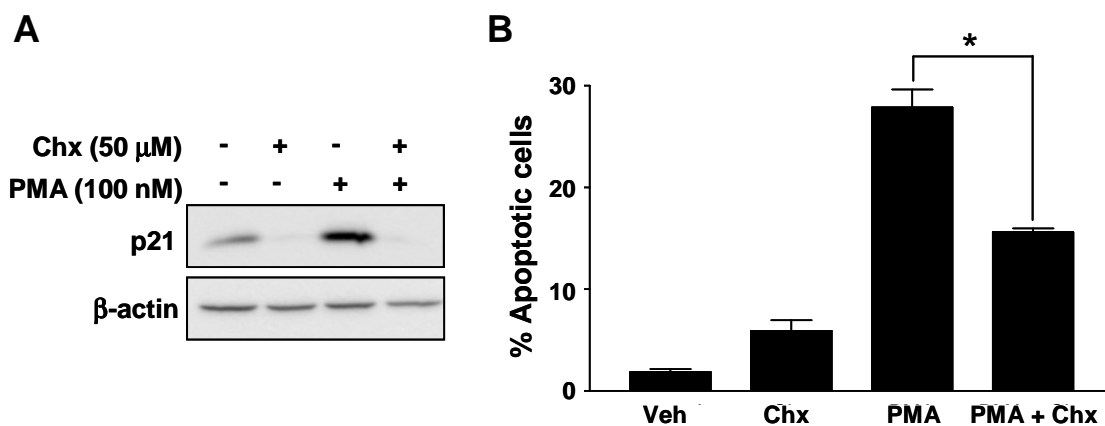
A

B

Figure III.12 Inhibition of protein synthesis reduces PMA-induced apoptosis. *Panel A.* Cycloheximide (Chx) inhibits the induction of p21. *Panel B.* LNCaP cells were treated with 50 µM Chx 40 min prior to and during stimulation with 100 nM PMA. Data represent the mean ± S.E.M. of three independent experiments, *p<0.05.

III.2.2 PMA rapidly induces changes in gene expression levels

To address the first question, a time-dependent analysis of transcriptional changes in response to PMA (100 nM, 1 h) was carried out as described in section II.13. Applying the criteria for significance as mentioned in the Material and Methods section (Fig. II.7), 4949 genes displayed a significant change ≥ 2-fold in PMA-treated LNCaP cells compared to vehicle (ethanol) at different time points after treatment. We observed a variety of patterns of changes in expression over time, which allowed the categorization into either of the following groups: up- *vs.* down-regulated, and early- *vs.* late-regulated genes (Fig. III.13A). Interestingly, most of all altered genes were found to be regulated within the first 4 h after stimulation. There was a striking difference between the number of genes that were transiently regulated (Fig. III.13B, Panels 1-3) and those that exhibited sustained changes (Fig. III.13B, Panels 4-6). The latter represents the time-course of regulation for the majority of genes.
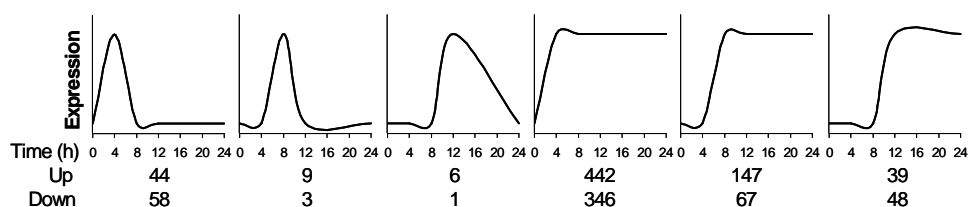
A
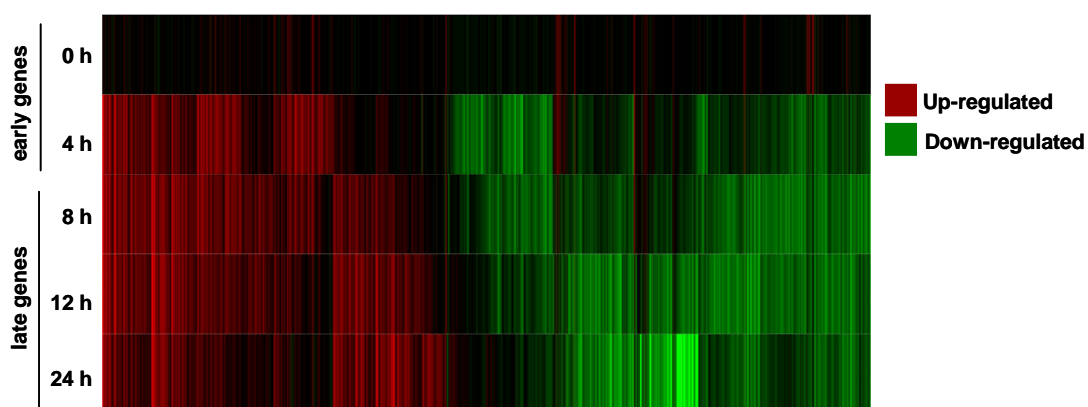
B

Figure III.13 Genome-wide expression analysis reveals different temporal patterns of gene expression with the majority of changes in gene expression occurring 4 h after PMA treatment. *Panel A.* Expression levels change over time. The heat map shows 4949 genes which are significantly altered 0, 4, 8, 12, and 24 h after treatment with PMA. The number of genes with changes in expression levels differs between time points. *Panel B.* Genes can be classified into early (0-4 h) and late (8-24 h) regulated genes. Genes were filtered with respect to transient (panels 1-3) or sustained (panels 4-6) changes. In both sets, the majority of changes in gene expression occurs 4 h after PMA treatment.

III.2.3 Selection of PMA-regulated genes according to their Gene Ontologies

To further characterize the distribution of PMA-regulated genes across biological functions, genes were categorized according to six Gene Ontology biological processes, which led to functional classification of 1280 genes. Out of these, 7% are involved in apoptosis/survival, 17% in proliferation, 13% in differentiation, 4% in oncogenesis, 22% are transcription factors, and 37% are encoding for signal transduction molecules (Fig. III.14A). In addition, these 1280

genes were classified into early- and late-regulated genes. In addition and in line with previous analysis conducted during these studies, most of the regulated genes were altered within 4 h after treatment with PMA (Fig. III.14B).
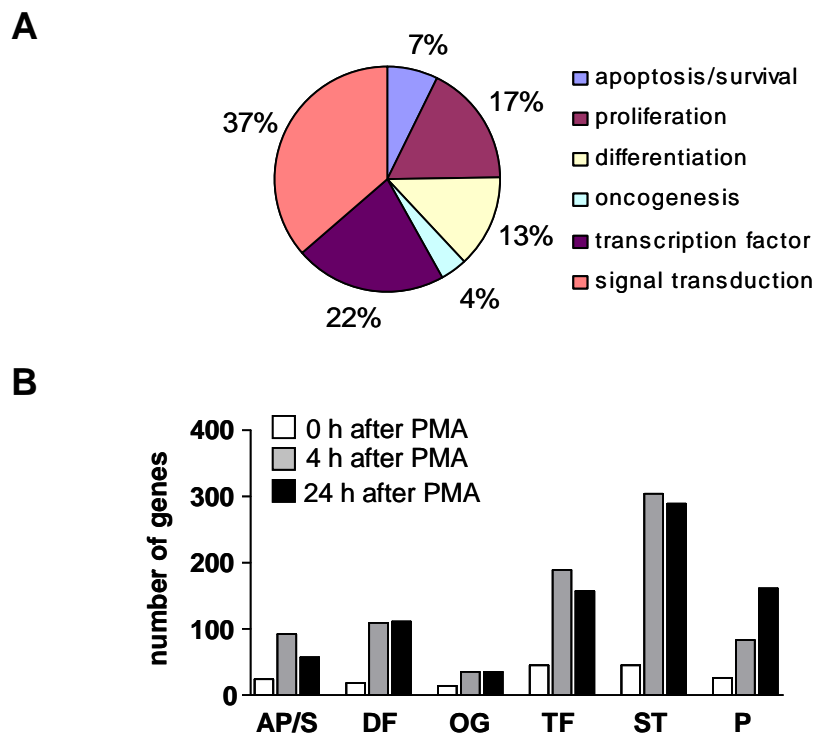
A

B

Figure III.14 Classification of regulated genes according to their biologic functions. *Panel A.* The 4949 PMA-regulated genes shown in the heat map were filtered according to their Gene Ontology biological processes (GO) as indicated, resulting in a functional classification of 1280 genes. Most of the PMA-regulated genes are related to transcription factors (TF) and signal transduction (ST) compared to apoptosis/survival (AP/S), differentiation (DF), oncogenesis (OG), or proliferation (P). *Panel B.* The 1280 genes categorized according to their GO were further classified into early (0-4 h) and late (4-24 h) regulated genes. The number of regulated genes at indicated time points after PMA treatment shows that unlike early responsive genes, regulation of late regulated genes lacks a dynamic over time.

III.2.4 Isozyme-specific depletion of PKCs in LNCaP cells

As individual PKC isozymes exert different functions in prostate cancer cells, it is desirable to determine whether the three PMA-responsive PKC isozymes present in LNCaP cells (PKCα, PKCδ and PKCϵ) could potentially regulate different subsets

of genes. To this end, a genome-wide expression analysis in LNCaP cells in which each individual PKC isozyme was depleted by RNAi was carried out. Various RNAi duplexes were tested and the two most effective and specific for each PKC isozyme were selected for these studies, which minimized the chances of "off-target" effects of the RNAi. Two different control RNAi sequences were also used. As shown in Fig. III.15, a nearly complete depletion for all RNAi duplexes was achieved, and importantly, knock-down was PKC isozyme-specific.
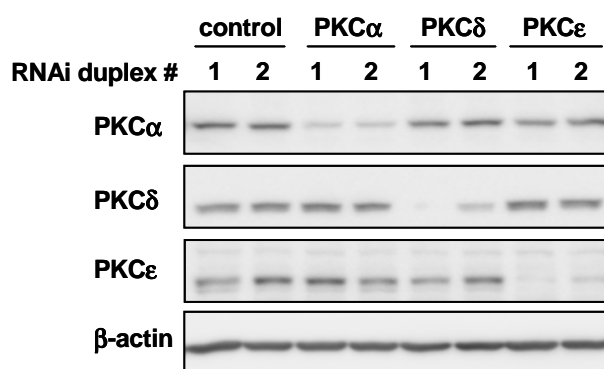
Figure III.15 Depletion of PKCs is isozyme specific. Western blot analysis conducted 48 h post transfection of LNCaP cells with two different RNAi duplexes (120 pmol) shows highly specific knockdown of each PKC isozymes.

III.2.5 Reproducibilty between two independent microarray experiments

To verify the reproducibility of the microarray experiments, genes regulated by PMA at 4 h after treatment in the first microarray experiment were compared with those of the 4 h time point from cells transfected with non-specific control siRNA in the second microarray experiment. Despite this difference between the samples, among the 50 most regulated genes a concordance of 96% between the two experiments was found, thus indicating a high degree of reproducibility (Table III.2).

Up-regulated genes

	Gene symbol	log2Rat (PMA vs.Veh)	
		1st ARRAY	2nd ARRAY
1	MMP10	10.2	10.5
2	DUSP5	9.9	7.8
3	PHLDA1	9.9	10.3
4	CCL2	9.8	11.0
5	IL8	9.8	10.3
6	EDN1	9.0	9.1
7	MAFF	8.8	7.3
8	EMP1	8.8	8.7
9	MMP1	8.6	10.8
10	ITGA2	8.6	7.8
11	EGR1	8.5	4.7
12	MET	8.3	9.0
13	C6orf145	8.1	8.0
14	TNFAIP3	7.9	8.1
15	BIRC3	7.8	7.4
16	RSAD2	7.8	6.3
17	SYTL2	7.7	7.3
18	C8orf4	7.6	6.3
19	LIPG	7.5	8.7
20	KRT34	7.4	7.7
21	SERPINB2	7.4	8.4
22	C3orf52	7.2	8.5
23	MMP12	7.1	8.2
24	GADD45B	7.0	7.6
25	HMOX1	7.0	4.6
26	GBP1	6.9	7.0
27	TNFAIP3	6.9	7.8
28	IGF2BP2	6.8	7.4
29	HEG1	6.8	7.1
30	SFN	6.8	6.8
31	CCL20	6.8	8.8
32	CYR61	6.7	7.3
33	TUBB6	6.7	6.0
34	TNF	6.6	7.6
35	LEPREL1	6.6	6.9
36	KRT20	6.5	3.0
37	PGBD5	6.5	7.1
38	CLDN1	6.5	7.6
39	FHL2	6.5	7.5
40	ARL14	6.5	6.7
41	GLIPR1	6.4	6.7
42	PLEKHC1	6.4	N.R.
43	C6orf148	6.4	N.R.
44	BCL2A1	6.3	7.9
45	PLAC8	6.3	5.9
46	TNFRSF12A	6.3	6.0
47	CACNA1G	6.2	7.1
48	KLF4	6.2	6.5
49	ULBP2	6.2	5.1
50	EDN2	6.2	7.2

Down-regulated genes

	Gene Symbol	log2Rat (PMA vs. Veh)	
		1st ARRAY	2nd ARRAY
1	TXNIP	-6.9	-6.8
2	PIK3R1	-4.7	-5.4
3	KLK2	-4.7	-5.6
4	SPRY1	-4.6	-5.9
5	PSRC1	-4.6	-5.3
6	TRIM48	-4.5	-4.3
7	ADRB2	-4.4	-6.9
8	DKFZP434P211	-4.3	-5.2
9	B3GNT1	-4.2	-4.5
10	RAB3A	-4.2	-3.4
11	GATA2	-4.0	-3.6
12	SESN1	-4.0	-4.6
13	RIN2	-3.9	-3.1
14	HOXC6	-3.8	-4.3
15	RAB36	-3.7	-3.2
16	SLC25A12	-3.5	-3.8
17	PTGFR	-3.5	-3.5
18	SLITRK3	-3.5	-4.4
19	C8orf51	-3.4	-4.4
20	FZD4	-3.4	-3.2
21	ASB13	-3.4	-3.6
22	FRY	-3.3	-2.3
23	SMAD6	-3.3	-4.4
24	RPGRIP1L	-3.3	-2.2
25	TSC22D3	-3.3	-3.7
26	POLG2	-3.3	-2.6
27	RASL11B	-3.3	-4.4
28	SUOX	-3.3	-3.0
29	ZNF692	-3.3	-3.1
30	THNSL1	-3.2	-2.4
31	AKAP1	-3.2	-3.1
32	HSPA1A /1B	-3.2	-2.5
33	F5	-3.2	-1.1
34	ATAD4	-3.2	-3.4
35	PMS1	-3.1	-2.7
36	ATF7IP	-3.1	-3.5
37	VIPR1	-3.1	-3.4
38	TTK	-3.1	-2.6
39	SALL2	-3.0	-3.2
40	ZMYM3	-3.0	-3.2
41	NR2F2	-3.0	-2.8
42	GPRIN2	-2.9	-3.2
43	WNT5A	-2.9	-3.1
44	KIF20A	-2.9	-4.2
45	GSPT2	-2.9	-2.5
46	KIAA0984	-2.9	N.R.
47	PPP1R3D	-2.9	-3.1
48	DFFB	-2.9	-3.6
49	SUHW4	-2.9	N.R.
50	LGR4	-2.9	-3.9

Table III.2 Reproducibility of gene expression analyses. There is a concordance of 96% between two independent microarray experiments for genes regulated at 4 h after PMA treatment. (N.R. = Not Represented).

III.2.6 Principal component analysis

A first estimate of the variability in gene expression across the whole genome can be obtained by prinicipal component analysis (PCA), in which the global variation in gene expression among all samples is analyzed. Using this approach, profound changes in PMA-treated samples were observed when compared to vehicle-treated LNCaP cells. Importantly, comparison of PCA for samples transfected with either control RNAi or PKC isoform-specific RNAi revealed that PKCδ-depleted samples were positioned away from the rest, suggesting a high number of genes specifically regulated by this isoform in response to PMA (Fig. III.16).
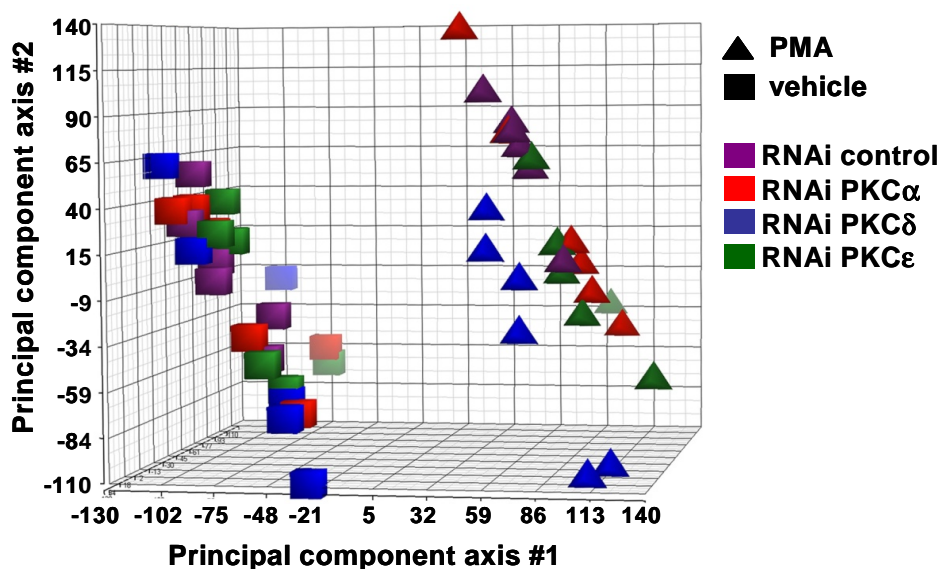
Figure III.16 Principal component analysis (PCA). PCA represents the global variation in three dimensions among all of the samples transfected with either control RNAi or PKC isoform-specific RNAi and treated with either vehicle or PMA. Plots are derived from expression values for all genes on the microarray. PKCδ-depleted and PMA-treated samples are located at unique positions, which indicates a higher number of genes specifically regulated by PKCδ.

III.2.7 PKCδ and PKCε have major, but opposing, roles in gene expression

The next goal was to determine whether PKC isozymes have the ability to selectively regulate gene expression. PKC isozyme-specific genes were defined as those which displayed ≥ 1.5-fold change in expression upon depletion of one PKC with changes < 1.5-fold upon depletion of the other two PKCs. This analysis revealed 300 and 439 genes regulated by PKCs under normal growth conditions (vehicle) and in response to PMA, respectively. Out of these, 215 (vehicle) and 302 (PMA) genes were found to be regulated by one specific PKC isozyme, resulting in well-defined isozyme-specific patterns. Surprisingly, the most represented patterns were those for isozyme-specific gene regulation by PKCδ and PKCε. Even more, PKCδ was primarily involved in the control of PMA-regulated genes, while PKCε primarily regulated gene expression in the absence of PMA (Fig. III.17). On the other hand, PKCα showed little contribution to specific regulated genes, either in the presence or absence of PMA.
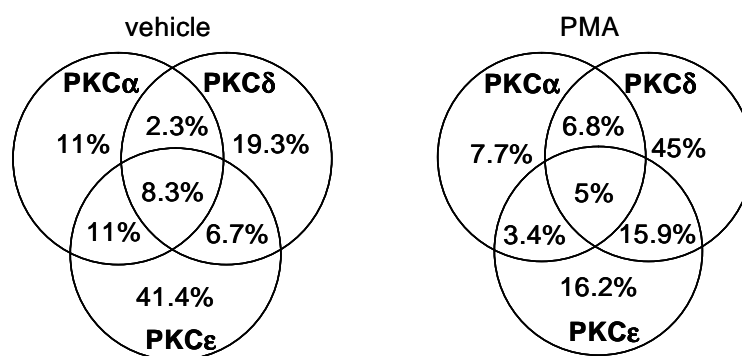
Figure III.17 PKC-isozyme-specific changes in transcription 4 h after PMA treatment assign major but opposing roles to PKCδ and PKCε. Comparative analysis in which the fold-change PMA/vehicle for one PKC isoform is ≥ 1.5-fold upon knockdown of this isoform revealed that 67% of all PKC-isozyme-regulated genes in the vehicle-treated group are controlled exclusively by PKCε whereas 45% of all PKC-regulated genes in response to PMA are solely controlled by PKCδ. The total number of genes found to be regulated by PKC isozymes was set to 100%.

Furthermore, analysis of up- and down-regulated genes separately under either vehicle- or PMA-treated conditions revealed that knockdown of PKCε mostly up-regulated gene expression (46.8% vehicle and 36.1% PMA) (Fig. III.18A), suggesting that PKCε primarily reduces gene expression. In contrast, knockdown of PKCδ led predominantly to down-regulation of genes (52% vehicle and 63% PMA) (Fig. III.18B), arguing for a role of PKCδ in the induction of gene expression. These results indicate a major role for PKCε as a negative regulator and PKCδ as a positive regulator of transcription.
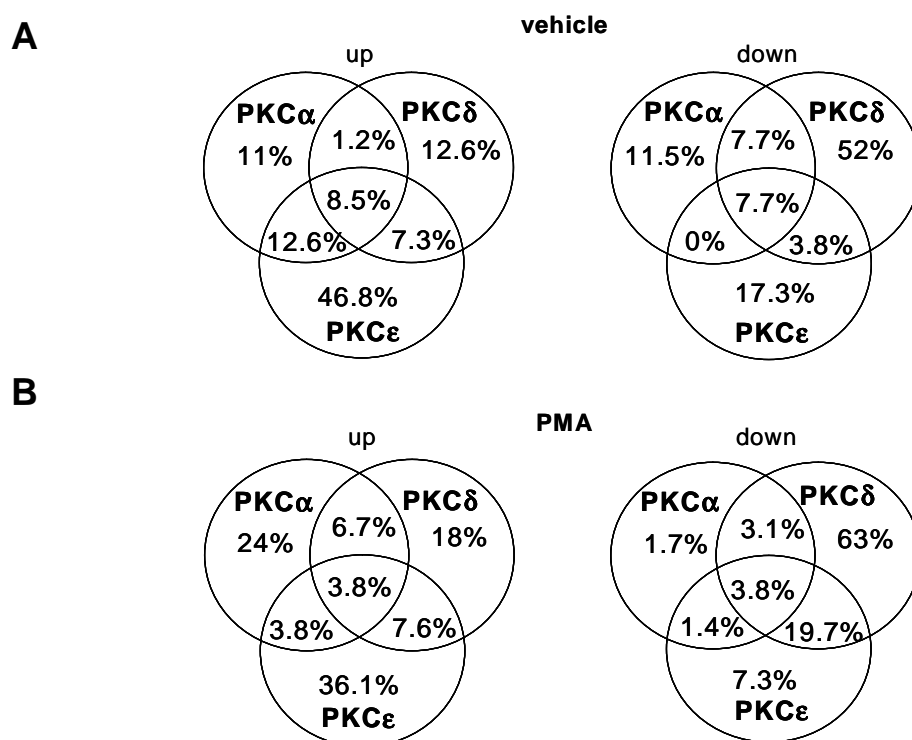
Figure III.18 PKC isoform-specific regulation of basal gene expression and after PMA treatment. Comparative analysis in which the fold change PMA/vehicle for one PKC isoform is ≥ 1.5-fold (the fold change PMA/vehicle for the other two PKC isozymes is < 1.5-fold variation with respect to the control). *Panel A.* Analysis of up- and down-regulated genes separately under vehicle conditions. Basal expression knockdown of PKCε up-regulates 47% of all genes up-regulated by PKCs whereas knockdown of PKCδ down-regulates 52% of the genes down-regulated by all PKCs. *Panel B.* In response to PMA 36% of all PKC-regulated genes are up-regulated after knockdown of PKCε and 63% are down-regulated after knockdown of PKCδ.

III.2.8 PKCδ as a master regulator of transcription

Next, the analysis was focused on genes that changed significantly upon PMA treatment in the presence of all PKC isozymes but had a significantly decreased fold change in response to PMA when PKC isozymes were silenced. The stringency for determining if a gene was specifically regulated by one particular PKC isozyme was increased by including only genes that had a $\geq$ 1.5-fold change in expression for one isoform knockdown and < 1.25-fold change in the two other isoform knockdowns when compared to samples treated with control siRNA and PMA. Using these criteria, 75 genes could be identified to be regulated specifically by PKCδ, whereas PKCα and PKCε had negligible impact on gene expression (0 and 4 specific genes, respectively) (Table III.3). Altogether, these results argue for a prominent role for PKCδ in the transcriptional control of PMA-mediated responses. On the other hand, analysis of genes that lost basal expression by a selective PKC RNAi indicated that although PKCδ was the major player, PKCε had a stronger role in basal transcription of genes in LNCaP cells (Table III.4).

Gene Symbol	Fold change (PMA vs. vehicle)			
	control siRNA	siRNA PKC alpha	siRNA PKC delta	siRNA PKC epsilon
CCL20	431.97	445.356	205.778	371.217
LIPG	412.064	380.913	138.744	348.031
C3orf52	352.221	349.808	140.401	302.386
SERPINB2	347.568	277.507	69.0852	280.939
MMP12	289.549	265.599	100.944	285.6
KIAA1199	279.829	268.394	84.5418	222.694
BCL2A1	231.687	261.559	41.0672	231.023
LBH	229.911	181.189	66.104	180.408
FOSL1	177.466	197.121	58.8825	166.614
KHDC1 /// RP11	173.491	185.242	59.691	150.39
IL2RG	150.179	132.166	58.1727	142.704
NAV2	141.685	124.774	57.2503	137.425
C6orf54	140.333	148.953	64.4421	126.33
GEM	139.116	104.458	25.2081	154.469
KIAA1462	134.649	138.682	42.0577	131.987
KLF6	118.65	105.594	49.7286	89.5544
ZEB1	111.113	96.0691	52.8667	98.1746
ALOXE3	80.6271	91.4754	39.8217	82.6679
ARID3B	69.8016	54.2586	22.8919	59.2662
GPRC5A	65.3548	78.6696	11.7494	52.1436
TRAF1	52.8591	58.7909	15.2639	46.34
LIF	49.6374	51.29	17.5727	51.5552
LAMB3	48.2196	57.5214	23.6052	50.7047
PPP1R15A	44.8156	37.2712	12.9591	39.9825
FBN1	26.8365	26.0985	10.4595	30.461
LOC100128443	24.1457	23.4664	5.97764	19.0712
SPHK1	22.7177	28.0275	3.29861	24.7489
CAMSAP1	19.6096	17.2473	9.79626	17.7953
ICOSLG	19.5864	18.9457	9.2869	18.0136
CCRN4L	18.3284	15.3042	6.72496	18.267
LDLR	18.1358	13.6885	8.30123	15.2696
ETS2	17.6968	15.9484	5.2811	16.0537
GPR87	15.9557	12.7265	3.6525	15.6914
CD4	11.4373	9.59886	3.3085	9.41094
PDLIM7	10.723	8.61031	5.1742	10.333
FEM1B	9.86614	9.71118	3.90214	8.53524
UGCG	6.97515	5.37178	3.47926	5.36878
RYBP	6.90635	6.23919	3.26558	5.89797
LYST	6.73711	5.81888	3.26899	5.43824
ITPR3	6.46632	6.46812	3.2132	5.19414
USP36	5.85851	6.49457	2.49393	5.22142
OAS1	5.77975	4.92854	2.63296	4.39302
APOBEC3A	5.38297	6.27105	1.48176	5.87304
SLC22A1	5.08514	6.11884	1.61635	3.89961
PLAGL2	4.95312	4.91819	2.31105	4.34918
CDKN2A	4.45763	4.27048	1.94775	3.48499
DENND3	4.45107	5.56148	1.30471	3.41965
IL1RN	3.80724	3.77067	1.0391	3.41129
TTC9	3.73481	4.44471	1.78045	4.08914
KIAA0999	3.70932	2.9546	1.56697	3.11012
CTSB	3.41354	3.20394	1.36195	2.61311
TRPC1	3.36842	2.86229	1.24457	3.67032
MYO9B	3.20274	3.14437	1.20856	2.66726
SOCS1	3.06965	2.65086	1.31112	3.37385
TPBG	3.03726	3.7882	1.26595	3.45281
SLC15A1	2.76128	2.42382	1.2857	3.28669
TNFRSF11B	2.17107	1.94894	1.02276	1.82696
MRPS11	-2.07019	-1.63141	1.01607	-1.88649
ERCC6L	-2.50111	-2.21877	-1.13322	-1.9744
RICS	-2.78452	-2.32582	-1.10022	-2.76961
FZD1	-3.67286	-3.48945	-1.75885	-3.3002
SETBP1	-3.92599	-3.7889	-1.88683	-3.82427
HJURP	-4.36168	-3.5118	-2.16685	-3.73219
ADAM7	-4.61817	-3.61813	-1.74444	-4.66567
PALMD	-6.64709	-5.95581	-2.96025	-7.37101
EPOR	-8.17631	-7.08552	-3.23777	-6.75039
PPP1R3D	-8.58931	-9.61791	-4.1307	-9.6654
KIF2C	-9.36199	-8.47474	-4.45154	-7.66166
GRHL2	-11.9138	-12.659	-5.73562	-9.51378
TRIM48	-20.0484	-21.2956	-6.81481	-15.5338
SLITRK3	-20.4579	-19.6886	-6.96534	-18.1756
SMAD6	-20.6522	-17.6457	-8.34856	-17.7705
C8orf51	-21.3233	-24.3322	-8.48837	-22.1655
OSR2	-26.5443	-21.5834	-4.636	-20.4407
SPRY1	-60.0994	-53.9636	-17.4948	-59.9429

Table III.3 PKCδ-specific regulated genes. Applying stringent filters (reduction of PMA-induced fold change ≥ 1.5-fold upon knockdown of one PKC isozyme and < 1.25-fold upon knockdown of the two remaining PKC isozymes), 75 genes specific for PKCδ are identified.

Gene Symbol	Fold change (PMA vs. vehicle)			
	control siRNA	siRNA PKC alpha	siRNA PKC delta	siRNA PKC epsilon
BIRC3	171.118	147.828	203.254	75.6516
CYR61	157.834	188.299	125.911	78.7102
RGS2	23.621	18.067	24.0415	9.03592
AMIGO2	-2.7108	-2.29536	-2.09736	1.09313

Table III.4 **PKCε-specific regulated genes.** Applying stringent filters (reduction of PMA induced fold change ≥ 1.5-fold upon knockdown of one PKC isozyme and < 1.25-fold upon knockdown of the two remaining PKC isozymes), 4 genes specific for PKCε are identified.

III.2.9 Validation of microarray studies by RT-PCR

In order to validate the results obtained in the microarray studies, a subset of genes specifically regulated by PKCδ (*BCL2A1, FOSL1, TRAF1, SERPINB2, SPHK1, PPP1R15A*) was selected for their well known and important functions, such as apoptosis signaling or proliferation, as outlined below:

BCL2A1 encodes a member of the BCL-2 protein family. The proteins of this family form hetero- or homodimers. They act as anti- and pro-apoptotic regulators that are involved in a wide variety of cellular activities, including tumorigenesis. This gene is a direct transcription target of NF-κB in response to inflammatory mediators, and it is up-regulated by different extracellular signals, such as phorbol ester and the inflammatory cytokines TNFα and IL-1, which suggests a cytoprotective function essential for cell survival [101].

FOSL1 belongs to the Fos gene family which consists of 4 members (FOS, FOSB, FOSL1, and FOSL2). These genes encode proteins which are components of the transcription factor complex AP-1. FOS proteins have been implicated in cell proliferation, differentiation, and transformation [102, 103].

Tumor necrosis factor receptor-associated factors (TRAFs) are cytoplasmic adapter proteins that link a wide variety of cell surface receptors to the apoptotic signaling cascade [104]. Specifically, TRAF1 has been implicated in the modulation

of TNFα signaling and subsequent apoptosis, where it can exert both pro- and antiapoptotic effects [105].

SERPINB2, also known as Plasminogen activator inhibitor-2 (PAI-2) regulates proliferation and differentiation of monocytes [106]. Intracellular PAI-2 is an important factor in regulating cell death in TNFα-mediated inflammatory processes through inhibition of a proteinase involved in TNFα-induced apoptosis [107].

Sphingosine kinase (SPHK) is the enzyme that catalyzes the phosphorylation of sphingosine to sphingosine-1-phosphate (SPP), which is a lipid messenger with intracellular and extracellular functions, including proliferation and survival [108].

Protein phosphatase 1, regulatory (inhibitor) subunit 15A (PPP1R15A) is a member of a group of genes whose transcript levels are increased following stressful growth arrest conditions and treatment with DNA-damaging agents. The induction of this gene by ionizing radiation occurs in certain cell lines regardless of p53 status, and its protein response is correlated with apoptosis following ionizing radiation [109].

Quantitative RT-PCR was performed using primers specific for the aforementioned genes and cDNA transcribed from the RNA that has been initially obtained for the global gene expression analysis. There was a remarkable agreement between microarray data and qPCR analysis for all selected genes (Fig. III.19). This indicated a high degree of reliability of the genome-wide expression analysis on the one hand and highlighted the importance of PKCδ for the induction of these genes on the other.

FOSL1
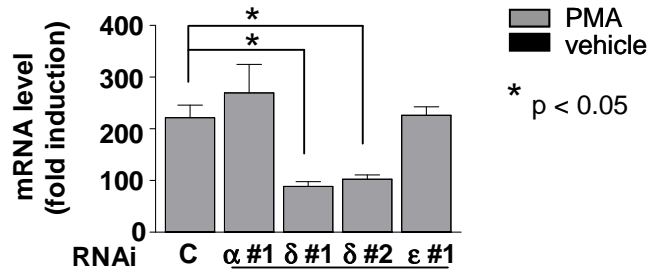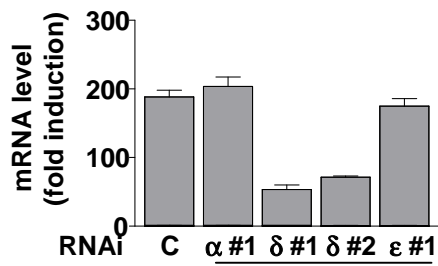
BCL2A1
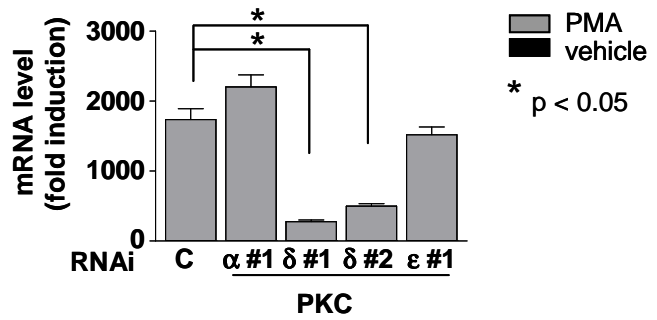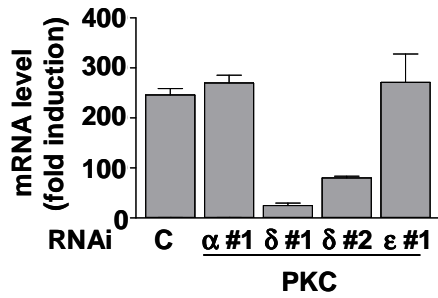
SERPINB2
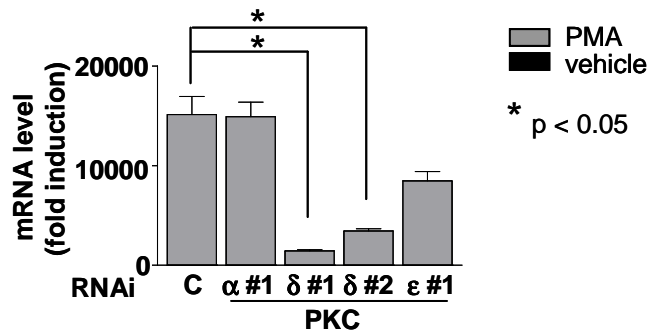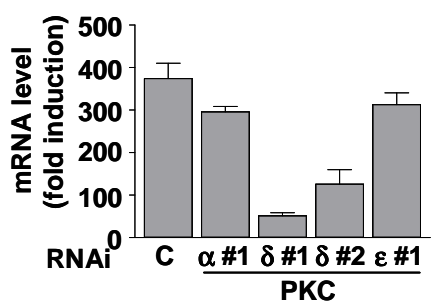
TRAF1
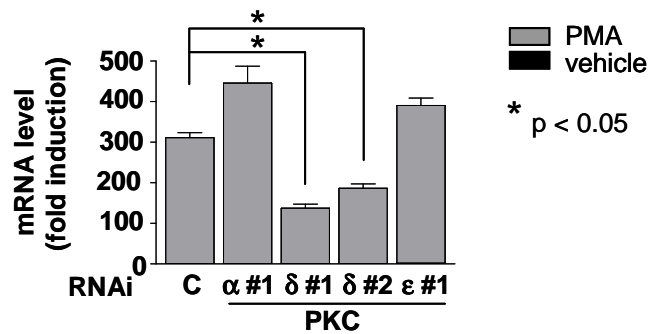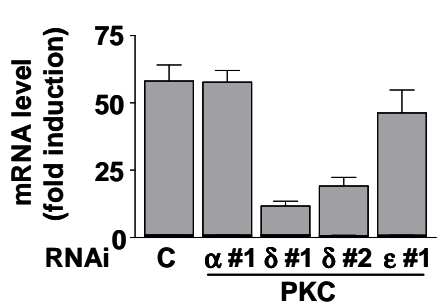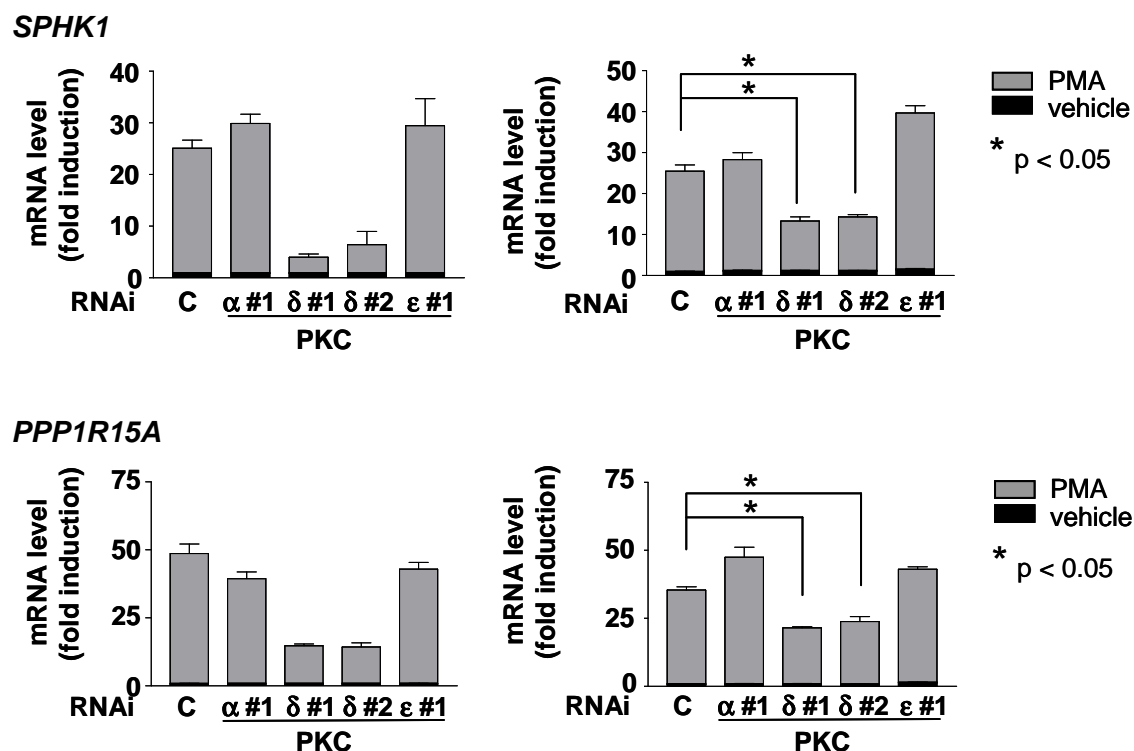
SPHK1

PPP1R15A

Figure III.19 Validation of microarray studies confirms a high reliability of the genome-wide expression analysis. GCRMA data of *FOSL1*, *BCL2A1*, *SERPINB2*, *TRAF1*, *SPHK1*, and *PPP1R15A* obtained in the microarray study were normalized to GAPDH (left side of each panel). Data of the quantitative RT-PCR were normalized to 18S (right side of each panel). In order to analyze PKCδ-specific genes two different RNAis for PKCδ were used. For control and the PKCα and PKCε isoforms one specific siRNA was used. Fold changes were referred to samples transfected with control RNAi and treated with vehicle. Data represent the mean ± S.E.M. of three independent experiments, *p<0.05.

III.2.10 Identification of novel genes implicated in PMA-induced and PKCδ-mediated apoptosis in LNCaP cells

As described earlier, PKCδ is the primary mediator of PMA-induced apoptosis in LNCaP cells. In order to determine the potential involvement of candidate genes in this effect, a selective RNAi-mediated knockdown experiment for 4 different PKCδ-regulated genes (*BCL2A1, FOSL1, TRAF1, SERPINB2)* was conducted. Transfection of the specific ON-TARGET®plus SMARTpool siRNAs into LNCaP cells prevented the up-regulation of each corresponding mRNA by PMA (Fig. III.20A).

Remarkably, siRNA against either *BCL2A1* or *FOSL1*, but not of *SERPINB2* and *TRAF1*, significantly reduced the apoptotic effect of PMA in LNCaP cells (Fig. III.20B).
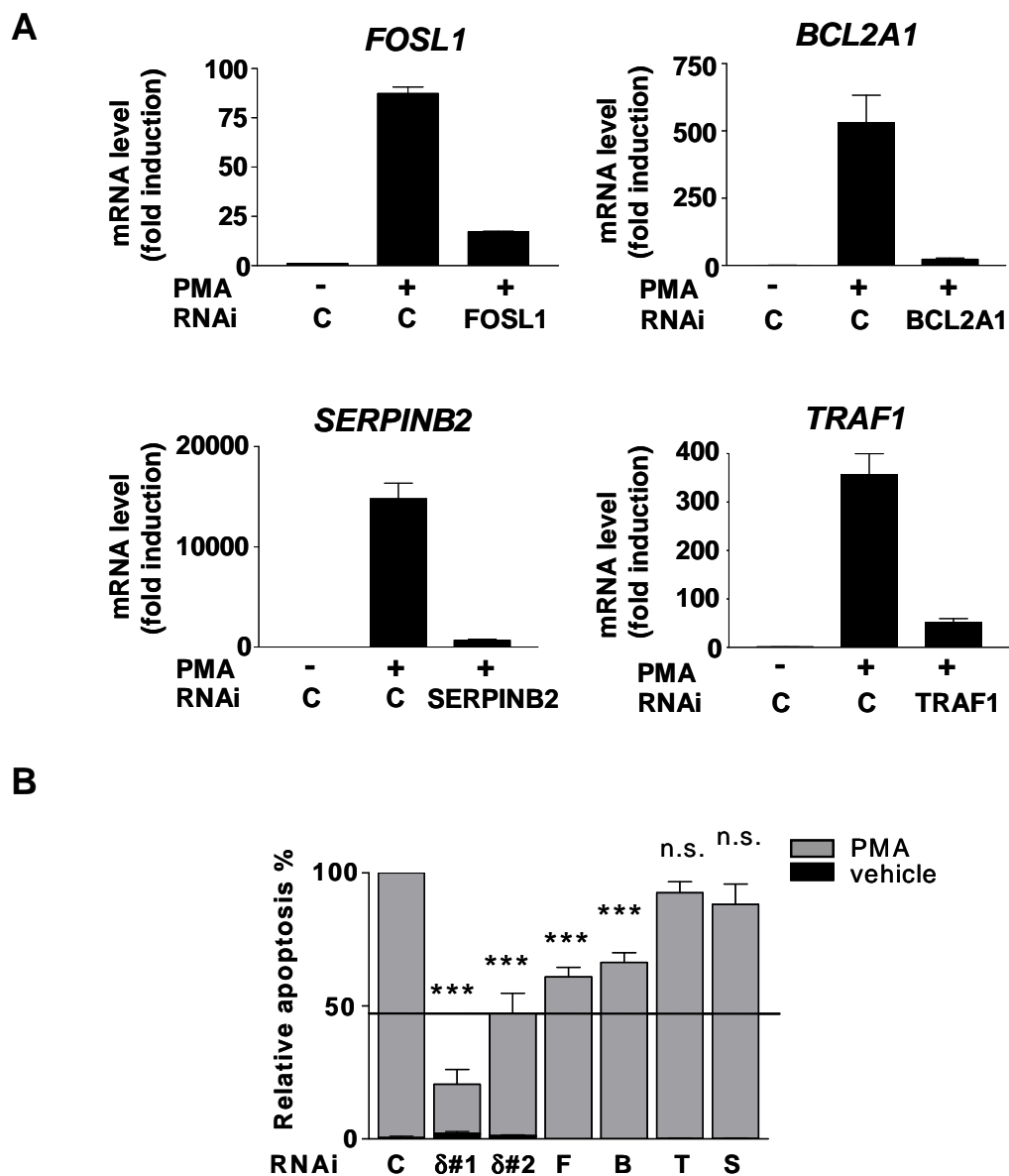
Figure III.20 *FOSL1*, *BCL2A1* **and PKCδ play an important role in PMA-induced apoptosis in LNCaP cells.** *Panel A.* RNA interference efficiently prevents an increase in mRNA levels of PKCδ-dependent genes as measured by quantitative RT-PCR. Data represent the mean ± S.E.M. of three independent experiments. *Panel B.* Percentage of apoptotic LNCaP cells was assessed 24 h after treatment with PMA (100 nM) by nuclear staining with DAPI. Similar to depletion of PKCδ, reduction of mRNA levels significantly reduces the PMA-induced apoptosis for *BCL2A1* (B) and *FOSL1* (F). Knockdown of *SERPINB2* (S) and *TRAF1* (T) does not significantly decrease PMA-induced apoptosis. Data represent the mean ± S.E.M. of three independent experiments, ***p<0.001.

To minimize the chance of "off-target" effects of RNAi we carried out additional experiments using two different RNAi duplexes for *FOSL1* and *BCL2A1*, and observed similar results (Fig. III.21A and B).

A
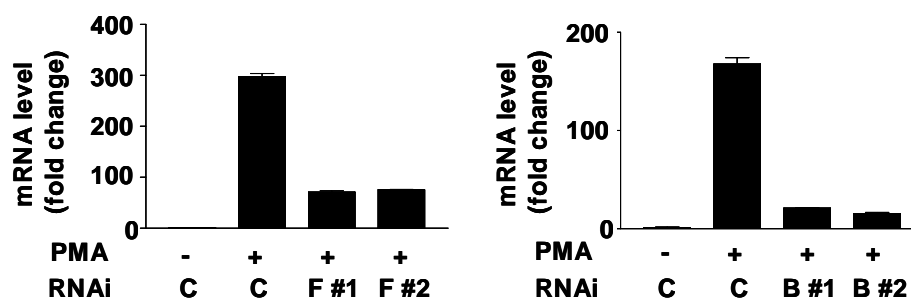
B
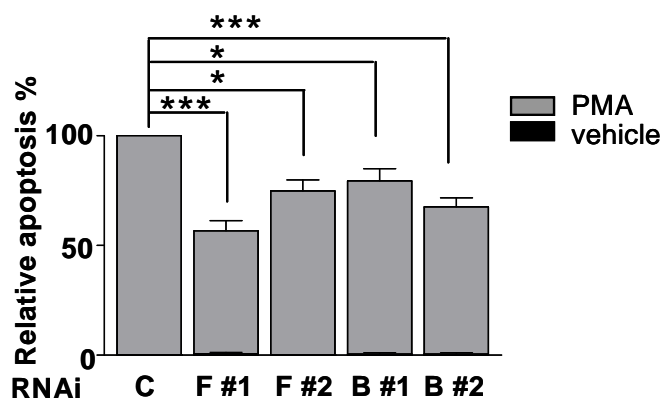
Figure III.21 *FOSL1* **and** *BCL2A1* **mediate PMA-induced apoptosis.** LNCaP cells transfected with one control RNAi duplex (240 pmol) or two different specific RNAi duplexes (240 pmol) for each gene were stimulated with PMA (100 nM). *Panel A.* RNA interference efficiently prevents an increase in mRNA levels of PKCδ-dependent genes. Data represent the mean ± S.E.M. of three independent experiments. *Panel B.* Percentage of apoptotic LNCaP cells was assessed 24 h after treatment with PMA (100 nM) by nuclear staining with DAPI. Data confirm the results obtained after transfection with SMARTpool RNAi for *FOSL1* and *BCL2A1*. Data represent the mean ± S.E.M. of three independent experiments, *p<0.05 and ***p<0.001.

III.2.11 PKCδ-mediated transcriptional regulation is required for etoposide-induced apoptosis

To further validate the genes regulated by PKCδ in PMA-induced apoptosis, and to further support the concept of PKCδ's involvement in gene regulation during programmed cell death, etoposide was used as a different means to induce apoptosis in LNCaP cells (Fig. III.22). Importantly, the involvement of PKCδ in up-regulation of candidate genes was confirmed in LNCaP cells subjected to etoposide treatment.
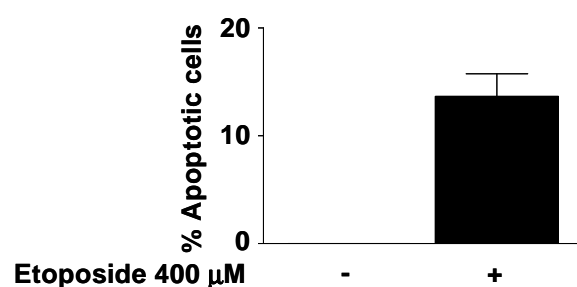

Figure III.22 Etoposide induces apoptosis in LNCaP cells. Induction of apoptosis by etoposide (400 µM) was assessed by staining with DAPI 5 h after treatment and evaluating cells for chromatin fragmentation. Data represent the mean ± S.E.M. of three independent experiments.

Interestingly, cells treated with etoposide showed a similar pattern of induction of *FOSL1, BCL2A1, SERPINB2* and *TRAF1* (Fig. III.23).
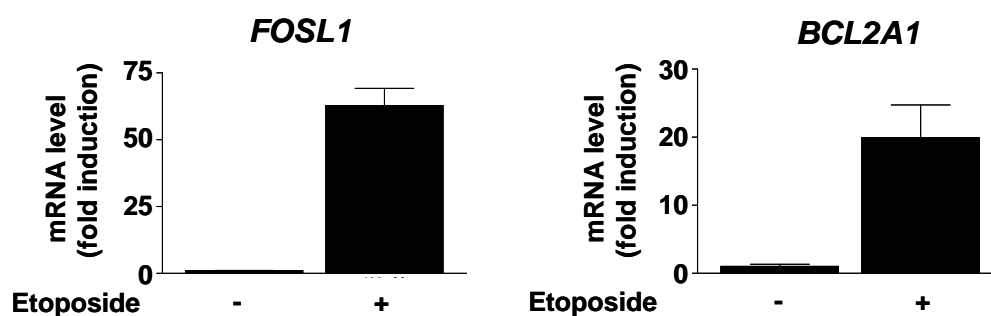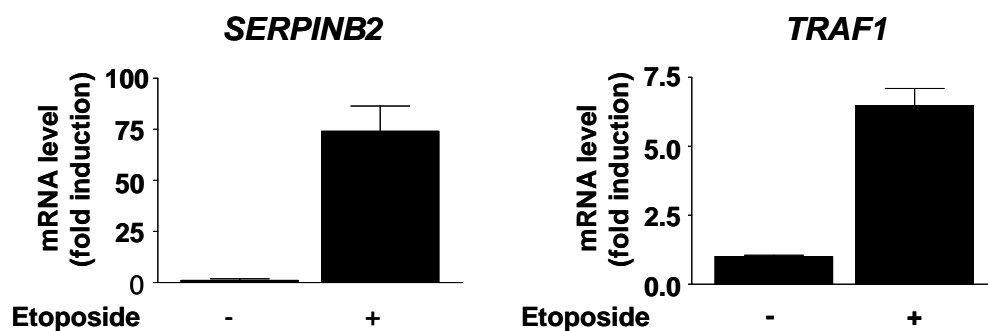
Figure III.23 Etoposide induces mRNA levels of *FOSL1*, *BCL2A1*, *SERPINB2* and *TRAF1* in LNCaP cells. Treatment of LNCaP cells with etoposide for 5 h (400µM) results in the induction of mRNA levels of *FOSL1*, *BCL2A1*, and *SERPINB2*. Data represent the mean ± S.E.M. of three independent experiments.

To evaluate the role of PKCδ in this model, knockdown of PKCδ was conducted prior to the induction of apoptosis with etoposide (Fig. III.24A). Reduced apoptosis could be observed when cells had been depleted of PKCδ (Fig. III.24B). This confirms that PKCδ is a strong mediator of etoposide-induced apoptosis in LNCaP cells, as described for other cell types [110, 111]. Most importantly, silencing of PKCδ blunted mRNA induction of all of the four candidate genes by etoposide. (Fig. III.24C).
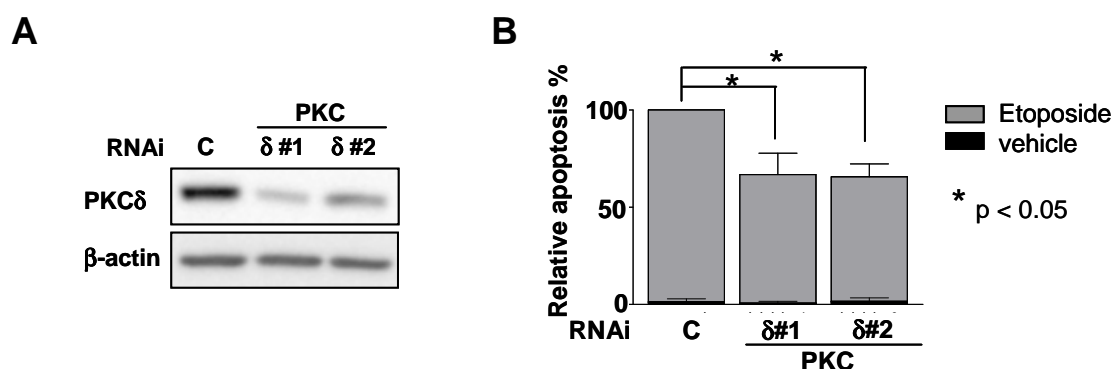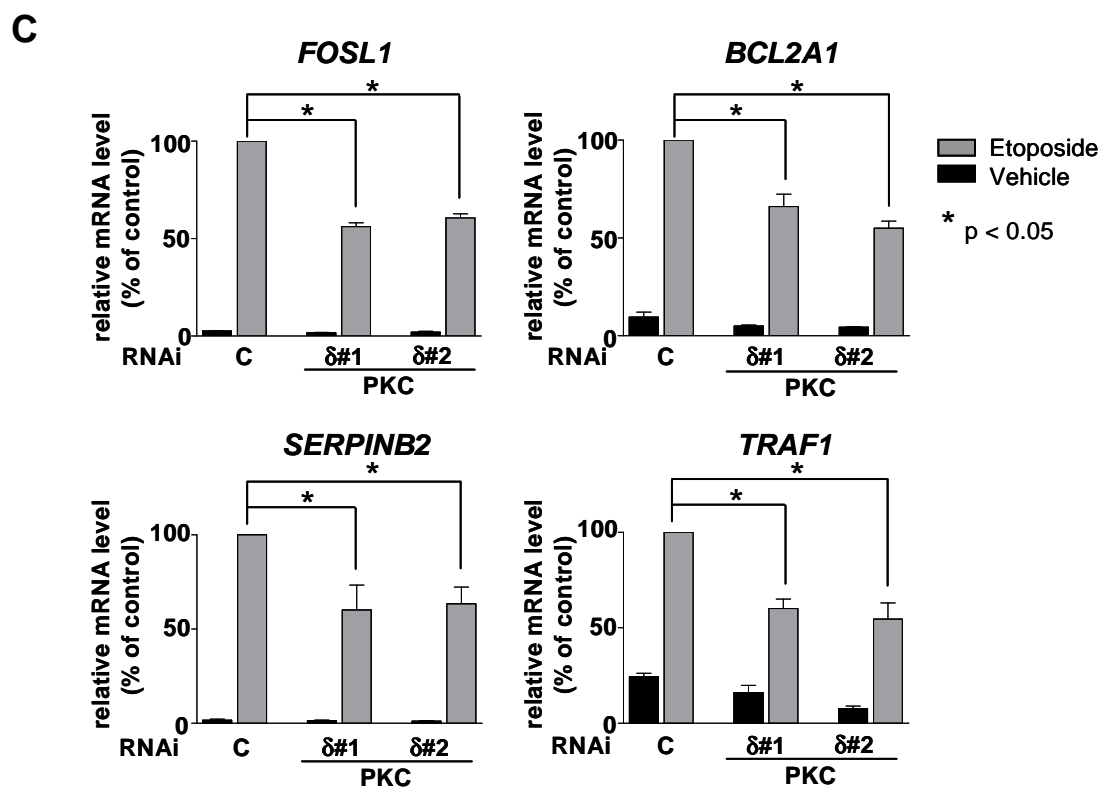
Figure III.24 *FOSL1, BCL2A1, SERPINB2* and *TRAF1* **are induced by etoposide in a PKCδ-dependent manner.** *Panel A.* Western blot analysis shows sufficient knockdown of PKCδ. *Panel B.* Treatment of LNCaP cells transfected with two separate siRNAs for PKCδ (120 pmol) with etoposide (400 µM) reduces apoptosis. Apoptosis was determined 48 h after stimulation with etoposide (400 µM), showing a significant reduction for the samples depleted of PKCδ. *Panel C.* Treatment of LNCaP cells with etoposide (400 µM) reveals a significant PKCδ dependent induction of *FOSL1*, *BCL2A1*, *SERPINB2*, and *TRAF1*. The induction of all four genes is significantly reduced when PKCδ is silenced. Samples transfected with control siRNA and treated with etoposide were arbitrarily set to 100%. Data represent the mean ± S.E.M. of three independent experiments, *p<0.05.

IV DISCUSSION

IV.1 Bryostatin 1 inhibits PMA-induced apoptosis in LNCaP cells

Bryostatin 1, a macrocylic lactone derived from the marine species *Bugula neritina*, has been reported previously to exert anti-proliferative and apoptotic effects in numerous cancer cell lines [112-114]. Moreover, it has been used successfully for tumor treatment in animal studies [69, 71] and is currently being investigated in clinical trials against various solid tumor as well as hematologic malignancies [73, 74, 76, 77]. However, the effect of bryostatin 1 on prostate cancer cells is unknown. Bryostatin 1 is a potent ligand at the C1 domain of PKCs, similar to the phorbol ester PMA, which is known to induce apoptosis in the prostate cancer cell line LNCaP. Given the described anti-cancer effects of bryostatin 1 on the one hand and the pro-apoptotic effect of PMA on LNCaP cells on the other, one aim of this study was to assess the effect of bryostatin 1 on LNCaP prostate cancer cells on its own and whether it augments, attenuates or does not affect PMA-induced apoptosis in this cell line.

To validate previous findings, LNCaP cells were first treated with PMA alone. Here, PMA increased the rate of apoptosis in a dose-dependent manner. Based on this finding, the concentration of PMA used for further experiments was determined to be 100 nM. In contrast, bryostatin 1 failed to induce apoptosis at any used concentration. More importantly, bryostatin 1 decreased and ultimately blocked PMA-induced apoptosis in LNCaP cells dose-dependently. Remarkably, the expression levels of the anti-apoptotic proteins MCL1, BCL-XL and BCL-2 were not found to be altered, suggesting that bryostatin 1 does not act through the induction of *de novo* synthesis of these proteins. Also the well-described phosphorylation of p38 and dephosphorylation of pAkt by PMA were unaffected by bryostatin 1, indicating that at least a subset of PMA-induced effects were still executed.

Another well-known effect of PMA is the release of TNFα and other factors from LNCaP cells. Therefore, the question whether bryostatin 1 affects the composition of the conditioned medium (CM) was addressed. Indeed, whereas CM-PMA was capable of inducing apoptosis in naïve LNCaP cells, CM-Bryo1 and, more importantly, CM-Bryo1+PMA failed to induce apoptosis. As with cells that are directly treated with PMA and bryostatin 1, cells that received CM-Bryo1+PMA still exhibited phosphorylation of p38, which was maintained over several hours, as well as phosphorylation of JNK and dephosphorylation of pAkt. Taken together, these data are in favor with the hypothesis that bryostatin 1 prevents PMA from triggering the release of pro-apoptotic factors to the CM, while others are still being secreted and are capable of triggering a cascade that leads ultimately to the phosphorylation of p38 and JNK and dephosphorylation of pAkt, respectively. Although a cytokine array did not reveal any obvious difference in the secretion of pro-apoptotic factors, probably due to issues of sensitivity [94], a more accurate measurement employing ELISA revealed that PMA-induced secretion of TNFα is essentially blunted by bryostatin 1. PMA, in turn, depends on the autocrine secretion of this cytokine for killing prostate cancer cells [57]. The impaired TNFα secretion by PMA when cells are simultaneously treated with bryostatin 1 seems to fully account for the functional antagonism. Indeed, adding back this cytokine at similar final concentrations as those normally observed in CM-PMA fully restores the apoptotic activity. It is interesting that bryostatin 1 promotes apoptosis and TNFα release from leukemia cells [115, 116], suggesting a strict cell type dependency for the differential killing ability of this agent.

Our laboratory established that TNFα release from prostate cancer cells induced by PMA is mediated by PKCδ [57]. This paradigm has been recently validated in vascular smooth muscle cells [117]. Moreover, it appears that none of the other PKC isozymes expressed in LNCaP cells can compensate for the loss of

PKCδ, as the single knockdown of PKCδ decreased both the rate of apoptosis and the release of TNFα followed by treatment with PMA. These findings highlight PKCδ to be the most critical PKC isozyme in mediating PMA-induced apoptosis in LNCaP cells. It is a well known phenomenon that PKCδ needs to be translocated to the plasma membrane in a fashion as depicted in Fig. I.7. This raised the question whether translocation to the plasma membrane and subsequent activation of PKCδ is impaired upon treatment with bryostatin 1. As a matter of fact, bryostatin 1 selectively translocated PKCδ, but not PKCα or PKCε, to the nuclear membrane and importantly, almost completely blocked PMA-induced translocation of PKCδ to the plasma membrane. One possible explanation by which this prevents the release of TNFα is the necessity of TACE/ADAM17 phosphorylation (TNFα converting enzyme). As TACE is a membrane bound enzyme [118], phosphorylation could either happen directly through PKCδ or by PKC downstream effector kinases, as previously reported [119]. Either way, the data presented here demonstrate that relocalization of PKCδ to the plasma membrane of LNCaP cells is required for promoting an apoptotic response. Remarkably, expression of a membrane (myr) targeted PKCδ in LNCaP cells is sufficient to promote apoptosis, and conversely limiting the access of PKCδ to the plasma membrane prevents the apoptotic effect of PMA.

The ability of bryostatin 1 to differentially translocate PKC isozymes is a well-documented phenomenon. Early studies using GFP-tagged PKCs revealed distinctive patterns of translocation for PKC isozymes in living cells in response to different PKC activators and other stimuli. In this regard, it is striking that ligands that are all capable of binding with high affinity to the C1 domains confer such distinct patterns of PKC relocalization, a paradox that is particularly observed for PKCδ [82, 120]. The pattern of translocation of PKCδ in LNCaP cells resembles that observed originally in CHO cells, in which bryostatin 1 translocates PKCδ predominantly to the nuclear membrane [82]. Our studies revealed that in LNCaP cells bryostatin 1

prevents PKCδ translocation to the plasma membrane by PMA while still allowing for nuclear membrane relocalization of PKCδ, and without significantly affecting translocation of PKCα or PKCε to the plasma membrane. The circumstance that some of the PMA-induced effects were still observed in LNCaP cells, *i.e.* phosphorylation of p38 and JNK as well as dephosphorylation of pAkt, is in line with the observation that bryostatin 1 specifically affects PKCδ activity, but not the function of PKCα or PKCε. As reported previously, PKCα significantly contributes to the phosphorylation of p38 and the dephosphorylation of pAkt [57] (see Fig. I.9). On the other hand, these findings indicate that activation of p38 and inactivation of Akt may be required for apoptosis in LNCaP cells, but these events are not sufficient for the induction of apoptosis on their own.

The results reported here strongly support the hypothesis that bryostatin 1 exerts its anti-apoptotic effects in LNCaP cells through a functional antagonism driven by mislocalization of PKCδ, ultimately restraining the access of this kinase to plasma membrane substrates. The basis for the differential subcellular translocation by PMA and bryostatin 1 remains to be determined. The interactions between the C1 domain in PKCs, C1 domain ligands, and the lipid bilayers are complex and not totally understood.

Previous studies conducted by Peter Blumberg and co-workers established that a key determinant for conferring ligand selectivity for PKC translocation is lipophilicity [120]. It is tempting to speculate that the differential relocalization pattern of PKCδ by PMA and bryostatin 1 is due to distinct hydrophobic interactions with the lipid bilayer. Binding of a C1 ligand into a hydrophilic cleft at the C1 domain leads to an overall more hydrophobic composition of this domain, thus allowing for lipophilic interactions with the plasma membrane and the subsequent insertion of this domain into the lipid bilayer. Additional interactions between the side-chains of the ligand and the membrane may be therefore key for dictating intracellular selectivity through specific

association with membrane components. Another mechanism by which localization of PKCδ may be differentially regulated is that binding of different ligands confers differential interaction between PKCδ and various interacting proteins, which then direct the kinase to distinct localizations within the cell.

Taken together, the data presented here indicate that bryostatin 1 does not induce apoptosis in the prostate cancer cell line LNCaP and impairs the PKCδ-dependent release of TNFα, thereby attenuating the apoptotic effect of PMA. As several chemotherapeutic agents depend on PKCδ to promote prostate cancer cell death [121], these data suggest that bryostatin 1 may have limited effectiveness in combination therapies with certain anti-cancer agents for prostate cancer treatment.

IV.2 PKC regulation of gene expression

Given the overall importance of PKC isozymes in triggering PMA-induced apoptosis, the question whether PKC activation in general and isozyme-specific activation in particular has an impact on transcriptional regulation in LNCaP cells in the context of PMA-induced apoptosis was addressed. Treatment of LNCaP cells with the protein synthesis inhibitor Chx prior to the application of PMA resulted in a signifcantly reduced apoptotic effect of PMA, suggesting that triggering the apoptotic process requires *de novo* synthesis of proteins and therefore, presumably, of mRNA as well. In our study we focused on three different aspects: (1) The time-course of changes in global gene expression after PMA treatment; (2) Classification of the response to PMA exposure in biological functions (Gene Ontologies) and (3) Functional relevance of PKC isozymes on gene expression in LNCaP cells.

By conducting a longitudinal study observing changes of global gene expression over 24 h after exposure to PMA, it was possible to determine that major changes take place initially after drug exposure and reach their peak within 4 h. At later stages, alterations in gene expression can be observed only in a relatively small proportion of genes. Investigating changes in gene expression in relation to PMA-induced apoptosis at 4 h allowed for the maximum of altered genes to be included and reduced the evaluation of secondary regulated genes, which are likely to be included at later stages. Of the genes regulated in this time frame most are related to signal transduction and modulation of transcription, indicating profound changes in essential cell fate determinants. In conclusion, genome-wide expression analysis in combination with exposure to a specific drug can be useful for further analysis of specific signaling pathways in response to this particular drug.

To determine the role of PKC isozyme-specific functions, knockdown of PKCα, PKCδ or PKCε was successfully achieved using RNAi and subsequent gene expression analysis was carried out in response to PMA. Although stable knockdown

is desirable, it is not feasible in this model as LNCaP cells transition from an androgen-dependent state to an androgen-independent state upon long-term culturing. This, in turn, affects the response to PMA [122, 123]. The robustness of the microarray experiments is underscored by the high similarity between genes regulated by PMA after 4 h in the longitudinal microarray study and the genes regulated by PMA in the sample using control siRNA. A rough estimate of variability in gene expression across the whole genome was obtained by principal component analysis (PCA), which revealed profound changes between PMA- and vehicle-treated LNCaP cells. Importantly, comparison of PCA for samples transfected with either control RNAi or PKC isoform-specific RNAi revealed that PKCδ-depleted samples were differentially positioned, suggesting a high number of genes specifically regulated by this isoform in the context of PMA induced apoptosis. Most interestingly, distinct, stimulus-dependent roles for PKC isozymes were identified. In cells not exposed to PMA (only growing in normal medium containing FBS), knockdown of PKCε evoked the largest change in gene expression. Moreover, depletion of this isoform resulted predominantly in up-regulation, rather than down-regulation of genes. These data suggest that PKCε may function in favor of a normal, proliferative state in line with previous descriptions as a mitogenic and pro-survival kinase. PKCε has been linked to prostate cancer progression in particular [10, 96, 124-127] and has been assigned to oncogenic functions in a broad variety of tissues [128]. In contrast to these observations, exposure to PMA, which is followed by apoptosis in LNCaP cells, is accompanied by changes in gene expression that are primarily mediated by PKCδ. Interestingly, and in opposite to PKCε, PKCδ alters the gene expression levels predominantly by up-regulation. Taken together, these findings suggest that the pro-survival kinase PKCε may act as a more repressing kinase, as depletion of PKCε from LNCaP cells resulted in up-regulation of gene expression. In contrast, the pro-apoptotic kinase PKCδ predominantly controls pathways that lead to the activation of

gene transcription. Moreover, our results suggest that PKCε may be more relevant in controlling gene expression under "physiological" conditions whereas PKCδ may have relevant roles in response to phorbol ester stimulation.

To narrow the number of genes regulated by PKC isozymes, more stringent criteria were applied (reduction of PMA-induced fold change ≥ 1.5-fold upon knockdown of one PKC isozyme and < 1.25-fold upon knockdown of the two remaining PKC isozymes). This analysis revealed that 75 PMA-regulated genes were specifically induced by PKCδ, whereas PKCα and PKCε had negligible impact on gene expression. This finding confirms the results obtained in the principal component analysis and argues for PKCδ as a master regulator of the genome in the response to phorbol ester stimulation.

To further validate the data generated in the microarray experiments, quantitative RT-PCR (qRT-PCR) was performed on PKCδ-regulated genes (*BCL2A1, FOSL1, TRAF1, SERPINB2, SPHK1, PPP1R15A*), which were chosen upon their already known involvement in the control of apoptosis. The remarkable agreement between microarray data and qRT-PCR analysis for all selected genes is indicative of a high degree of accuracy and reliability of the genome-wide expression analysis.

Given the importance of selected PKCδ-regulated genes in apoptosis, it was of interest to evaluate their functional relevance in PMA-induced apoptosis in LNCaP cells. To achieve this goal, LNCaP cells had to be transfected with pooled siRNA prior to the treatment with PMA, so that the interfering RNA was already present at the onset of gene transcription, thus preventing an increase of the mRNA. Indeed, this approach proved to be successful, as mRNA levels of genes of interest could be blunted in the presence of siRNA and PMA. Knockdown of some genes regulated by PKCδ, but not all, was able to reduce the apoptotic response of PMA. The results showed that none of the single knockdowns prevented PMA-induced apoptosis as efficiently as the depletion of PKCδ. This observation may have two reasons. First,

PKCδ signaling results in the transcription of multiple genes that synergistically act on the activation of apoptosis, and second, phosphorylation of target proteins by PKCδ may lead to other pro-apoptotic functions than transcriptional regulation. However, these two processes might not be independent from each other. As already demonstrated in this study, PKCδ is critical for the release of TNFα, which leads to the assembly of the DISC and subsequently to caspase activation on the one hand. On the other hand, binding of TNFα to its receptor can lead to the activation of transcription, in part through the NFκB pathway [129]. Indeed, *SERPINB2, FOSL1* and *BCL2A1* have been described to undergo transcriptional activation in response to TNFα treatment, and BCL2A1 is a known target of the NFκB pathway [101, 102, 130].

Since above-mentioned knockdown studies had been conducted with pooled siRNA targeting multiple sequences of the same mRNA, there was a possibility that off-target effects might have occurred. To reduce the potential impact of off target effects of pooled siRNA, knockdown of *FOSL1* and *BCL2A1* was also performed using two separate siRNAs. Again, transfection of a single siRNA prevented gene induction and apoptosis by PMA, suggesting specific involvement of these genes.

The fact that etoposide-induced apoptosis requires PKCδ as well as the induction of PKCδ target genes in a similar manner as it is required for PMA-induced apoptosis serves as a proof of concept and suggests that a general involvement of PKCδ upstream of the pro-apoptotic signaling is mandatory for the induction of apoptosis [131]. In addition, the requirement of PKCδ in etoposide-induced apoptosis indicates a stimulus-independent function for PKCδ as a regulator of apoptosis. Although there is some evidence that *BCL2A1* may be influenced by the PLC-DAG-PKC signaling axis [132], the involvement of this gene in the positive regulation of apoptosis is a surprising result as the majority of reports demonstrate an anti-apoptotic function for *BCL2A1* [132, 133]. *FOSL1* is a member of the AP-1

transcription complex and is also known to support growth and survival in transformed cells [134]. In addition, knockdown of FOSL1 induces apoptosis in a variety of cancer cells [135]. However, overexpression of *FOSL1* in glioblastoma cells induces apoptosis [136] and increases the sensitivity against erlotinib, an inhibitor of the EGFR signaling pathway [137]. This and the results shown here indicate that biological functions of certain gene products may vary dependent on the cellular context rather than on the apoptotic stimulus, as shown by concomitant increase of apoptosis and up-regulation of *BCL2A1* and *FOSL1* by both PKCδ-dependent apoptosis-inducing agents, PMA and etoposide.

Taken together, this is the first comprehensive evaluation of transcriptional dynamics of LNCaP cells in response to the PKC activator PMA. In addition, genome-wide expression analysis revealed distinct roles for PKC isozymes during normal growth/proliferation and apoptosis and how signaling molecules impact the regulation of transcription in a genome-wide scale.

V SUMMARY

Prostate cancer is the leading cause of cancer related deaths in men in the United States and is characterized by altered expression patterns of PKC isozymes, among other genetic and epigenetic disturbances. PKCs are involved in multiple cellular processes including cell survival, proliferation, apoptosis and differentiation. The current concept is that the effect is isozyme-, cell type- and stimulus-dependent. Activation of PKCs occurs through binding of ligands to their C1 domain and can be of endogenous (DAG) or exogenous (PMA, bryostatin 1) nature. Treatment of LNCaP prostate cancer cells with PMA resulted in apoptosis. However, application of a different C1 ligand, bryostatin 1, did not induce apoptosis. More importantly, bryostatin 1 blocked PMA induced apoptosis, as it prevented the PMA-induced release of TNFα. Of all DAG-reponsive PKC isozymes in LNCaP cells PKCδ was shown to be critical for the induction of apoptosis and release of TNFα. Translocation to the plasma membrane of this PKC isozyme is required for the PMA-induced release of TNFα from this cell line. The data presented here show that bryostatin 1 prevented proper translocation of PKCδ, but not of PKCα or PKCϵ, by PMA. Thus, PKCδ acts as a master regulator of apoptosis and is misdirected by bryostatin 1, thereby preventing PMA-induced apoptosis. In addition, PKCs are involved in the regulation of transcription. In the first comprehensive evaluation of transcriptional dynamics in response to PMA in the present study microarray analysis revealed distinct roles of PKC isozymes during normal growth and apoptosis. Furthermore, it was shown how signaling molecules affect expression patterns and novel downstream targets of PKCδ were identified that are directly involved in apoptosis. On the basis of these results it is tempting to speculate that loss or dysfunction of PKCδ contributes to the diminished apoptotic response of prostate cancer cells and that restoration of PKCδ might be of therapeutic benefit. In addition, the results

indicate that bryostatin 1 may have limited effectiveness in the treatment of prostate

cancer in humans.

VI REFERENCES

1.   Jemal, A., et al., *Cancer Statistics, 2010.* CA Cancer J Clin.

2.   Wang, S., et al., *Prostate-specific deletion of the murine Pten tumor suppressor gene leads to metastatic prostate cancer.* Cancer Cell, 2003. **4**(3): p. 209-21.

3.   Majumder, P.K., et al., *Prostate intraepithelial neoplasia induced by prostate restricted Akt activation: the MPAKT model.* Proc Natl Acad Sci U S A, 2003. **100**(13): p. 7841-6.

4.   Cao, C., et al., *Inhibition of mammalian target of rapamycin or apoptotic pathway induces autophagy and radiosensitizes PTEN null prostate cancer cells.* Cancer Res, 2006. **66**(20): p. 10040-7.

5.   Hofmann, J., *Protein kinase C isozymes as potential targets for anticancer therapy.* Curr Cancer Drug Targets, 2004. **4**(2): p. 125-46.

6.   Cornford, P., et al., *Protein kinase C isoenzyme patterns characteristically modulated in early prostate cancer.* Am J Pathol, 1999. **154**(1): p. 137-44.

7.   Powell, C.T., et al., *Persistent membrane translocation of protein kinase C alpha during 12-0-tetradecanoylphorbol-13-acetate-induced apoptosis of LNCaP human prostate cancer cells.* Cell Growth Differ, 1996. **7**(4): p. 419-28.

8.   Koren, R., et al., *Expression of protein kinase C isoenzymes in benign hyperplasia and carcinoma of prostate.* Oncol Rep, 2004. **11**(2): p. 321-6.

9.   Aziz, M.H., et al., *Protein kinase Cvarepsilon mediates Stat3Ser727 phosphorylation, Stat3-regulated gene expression, and cell invasion in various human cancer cell lines through integration with MAPK cascade (RAF-1, MEK1/2, and ERK1/2).* Oncogene.

10.   Wu, D., et al., *Protein kinase cepsilon has the potential to advance the recurrence of human prostate cancer.* Cancer Res, 2002. **62**(8): p. 2423-9.

11.   Xiao, L., et al., *Phorbol ester-induced apoptosis and senescence in cancer cell models.* Methods Enzymol, 2008. **446**: p. 123-39.

12.   He, H., et al., *Phorbol ester phorbol-12-myristate-13-acetate induces epithelial to mesenchymal transition in human prostate cancer ARCaP(E) cells.* Prostate.

13.   Metzger, E., et al., *Phosphorylation of histone H3T6 by PKCbeta(I) controls demethylation at histone H3K4.* Nature. **464**(7289): p. 792-6.

14.   Fujii, T., et al., *Involvement of protein kinase C delta (PKCdelta) in phorbol ester-induced apoptosis in LNCaP prostate cancer cells. Lack of proteolytic cleavage of PKCdelta.* J Biol Chem, 2000. **275**(11): p. 7574-82.

15.   Taylor, R.C., S.P. Cullen, and S.J. Martin, *Apoptosis: controlled demolition at the cellular level.* Nat Rev Mol Cell Biol, 2008. **9**(3): p. 231-41.

16.   Riedl, S.J. and G.S. Salvesen, *The apoptosome: signalling platform of cell death.* Nat Rev Mol Cell Biol, 2007. **8**(5): p. 405-13.

17.   Browne, K.A., et al., *Cytosolic delivery of granzyme B by bacterial toxins: evidence that endosomal disruption, in addition to transmembrane pore formation, is an important function of perforin.* Mol Cell Biol, 1999. **19**(12): p. 8604-15.

18.   Froelich, C.J., V.M. Dixit, and X. Yang, *Lymphocyte granule-mediated apoptosis: matters of viral mimicry and deadly proteases.* Immunol Today, 1998. **19**(1): p. 30-6.

19.   Froelich, C.J., et al., *New paradigm for lymphocyte granule-mediated cytotoxicity. Target cells bind and internalize granzyme B, but an endosomolytic agent is necessary for cytosolic delivery and subsequent apoptosis.* J Biol Chem, 1996. **271**(46): p. 29073-9.

20.   Sarin, A., et al., *Target cell lysis by CTL granule exocytosis is independent of ICE/Ced-3 family proteases.* Immunity, 1997. **6**(2): p. 209-15.

21.   Trapani, J.A., et al., *Efficient nuclear targeting of granzyme B and the nuclear consequences of apoptosis induced by granzyme B and perforin are caspase-dependent, but cell death is caspase-independent.* J Biol Chem, 1998. **273**(43): p. 27934-8.

22.   Froelich, C.J., et al., *Granzyme B/perforin-mediated apoptosis of Jurkat cells results in cleavage of poly(ADP-ribose) polymerase to the 89-kDa apoptotic fragment and less abundant 64-kDa fragment.* Biochem Biophys Res Commun, 1996. **227**(3): p. 658-65.

23.   Beresford, P.J., et al., *Granzyme A loading induces rapid cytolysis and a novel form of DNA damage independently of caspase activation.* Immunity, 1999. **10**(5): p. 585-94.

24.   Beresford, P.J., et al., *Granzyme A activates an endoplasmic reticulum-associated caspase-independent nuclease to induce single-stranded DNA nicks.* J Biol Chem, 2001. **276**(46): p. 43285-93.

25.   Fan, Z., et al., *Tumor suppressor NM23-H1 is a granzyme A-activated DNase during CTL-mediated apoptosis, and the nucleosome assembly protein SET is its inhibitor.* Cell, 2003. **112**(5): p. 659-72.

26.   Orrenius, S., B. Zhivotovsky, and P. Nicotera, *Regulation of cell death: the calcium-apoptosis link.* Nat Rev Mol Cell Biol, 2003. **4**(7): p. 552-65.

27.   Danial, N.N. and S.J. Korsmeyer, *Cell death: critical control points.* Cell, 2004. **116**(2): p. 205-19.

28.   Riedl, S.J. and Y. Shi, *Molecular mechanisms of caspase regulation during apoptosis.* Nat Rev Mol Cell Biol, 2004. **5**(11): p. 897-907.

29.   Kim, H.E., et al., *Formation of apoptosome is initiated by cytochrome c-induced dATP hydrolysis and subsequent nucleotide exchange on Apaf-1.* Proc Natl Acad Sci U S A, 2005. **102**(49): p. 17545-50.

30.   Yu, X., et al., *A structure of the human apoptosome at 12.8 A resolution provides insights into this cell death platform.* Structure, 2005. **13**(11): p. 1725-35.

31.   Yoshida, H., et al., *Apaf1 is required for mitochondrial pathways of apoptosis and brain development.* Cell, 1998. **94**(6): p. 739-50.

32.   Ammelburg, M., T. Frickey, and A.N. Lupas, *Classification of AAA+ proteins.* J Struct Biol, 2006. **156**(1): p. 2-11.

33.   Canman, C.E., et al., *Activation of the ATM kinase by ionizing radiation and phosphorylation of p53.* Science, 1998. **281**(5383): p. 1677-9.

34.   Khanna, K.K. and S.P. Jackson, *DNA double-strand breaks: signaling, repair and the cancer connection.* Nat Genet, 2001. **27**(3): p. 247-54.

35.   Chehab, N.H., et al., *Phosphorylation of Ser-20 mediates stabilization of human p53 in response to DNA damage.* Proc Natl Acad Sci U S A, 1999. **96**(24): p. 13777-82.

36.   Siliciano, J.D., et al., *DNA damage induces phosphorylation of the amino terminus of p53.* Genes Dev, 1997. **11**(24): p. 3471-81.

37.   Yu, J. and L. Zhang, *The transcriptional targets of p53 in apoptosis control.* Biochem Biophys Res Commun, 2005. **331**(3): p. 851-8.

38.   Baldwin, E.L. and N. Osheroff, *Etoposide, topoisomerase II and cancer.* Curr Med Chem Anticancer Agents, 2005. **5**(4): p. 363-72.

39.   Yoshida, K., et al., *Protein kinase C delta activates topoisomerase IIalpha to induce apoptotic cell death in response to DNA damage.* Mol Cell Biol, 2006. **26**(9): p. 3414-31.

40.   Lowe, S.W., et al., *p53-dependent apoptosis modulates the cytotoxicity of anticancer agents.* Cell, 1993. **74**(6): p. 957-67.

41.   Griner, E.M. and M.G. Kazanietz, *Protein kinase C and other diacylglycerol effectors in cancer.* Nat Rev Cancer, 2007. **7**(4): p. 281-94.

42.   Kazanietz, M.G., *Targeting protein kinase C and "non-kinase" phorbol ester receptors: emerging concepts and therapeutic implications.* Biochim Biophys Acta, 2005. **1754**(1-2): p. 296-304.

43.   Newton, A.C., *Regulation of the ABC kinases by phosphorylation: protein kinase C as a paradigm.* Biochem J, 2003. **370**(Pt 2): p. 361-71.

44.   Dutil, E.M., et al., *In vivo regulation of protein kinase C by trans-phosphorylation followed by autophosphorylation.* J Biol Chem, 1994. **269**(47): p. 29359-62.

45.   Hansra, G., et al., *Multisite dephosphorylation and desensitization of conventional protein kinase C isotypes.* Biochem J, 1999. **342 (Pt 2)**: p. 337-44.

46.   Hansra, G., et al., *12-O-Tetradecanoylphorbol-13-acetate-induced dephosphorylation of protein kinase Calpha correlates with the presence of a membrane-associated protein phosphatase 2A heterotrimer.* J Biol Chem, 1996. **271**(51): p. 32785-8.

47.   Sontag, E., J.M. Sontag, and A. Garcia, *Protein phosphatase 2A is a critical regulator of protein kinase C zeta signaling targeted by SV40 small t to*

promote cell growth and NF-kappaB activation. Embo J, 1997. **16**(18): p. 5662-71.

48.   England, K., et al., *Signalling pathways regulating the dephosphorylation of Ser729 in the hydrophobic domain of protein kinase Cepsilon upon cell passage.* J Biol Chem, 2001. **276**(13): p. 10437-42.

49.   Prevostel, C., et al., *Protein kinase C(alpha) actively downregulates through caveolae-dependent traffic to an endosomal compartment.* J Cell Sci, 2000. **113 (Pt 14)**: p. 2575-84.

50.   Lee, H.W., et al., *Bryostatin 1 and phorbol ester down-modulate protein kinase C-alpha and -epsilon via the ubiquitin/proteasome pathway in human fibroblasts.* Mol Pharmacol, 1997. **51**(3): p. 439-47.

51.   Lu, Z., et al., *Activation of protein kinase C triggers its ubiquitination and degradation.* Mol Cell Biol, 1998. **18**(2): p. 839-45.

52.   Gao, T. and A.C. Newton, *The turn motif is a phosphorylation switch that regulates the binding of Hsp70 to protein kinase C.* J Biol Chem, 2002. **277**(35): p. 31585-92.

53.   Denning, M.F., et al., *Caspase activation and disruption of mitochondrial membrane potential during UV radiation-induced apoptosis of human keratinocytes requires activation of protein kinase C.* Cell Death Differ, 2002. **9**(1): p. 40-52.

54.   Li, L., et al., *Protein kinase Cdelta targets mitochondria, alters mitochondrial membrane potential, and induces apoptosis in normal and neoplastic keratinocytes when overexpressed by an adenoviral vector.* Mol Cell Biol, 1999. **19**(12): p. 8547-58.

55.   Majumder, P.K., et al., *Mitochondrial translocation of protein kinase C delta in phorbol ester-induced cytochrome c release and apoptosis.* J Biol Chem, 2000. **275**(29): p. 21793-6.

56.   Yuan, Z.M., et al., *Activation of protein kinase C delta by the c-Abl tyrosine kinase in response to ionizing radiation.* Oncogene, 1998. **16**(13): p. 1643-8.

57.   Gonzalez-Guerrico, A.M. and M.G. Kazanietz, *Phorbol ester-induced apoptosis in prostate cancer cells via autocrine activation of the extrinsic apoptotic cascade: a key role for protein kinase C delta.* J Biol Chem, 2005. **280**(47): p. 38982-91.

58.   Tanaka, Y., et al., *Protein kinase C promotes apoptosis in LNCaP prostate cancer cells through activation of p38 MAPK and inhibition of the Akt survival pathway.* J Biol Chem, 2003. **278**(36): p. 33753-62.

59.   Haas, W., H. Sterk, and M. Mittelbach, *Novel 12-deoxy-16-hydroxyphorbol diesters isolated from the seed oil of Jatropha curcas.* J Nat Prod, 2002. **65**(10): p. 1434-40.

60.   Makkar, H.P.S., A.O. Aderibigbe, and K. Becker, *Comparative evaluation of non-toxic and toxic varieties of Jatropha curcas for chemical composition, digestibility, protein degradability and toxic factors.* Food Chem., 1998. **62**: p. 207-215.

61.   Makkar, H.P.S., et al., *Studies on Nutritive Potential and Toxic Constituents of Different Provenances of Jatropha curcas.* J. Agric. Food Chem., 1997. **45**: p. 3152-3157.

62.   Furstenberger, G., et al., *Skin tumor promotion by phorbol esters is a two-stage process.* Proc Natl Acad Sci U S A, 1981. **78**(12): p. 7722-6.

63.   Furstenberger, G. and F. Marks, *Growth stimulation and tumor promotion in skin.* J Invest Dermatol, 1983. **81**(1 Suppl): p. 157s-62s.

64.   Kazanietz, M.G., *Novel "nonkinase" phorbol ester receptors: the C1 domain connection.* Mol Pharmacol, 2002. **61**(4): p. 759-67.

65.   Kazanietz, M.G. and P.S. Lorenzo, *Phorbol esters as probes for the study of protein kinase C function.* Methods Mol Biol, 2003. **233**: p. 423-39.

66.   Wender, P.A., et al., *The rational design of potential chemotherapeutic agents: synthesis of bryostatin analogues.* Med Res Rev, 1999. **19**(5): p. 388-407.

67.   Kazanietz, M.G., et al., *Binding of [26-3H]bryostatin 1 and analogs to calcium-dependent and calcium-independent protein kinase C isozymes.* Mol Pharmacol, 1994. **46**(2): p. 374-9.

68.   Hennings, H., et al., *Bryostatin 1, an activator of protein kinase C, inhibits tumor promotion by phorbol esters in SENCAR mouse skin.* Carcinogenesis, 1987. **8**(9): p. 1343-6.

69.   Szallasi, Z., et al., *Differential regulation of protein kinase C isozymes by bryostatin 1 and phorbol 12-myristate 13-acetate in NIH 3T3 fibroblasts.* J Biol Chem, 1994. **269**(3): p. 2118-24.

70.   Pettit, G.R., et al., *Isolation and Structure of Bryostatin 1.* J. Am. Chem. Soc., 1982. **104**: p. 6846-6848.

71.   Hornung, R.L., et al., *Preclinical evaluation of bryostatin as an anticancer agent against several murine tumor cell lines: in vitro versus in vivo activity.* Cancer Res, 1992. **52**(1): p. 101-7.

72.   Schuchter, L.M., et al., *Successful treatment of murine melanoma with bryostatin 1.* Cancer Res, 1991. **51**(2): p. 682-7.

73.   Clamp, A.R., et al., *A phase II trial of bryostatin-1 administered by weekly 24-hour infusion in recurrent epithelial ovarian carcinoma.* Br J Cancer, 2003. **89**(7): p. 1152-4.

74.   Propper, D.J., et al., *A phase II study of bryostatin 1 in metastatic malignant melanoma.* Br J Cancer, 1998. **78**(10): p. 1337-41.

75.   Roberts, J.D., et al., *Phase I study of bryostatin 1 and fludarabine in patients with chronic lymphocytic leukemia and indolent (non-Hodgkin's) lymphoma.* Clin Cancer Res, 2006. **12**(19): p. 5809-16.

76.   Varterasian, M.L., et al., *Phase II trial of bryostatin 1 in patients with relapsed low-grade non-Hodgkin's lymphoma and chronic lymphocytic leukemia.* Clin Cancer Res, 2000. **6**(3): p. 825-8.

77.   Zonder, J.A., et al., *A phase II trial of bryostatin 1 in the treatment of metastatic colorectal cancer.* Clin Cancer Res, 2001. **7**(1): p. 38-42.

78.   Obrig, T.G., et al., *The mechanism by which cycloheximide and related glutarimide antibiotics inhibit peptide synthesis on reticulocyte ribosomes.* J Biol Chem, 1971. **246**(1): p. 174-81.

79.   Kingston, R.E., *Introduction of DNA into Mammalian Cells*, in *Current Protocols in Molecular Biology*, F.M. Ausubel, et al., Editors. 2003, John Wiley & Sons, Inc. p. 9.0.1-9.0.5.

80.   Shigekawa, K. and W.J. Dower, *Electroporation of eukaryotes and prokaryotes: a general approach to the introduction of macromolecules into cells.* Biotechniques, 1988. **6**(8): p. 742-51.

81.   Garcia-Bermejo, M.L., et al., *Diacylglycerol (DAG)-lactones, a new class of protein kinase C (PKC) agonists, induce apoptosis in LNCaP prostate cancer cells by selective activation of PKCalpha.* J Biol Chem, 2002. **277**(1): p. 645-55.

82.   Wang, Q.J., et al., *Differential localization of protein kinase C delta by phorbol esters and related compounds using a fusion protein with green fluorescent protein.* J Biol Chem, 1999. **274**(52): p. 37233-9.

83.   Bradford, M.M., *A rapid and sensitive method for the quantitation of microgram quantities of protein utilizing the principle of protein-dye binding.* Anal Biochem, 1976. **72**: p. 248-54.

84.   Laemmli, U.K., *Cleavage of structural proteins during the assembly of the head of bacteriophage T4.* Nature, 1970. **227**(5259): p. 680-5.

85.   Zoukhri, D., et al., *Lacrimal gland PKC isoforms are differentially involved in agonist-induced protein secretion.* Am J Physiol, 1997. **272**(1 Pt 1): p. C263-9.

86.   Meister, G. and T. Tuschl, *Mechanisms of gene silencing by double-stranded RNA.* Nature, 2004. **431**(7006): p. 343-9.

87.   Benjamini, Y. and Y. Hochberg, *Controlling the False Discovery Rate: a Practical and Powerful Approach to Multiple Testing.* Journal of the Royal Statistical Society. Series B (Methodological), 1995. **57**(1): p. 289-300.

88.   Benjamini, Y. and D. Yekutieli, *Quantitative trait Loci analysis using the false discovery rate.* Genetics, 2005. **171**(2): p. 783-90.

89.   Ogbourne, S.M., et al., *Antitumor activity of 3-ingenyl angelate: plasma membrane and mitochondrial disruption and necrotic cell death.* Cancer Res, 2004. **64**(8): p. 2833-9.

90.   Xiao, L., M. Eto, and M.G. Kazanietz, *ROCK mediates phorbol ester-induced apoptosis in prostate cancer cells via p21Cip1 up-regulation and JNK.* J Biol Chem, 2009. **284**(43): p. 29365-75.

91.   Gschwend, J.E., W.R. Fair, and C.T. Powell, *Bryostatin 1 induces prolonged activation of extracellular regulated protein kinases in and apoptosis of LNCaP human prostate cancer cells overexpressing protein kinase calpha.* Mol Pharmacol, 2000. **57**(6): p. 1224-34.

92.   Kitada, S., et al., *Bryostatin and CD40-ligand enhance apoptosis resistance and induce expression of cell survival genes in B-cell chronic lymphocytic leukaemia.* Br J Haematol, 1999. **106**(4): p. 995-1004.

93.   Thomas, A., et al., *Bryostatin induces protein kinase C modulation, Mcl-1 up-regulation and phosphorylation of Bcl-2 resulting in cellular differentiation and resistance to drug-induced apoptosis in B-cell chronic lymphocytic leukemia cells.* Leuk Lymphoma, 2004. **45**(5): p. 997-1008.

94.   Gingrich, J.C., D.R. Davis, and Q. Nguyen, *Multiplex detection and quantitation of proteins on western blots using fluorescent probes.* Biotechniques, 2000. **29**(3): p. 636-42.

95.   Solomon, A., et al., *Key feature of the catalytic cycle of TNF-alpha converting enzyme involves communication between distal protein sites and the enzyme catalytic core.* Proc Natl Acad Sci U S A, 2007. **104**(12): p. 4931-6.

96.   McJilton, M.A., et al., *Protein kinase Cepsilon interacts with Bax and promotes survival of human prostate cancer cells.* Oncogene, 2003. **22**(39): p. 7958-68.

97.   Ron, D. and M.G. Kazanietz, *New insights into the regulation of protein kinase C and novel phorbol ester receptors.* Faseb J, 1999. **13**(13): p. 1658-76.

98.   Wang, Q.J., et al., *The V5 domain of protein kinase C plays a critical role in determining the isoform-specific localization, translocation, and biological function of protein kinase C-delta and -epsilon.* Mol Cancer Res, 2004. **2**(2): p. 129-40.

99.   Gomel, R., et al., *The localization of protein kinase Cdelta in different subcellular sites affects its proapoptotic and antiapoptotic functions and the activation of distinct downstream signaling pathways.* Mol Cancer Res, 2007. **5**(6): p. 627-39.

100.   Schechtman, D. and D. Mochly-Rosen, *Isozyme-specific inhibitors and activators of protein kinase C.* Methods Enzymol, 2002. **345**: p. 470-89.

101.   Zong, W.X., et al., *The prosurvival Bcl-2 homolog Bfl-1/A1 is a direct transcriptional target of NF-kappaB that blocks TNFalpha-induced apoptosis.* Genes Dev, 1999. **13**(4): p. 382-7.

102.   Adiseshaiah, P., D.V. Kalvakolanu, and S.P. Reddy, *A JNK-independent signaling pathway regulates TNF alpha-stimulated, c-Jun-driven FRA-1 protooncogene transcription in pulmonary epithelial cells.* J Immunol, 2006. **177**(10): p. 7193-202.

103.   Belguise, K., et al., *FRA-1 expression level regulates proliferation and invasiveness of breast cancer cells.* Oncogene, 2005. **24**(8): p. 1434-44.

104.   Wang, X., et al., *Regulation of phorbol ester-mediated TRAF1 induction in human colon cancer cells through a PKC/RAF/ERK/NF-kappaB-dependent pathway.* Oncogene, 2004. **23**(10): p. 1885-95.

105. Lee, N.K. and S.Y. Lee, *Modulation of life and death by the tumor necrosis factor receptor-associated factors (TRAFs).* J Biochem Mol Biol, 2002. **35**(1): p. 61-6.

106. Yu, H., F. Maurer, and R.L. Medcalf, *Plasminogen activator inhibitor type 2: a regulator of monocyte proliferation and differentiation.* Blood, 2002. **99**(8): p. 2810-8.

107. Dickinson, J.L., et al., *Plasminogen activator inhibitor type 2 inhibits tumor necrosis factor alpha-induced apoptosis. Evidence for an alternate biological function.* J Biol Chem, 1995. **270**(46): p. 27894-904.

108. Sarkar, S., et al., *Sphingosine kinase 1 is required for migration, proliferation and survival of MCF-7 human breast cancer cells.* FEBS Lett, 2005. **579**(24): p. 5313-7.

109. Hollander, M.C., et al., *Mammalian GADD34, an apoptosis- and DNA damage-inducible gene.* J Biol Chem, 1997. **272**(21): p. 13731-7.

110. Blass, M., et al., *Tyrosine phosphorylation of protein kinase Cdelta is essential for its apoptotic effect in response to etoposide.* Mol Cell Biol, 2002. **22**(1): p. 182-95.

111. Reyland, M.E., et al., *Protein kinase C delta is essential for etoposide-induced apoptosis in salivary gland acinar cells.* J Biol Chem, 1999. **274**(27): p. 19115-23.

112. Stone, R.M., et al., *Bryostatin 1 activates protein kinase C and induces monocytic differentiation of HL-60 cells.* Blood, 1988. **72**(1): p. 208-13.

113. Wang, S., et al., *Effect of bryostatin 1 on taxol-induced apoptosis and cytotoxicity in human leukemia cells (U937).* Biochem Pharmacol, 1998. **56**(5): p. 635-44.

114. Wang, S., et al., *Bryostatin 1 enhances paclitaxel-induced mitochondrial dysfunction and apoptosis in human leukemia cells (U937) ectopically expressing Bcl-xL.* Leukemia, 1999. **13**(10): p. 1564-73.

115. Cartee, L., et al., *Protein kinase C-dependent activation of the tumor necrosis factor receptor-mediated extrinsic cell death pathway underlies enhanced apoptosis in human myeloid leukemia cells exposed to bryostatin 1 and flavopiridol.* Mol Cancer Ther, 2003. **2**(1): p. 83-93.

116. Wang, S., et al., *Induction of tumor necrosis factor by bryostatin 1 is involved in synergistic interactions with paclitaxel in human myeloid leukemia cells.* Blood, 2003. **101**(9): p. 3648-57.

117. Reddy, A.B., et al., *Aldose reductase regulates high glucose-induced ectodomain shedding of tumor necrosis factor (TNF)-alpha via protein kinase C-delta and TNF-alpha converting enzyme in vascular smooth muscle cells.* Endocrinology, 2009. **150**(1): p. 63-74.

118. Black, R.A., et al., *A metalloproteinase disintegrin that releases tumour-necrosis factor-alpha from cells.* Nature, 1997. **385**(6618): p. 729-33.

119.   Diaz-Rodriguez, E., et al., *Extracellular signal-regulated kinase phosphorylates tumor necrosis factor alpha-converting enzyme at threonine 735: a potential role in regulated shedding.* Mol Biol Cell, 2002. **13**(6): p. 2031-44.

120.   Wang, Q.J., et al., *The lipophilicity of phorbol esters as a critical factor in determining the pattern of translocation of protein kinase C delta fused to green fluorescent protein.* J Biol Chem, 2000. **275**(16): p. 12136-46.

121.   Sumitomo, M., et al., *Protein kinase Cdelta amplifies ceramide formation via mitochondrial signaling in prostate cancer cells.* J Clin Invest, 2002. **109**(6): p. 827-36.

122.   Gavrielides, M.V., et al., *Androgens regulate protein kinase Cdelta transcription and modulate its apoptotic function in prostate cancer cells.* Cancer Res, 2006. **66**(24): p. 11792-801.

123.   Lu, S., S.Y. Tsai, and M.J. Tsai, *Molecular mechanisms of androgen-independent growth of human prostate cancer LNCaP-AI cells.* Endocrinology, 1999. **140**(11): p. 5054-9.

124.   Aziz, M.H., et al., *Protein kinase Cepsilon interacts with signal transducers and activators of transcription 3 (Stat3), phosphorylates Stat3Ser727, and regulates its constitutive activation in prostate cancer.* Cancer Res, 2007. **67**(18): p. 8828-38.

125.   Meshki, J., et al., *Regulation of prostate cancer cell survival by protein kinase C {epsilon} involves Bad phosphorylation and modulation of the TNF{alpha}/JNK pathway.* J Biol Chem.

126.   Wu, D. and D.M. Terrian, *Regulation of caveolin-1 expression and secretion by a protein kinase cepsilon signaling pathway in human prostate cancer cells.* J Biol Chem, 2002. **277**(43): p. 40449-55.

127.   Wu, D., et al., *Integrin signaling links protein kinase Cepsilon to the protein kinase B/Akt survival pathway in recurrent prostate cancer cells.* Oncogene, 2004. **23**(53): p. 8659-72.

128.   Gorin, M.A. and Q. Pan, *Protein kinase C epsilon: an oncogene and emerging tumor biomarker.* Mol Cancer, 2009. **8**: p. 9.

129.   Schutze, S., T. Machleidt, and M. Kronke, *Mechanisms of tumor necrosis factor action.* Semin Oncol, 1992. **19**(2 Suppl 4): p. 16-24.

130.   Dear, A.E., et al., *Molecular mechanisms governing tumor-necrosis-factor-mediated regulation of plasminogen-activator inhibitor type-2 gene expression.* Eur J Biochem, 1996. **241**(1): p. 93-100.

131.   Humphries, M.J., et al., *Suppression of apoptosis in the protein kinase Cdelta null mouse in vivo.* J Biol Chem, 2006. **281**(14): p. 9728-37.

132.   Mandal, M., et al., *The BCL2A1 gene as a pre-T cell receptor-induced regulator of thymocyte survival.* J Exp Med, 2005. **201**(4): p. 603-14.

133. Sarkar, S.A., et al., *Cytokine-mediated induction of anti-apoptotic genes that are linked to nuclear factor kappa-B (NF-kappaB) signalling in human islets and in a mouse beta cell line.* Diabetologia, 2009. **52**(6): p. 1092-101.

134. Casalino, L., et al., *Fra-1 promotes growth and survival in RAS-transformed thyroid cells by controlling cyclin A transcription.* Embo J, 2007. **26**(7): p. 1878-90.

135. Ramos-Nino, M.E. and B. Littenberg, *A novel combination: ranpirnase and rosiglitazone induce a synergistic apoptotic effect by down-regulating Fra-1 and Survivin in cancer cells.* Mol Cancer Ther, 2008. **7**(7): p. 1871-9.

136. Shirsat, N.V. and S.A. Shaikh, *Overexpression of the immediate early gene fra-1 inhibits proliferation, induces apoptosis, and reduces tumourigenicity of c6 glioma cells.* Exp Cell Res, 2003. **291**(1): p. 91-100.

137. Halatsch, M.E., et al., *Candidate genes for sensitivity and resistance of human glioblastoma multiforme cell lines to erlotinib. Laboratory investigation.* J Neurosurg, 2009. **111**(2): p. 211-8.

138. Gonzalez-Guerrico, A.M., et al., *Molecular mechanisms of protein kinase C-induced apoptosis in prostate cancer cells.* J Biochem Mol Biol, 2005. **38**(6): p. 639-45.

VII INDEX OF FIGURES

VIII INDEX OF TABLES

IX ABBREVIATIONS

ABTS	2,2′-Azino-bis(3-ethylbenzothiazoline-6-sulfonic acid)
ADP	Adenosine-5'-diphosphate
AIDS	Acquired immune deficiency syndrome
Akt 1	v-akt murine thymoma viral oncogene homolog 1
ANOVA	Analysis of variance
Apaf-1	Apoptotic protease activating factor-1
ATM kinase	Ataxia-telangiectasia mutated kinase
ATP	Adenosine-5'-triphosphate
BAD	BCL-2 antagonist of cell death
BAK	BCL2-antagonist/killer 1
BAX	BCL2-associated X protein
BCL-2	B-cell-lymphoma-2
BCL2A1	BCL2-related protein A1
BCL-B	BCL2-like 10
BCL-W	BCL2-like 2
BCL-XL	BCL2-like 1
BH3	BCL-2 homology 3
BID	BH3-interacting domain death agonist
BIK	BCL-2-interacting killer
BIM	BCL-2-like-11
BMF	BCL-2 modifying factor
BOK	BCL-2-related ovarian killer
BRCA1	Breast cancer 1
bryo1	Bryostatin 1
BSA	Bovine serum albumine
C1-4 domain	Conserved domain 1-4
CARD	Caspase-recruitment domain
Chx	Cycloheximide
CM	Conditioned medium
CTL	Cytotoxic T lymphocytes
DAMP	Danger-associated molecular pattern
DAG	Diacylglycerol
DAPI	4′,6-Diamidin-2-phenylindol
DEAE-Dextran	Diaminoethyl-Dextran

DISC	Death-ligand induced signaling complex
DMSO	Dimethylsulfoxide
DNA	Deoxyribonucleic acid
cDNA	Complementary DNA or copy DNA
dNTP	2'-Deoxynucleoside 5'-triphosphate
DSB	Double strand break
EDTA	Ethylenediaminetetraacetic acid
EMT	Epithelial-to-mesenchymal transition
EGFP	Enhanced green fluorescent protein
EGFR	Epidermal growth factor receptor
ELISA	Enzyme-linked immunosorbent assay
ERK	Extracellular signal-regulated kinases
FADD	As-associated death domain protein
FAM (6-FAM)	6-Carboxyfluorescein
Fas	TNF receptor superfamily, member 6
FasL	Fas ligand
FBS	Fetal bovine serum
FDR	False recovery rate
Fig.	Figure
FW primer	Forward primer
GAPDH	Glyceraldehyde-3-phosphate dehydrogenase
GCRMA	GeneChip Robust Multiarray Averaging
GO	Gene Ontology biological processes
GPCR	G-Protein-Coupled Receptor
GrA	Granzyme A
GrB	Granzyme B
h	Hour(s)
HEPES	4-(2-hydroxyethyl)-1-piperazineethanesulfonic acid
H3K4me	Methylated histone H3 lysine 4
HMGB1	High mobility group protein B1
HRK	Harakiri (also known as death protein -5)
HRP	Horseradish peroxidase
HSP70	Heat shock protein 70
IP3	Inositol-1,4,5-trisphosphate
JNK	Mitogen-activated protein kinase 8
LB	Lysogeny broth

log	Logarithm
LSD1	Lysine specific demethylase 1
MAP Kinase	Mitogen-activated protein kinase
MAPKK	Mitogen-activated protein kinase kinase
MCL1	Myeloid cell leukemia sequence 1
MEK	Same as MAPKK
MES	2-(*N*-morpholino)ethanesulfonic acid
MGB probe	Minor groove binder probe
myr	Myristoylated
NB-ARC	Same as NOD
NK	Natural killer (cells)
NLS	Nuclear localization signal
NOD	Nucleotide-binding and oligomerization domain
N.R.	Not represented
OG	Oncogenesis
p	Phospho
P	Proliferation
PAI-2	Same as SERPINB2
PBS	Phosphate buffered saline
PCA	Prinicipal component analysis
PCR	Polymerase chain reaction
qPCR	Quantitative PCR
qRT-PCR	Quantitative RT-PCR
RT-PCR	Reverse transcriptase real-time PCR
PDK1	3-phosphoinositide-dependent protein kinase-1
PEP005	Ingenol-3-angelate
PIN	Prostate intraepithelial neoplasia
PI3K	Phosphoinositide 3-kinase
PIP2	Phosphoinositol-4,5-bisphosphate
PKC	Protein kinase C
aPKC	Atypical PKC
cPKC	Classical PKC
nPKC	Novel PKC
PLC	Phospholipase C
PMA	Phorbol 12-myristate 13-acetate
PP2A	Protein phosphatase 2A

PPP1R15A	Protein phosphatase 1, regulatory (inhibitor) subunit 15A
PS	Pseudosubstrate sequence
PTEN	Phosphate and tensin homolog 1
PUMA	BCL-2 binding component-3
PVDF	Polyvinylidenfluoride
RB1	Retinoblastoma 1
RISC	RNA induced silencing complex
RNA	Ribonucleic acid
dsRNA	Double-stranded RNA
mRNA	Messenger RNA
miRNA	MicroRNA
rRNA	Ribosomal RNA
siRNA	Small interfering RNA
RNase	Ribonuclease
RNAi	RNA interference
RNP	Ribonucleoprotein particle
RPMI medium	Roswell Park Memorial Institute medium
RT	Reverse transcription
RV primer	Reverse primer
SAPK	Mitogen-activated protein kinase 9
SDS	Sodium dodecyl sulfate
SDS-PAGE	SDS- polyacrylamide gel electrophoresis
S.E.M.	Standard error of the mean
SERPINB2	Plasminogen activator inhibitor-2
S.O.C.	Super optimal broth + glucose
SPP	Sphingosine-1-phosphate
SSPE	Sodium chloride, sodium phosphate (monobasic), ethylenediaminetetraacetic acid
SPHK	Sphingosine kinase
ST	Signal transduction
TACE/ADAM17	TNFα converting enzyme
TAE	Tris-Acetate-EDTA
TBS-T	Tris-Buffered Saline Tween-20
TF	Transcription factors
TM	Transmembrane domains
TNFα	Tumor necrosis factor-α

hTNFα	Human TNFα
TPA	12-O-tetradecanoylphorbol-13-acetate (same as PMA)
TRAF	Tumor necrosis factor receptor-associated factor
TRAIL	TNF-related apoptosis-inducing ligand
Tris	Tris(hydroxymethyl)aminomethane
V1-V5 domain	Variable domain 1-5
vs.	Versus
WD40 repeat	beta-transducin repeat containing 40 amino acids , often terminating in a tryptophan-aspartic acid (W-D) dipeptide.
XIAP	X-linked inhibitor of apoptosis

X PUBLICATIONS

X.1 Original Publications

Caino M.C.*, <u>von Burstin V.A.*</u>, Lopez-Haber C., Kazanietz M.G.

Differential regulation of gene expression by PKC isozymes as determined by genome-wide expression analysis.

J Biol Chem. 2011 Jan 20. Epub ahead of print; doi: 10.1074/jbc.M110.194332

Meshki J.*, Caino M.C.*, <u>von Burstin V.A.</u>, Griner E.M., Kazanietz M.G.

Regulation of prostate cancer cell survival by protein kinase C {epsilon} involves Bad phosphorylation and modulation of the TNF{alpha}/JNK pathway.

J. Biol. Chem. 2010 Aug 20;285(34): 26033-40.

<u>von Burstin V.A.</u>, Xiao L., Kazanietz M.G.

Bryostatin 1 inhibits phorbol ester-induced apoptosis in prostate cancer cells by differentially modulating PKC{delta} translocation and preventing PKC{delta} mediated release of TNF{alpha}

Mol. Pharmacol. 2010 Sep 1; 78(3):325-32.

Bollrath J.*, Phesse T.J.*, <u>von Burstin V.A.</u>, Putoczki T., Bennecke M., Bateman T., Nebelsiek T., Lundgren-May T., Canli O., Schwitalla S., Matthews V., Schmid R.M., Kirchner T., Arkan M.C., Ernst M., Greten F.R.

gp130-mediated Stat3 activation in enterocytes regulates cell survival and cell-cycle progression during colitis-associated tumorigenesis.

Cancer Cell. 2009 Feb 3;15(2):91-102.

Xiao L.*, Caino M.C.*, <u>von Burstin V.A.*</u>, Oliva J.L., Kazanietz M.G.

Phorbol ester-induced apoptosis and senescence in cancer cell models.

Methods. Enzymol. 2008;446:123-39.

*These authors contributed equally to this work.

X.2 Abstracts

<u>von Burstin V.A.*</u>, Caino M.C.*, Kazanietz M.G.

Genome-wide expression analysis reveals PKCδ as a master regulator of

transcription in prostate cancer cells.

25th Annual Student Symposium of the Graduate Group in Pharmacological Sciences

of the University of Pennsylvania, November 6, 2008, Philadelphia, PA

<u>von Burstin V.A.*</u>, Caino M.C.*, Lopez-Haber C., Kazanietz M.G.

PKCδ controls apoptosis in prostate cancer cells through regulation of transcriptional

network.

2009 FASEB Summer Research Conferences "Lipid signaling Pathways in Cancer",

July 19-24, 2009, Carefree Resort, Carefree, Arizona

*These authors contributed equally to this work.

XI CURRICULUM VITAE

Personal Information

Name	von Burstin
Maiden name	Därr
Given name	Vivian
Middle name	Annaluise
Date and place of birth	September 16, 1978, Houston, Texas
Nationality	German, American
Marital status	Married

Education

03/2007 – present	Ph.D. thesis work at the Department of Pharmacology at the University of Pennsylvania, PA, USA in the laboratory of Prof. Dr. Marcelo G. Kazanietz and under the supervision of Prof. Dr. Angelika M. Vollmar at the Department of Pharmacy and Pharmaceutical Biology, Ludwig-Maximilians University, Munich
12/2005 – 01/2007	Research in the laboratory of Prof. Dr. Florian R. Greten, Technical University of Munich. Focus on Stat3 in colitis and colitis associated carcinogenesis.
07/2005	Registration as a pharmacist at the Bavarian Chamber of Pharmacists, Munich.
06/2005	Licensing exam as pharmacist at the Bavarian Chamber of Pharmacists, Munich.
05/2004 – 04/2005	Final year trainee at the pharmacy of the Centre Hospitalière Universitaire Vaudois (CHUV) of Lausanne/Switzerland and at the local pharmacy, Spitzweg, Munich
02/2004	Graduation, School of Pharmacy, Freie Universität of Berlin
10/1998 – 02/2004	School of Pharmacy, Freie Universität of Berlin
09/1997 – 04/1998	Diplôme élémentaire en langue française (D.E.L.F.) at the Collège Internationale de Cannes, Cannes/France
06/1997	High School Graduation, Dientzenhofer Gymnasium, Bamberg

**Additional
work experience**

12/2005 – 01/2007	Part time pharmacist, Spitzweg Pharmacy, Munich
07/2005 – 11/2005	Full time pharmacist, Spitzweg Pharmacy, both Munich
09/1997 – 04/1998	Au-pair in Cannes/Fance

Special Skills

Laboratory	Common techniques in molecular biology, *i.e.* Western Blot, qRT-PCR, cloning and preparation of plasmids, gene silencing, genome wide expression analysis, tissue culture techniques, immunohistochemistry and immunocytochemistry, confocal imaging, histopathology of mouse small and large intestinum, mouse models of cancer associated inflammatory bowel disease.
Computer	Profound knowledge in common software computer applications, *i.e.* Microsoft Office, Adobe Photoshop, GraphPad Prizm software for statistical analysis.
Languages	German (native), French (fluently) and English (fluently)

Interests

Sports	Downhill Skiing, sailing, ballet, tennis
Music	Playing the piano (since 1984) and the violin (since 1990)

XII ACKNOWLEDGEMENTS